ABSTRACT

Title of Document:	THE REGULATION OF B CELL ACTIVATION BY MEMBRANE DAMAGE AND ANTIGEN DENSITY
	Heather E. Miller, Doctor of Philosophy, 2015
Directed By:	Dr. Wenxia Song, Associate Professor, Cell Biology and Molecular Genetics

Antibodies generated by B cells neutralize pathogens and pathogen-secreted toxins and flag them for immune clearance. Antibody responses are initiated via binding of cognate antigen to B-cell receptors (BCR). This induces BCR aggregation in lipid rafts, promoting BCR signaling and internalization of antigen for processing and presentation to T helper cells, which is essential for generating high affinity and long-lasting antibody responses. The ability of an immunogen to activate BCR signaling and internalization is necessary for efficient vaccines. To capture these immunogens, B cells circulate and migrate through blood and lymphoid tissues. During circulation, the plasma membrane of B cells may be damaged by mechanical forces and membrane-perforating toxins. The impact of plasma membrane damage on B-cell activation is unknown.

The first part of this thesis investigated the mechanism of plasma membrane repair in B cells and the effects of repair on BCR activation. My research reveals that

B cells rapidly repair membrane wounds provoked by streptolysin O, a pore forming bacterial toxin. Similar to the mechanism reported for fibroblasts and muscle cells, B cells repair by Ca^{2+} triggered lysosome exocytosis, which releases acid sphingomyelinase (ASM) to the plasma membrane to induce endocytosis of damaged membrane. Different from previous reports, ASM induces direct endocytosis of lipid rafts in the absence of the membrane invaginating lipid raft protein, caveolin. Importantly, it was discovered that BCR activation interferes with plasma membrane repair, while wounding inhibits BCR signaling and internalization by segregating BCRs from lipid rafts. These data suggest that plasma membrane repair and B cell activation interfere with one another due to competition for lipid rafts.

The second part of my thesis established and characterized a membrane-bound antigen system where all antigenic molecules are optimally oriented for BCR binding. Using the new system, we investigated the role of the density and valency of membrane-bound antigen on BCR activation. The results show that increases in the density but not valency of antigen on membranes significantly enhance the magnitudes of the early events of BCR activation, including BCR self-clustering, cell spreading on antigen-presenting surface, and protein tyrosine phosphorylation. The enhanced signaling is correlated with greater actin dynamics required for BCR aggregation, B-cell spreading and signaling. These results indicate that this model antigen will benefit quantitative studies of the molecular mechanisms underlying BCR activation, and also suggest that manipulations of molecular configuration and density can be applied to enhance the immunogenicity of vaccines.

THE REGULATION OF B CELL ACTIVATION BY MEMBRANE DAMAGE
AND ANTIGEN DENSITY

By

Heather E. Miller

Thesis submitted to the Faculty of the Graduate School of the
University of Maryland, College Park, in partial fulfillment
of the requirements for the degree of
Doctor of Philosophy
2015

Advisory Committee:
Wenxia Song, Ph.D., Chair
Arpita Upadhyaya, Ph.D.
Norma Andrews Ph.D.
Xiaoping Zhu, D.V.M, Ph.D.
Volker Briken, Ph.D.

Dedication

I dedicate this thesis to my parents and sister, for all of their endless and loving

support. I could not have accomplished this without them.

Acknowledgements

First, I would like to thank my advisor, Dr. Song, for all of her patience and help with everything. I learned so much from her and she has made me a better researcher.

Thank you, to all my committee members: Dr. Upadhyaya, Dr. Zhu, Dr. Frauwirth, Dr. Briken. I appreciate the knowledge and advice given.

Special thanks to Dr. Andrews, for her much needed guidance and knowledge; also for joining my committee late in the game. My membrane repair project would not have been possible without her support.

Much appreciation going to Dr. Upadhyaya, for her contribution to my TIRFM analysis, and allowing me to use her TIRF microscope, which several of my projects completely depended on.

To my collaborators: Thiago, Matthias, and Christy. I greatly appreciate Thiago's much needed ASM work to complete the lysosome exocytosis figure. I was lucky to have both Matthias and Thiago's help and support with the B cell membrane repair project. Lots of gratitude for all of Christy's analysis of the live images of the LifeAct B cells, her analysis contributed to finishing the antigen density project. Also Christy was always there for me when I needed help with analysis or working the TIRF microscope, which was a lot, so we really got to know each other.

To Dr. Muro and her graduate students, for providing the ASM KO mice.

To Amy Beaven, Ken Class, and Timothy Maugel, I thank them for the training and help with imaging and flow.

Lastly, but very important to me, I would like to thank my lab members (past and present) for all their help, support, and understanding. They have provided me with the perfect working environment and I am glad to have every one of them as friends. Karen was the first lab member I saw graduate and leave the lab. She is a great researcher and I learned a lot from her, especially about running Westerns. Katharina, Katie, and Vonetta have always been there for me since I joined the lab. They provided much needed help and advice on experiments, presentations, and writing. Katharina is one of the sweetest people I know and I am grateful we are good friends. Katie and Vonetta are fun to be with and they always make me laugh. Choahong joined the same time as me and we were close. We worked on experiments together and learned about TIRFM at the same time. I admire his hard work and success as a researcher. Mark, Melvin, and Senthil joined after me and they provided the lab with lots of humor. Mark was the best at live fluorescence imaging and I really appreciate his help with using the Leica and getting the fantastic images for the BCR and CT internalization. Michelle and Qian joined the lab several years later. I quickly became close to Michelle, she has an easy going personality and good sense of humor, I am glad she was there with me when so many people were graduating and the lab felt empty. I could always count on Michelle to help me with anything and she

contributed a lot to the lab and took on many of the responsibilities. Qian is such a hard worker and I am glad we got to teach immunology lab together, she was the best prep TA I ever worked with. Abby joined the lab just last year, she has such a sweet nature and I enjoy seeing her every time I go into the lab. I had a good time working with her and teaching her everything I know about the TIRF microscope.

Table of Contents

List of Figures

List of Abbreviations

Ab   Antibody

Abp1   Actin-binding protein 1

AF   Alexa Fluor

Ag   Antigen

AP-2   Adaptor protein-2

APC   Antigen presenting cell

ASM   Acid sphingomyelinase

Bam32   B lymphocyte adaptor molecule of 32 kilodaltons

BCR   B cell receptor

bFab   Monobiotinylated goat anti-mouse IgG and IgM Fab fragment

bHEL   Monobiotinylated hen egg lysozyme

βHex   β-Hexosaminidase

BLNK   B cell linker protein

Btk   Bruton's tyrosine kinase

DAG   Diacylglycerol

DAMP   Damage-associated molecular pattern

DC   Dendritic cell

DPA   Desipramine

EBV   Epstein-Barr virus

ER   Endoplasmic reticulum

ERK   Extracellular signal regulated kinase

ERM   Ezrin-Radixin-Moesin

ESCRT	Endosomal sorting complex required for transport
F-actin	Filamentous actin
Fc	Fragment crystallizable
FcγRIIB	Fc gamma receptor IIB
FDC	Follicular dendritic cell
FO	Follicular
FRC	Fibroblastic reticular cells
FRET	Fluorescence resonance energy transfer
GAP	GTPase-activating protein
GAS	Group A streptococcus
GC	Germinal center
GEF	Guanine-nucleotide exchange factor
Grb2	Growth factor receptor-bound protein 2
HEK 293	Human embryonic kidney 293
HEL	Hen egg lysozyme
IL	Interleukin
INF-γ	Interferon-γ
IP_3	Inositol triphosphate
IRM	Interference reflection microscopy
ITAM	Immunoreceptor tyrosine-based activation motif
ITIM	Immunoreceptor tyrosine-based inhibition motif
JNK	c-Jun NH2-terminal kinase
LAB	Linker of activated B cells

LMP2A   Latent membrane protein 2A

LPS   Lipopolysaccharide

MAPK   Mitogen activated protein kinase

MβDC   Methyl-β-cyclodextrin

MHCII   Major histocompatibility complex class II molecule

MZ   Marginal zone

NFAT   Nuclear factor of activated T cells

NFκB   Nuclear factor kappa-B

NLR   Nod-like receptor

NP   (4-hydroxy-3-nitrophenyl)acetyl

N-WASP   Neuronal Wiskott–Aldrich syndrome protein

NRK   Normal rat kidney epithelial cell

PAMP   Pathogen-associated molecular pattern

PBS   Phosphate buffered saline

PC   Plasma cell

PH   Pleckstrin homology

PI3K   Phosphatidylinositol 3-kinase

PIP_2 Phosphatidylinositol-4,5-bisphosphate

PIP_3 Phosphatidylinositol-3,4,5-triphosphate

PKC-β   Protein kinase C-β

PLCγ2   Phospholipase Cγ2

PS   Polysaccharide

PTK   Protein tyrosine kinase

pY	phosphotyrosine
Rag	Recombination-activating gene
SHIP1	SH2-domain containing inositol 5'-phosphatase 1
sIg	Surface immunoglobulin
SLO	Streptolysin O
SNARE	Soluble N-ethyl-maleimide-sensitive fusion protein attachment protein receptor
Syk	Spleen tyrosine kinase
Syts	Synaptotagmins
T1	Transitional B cells of type 1
T2	Transitional B cells of type 2
TCR	T cell receptor
TD	T cell dependent
TEM	Transmission electron microscopy
TGF-β	Transforming growth factor β
TI	T cell independent
TIRFM	Total internal fluorescence microscopy
TLR	Toll-like receptors
t-SNARE	Target SNARE
VAMP-7	Vesicle-associated membrane protein 7
v-SNARE	Vesicle SNARE
WASP	Wiskott–Aldrich syndrome protein
WT	Wild type

Chapter 1: Introduction

1.1 Innate and adaptive immunity

The vertebrate immune system is divided into two branches that protect the host from pathogens: the innate immunity and adaptive immunity. The innate immune response is the first line of defense against invading microbes and mediated by immune cells like neutrophils and macrophages. The activation of the innate immune responses depends on surface and internal receptors that recognize pathogen-associated molecular patterns (PAMPs) or host derived damage-associated molecular patterns (DAMPs) (*1, 2*). PAMPs such as lipoproteins and glycolipids present on bacterial surfaces or double stranded RNA made by viruses are recognized by pattern recognition receptors (PRRs), including Toll-like receptors (TLR), RIG-I like receptors, and Nod-like receptors (NLR) (*1-4*). The binding of PRRs to their respective PAMPs induces signaling, which leads to the production and secretion of cytokines that affect the development and activation of leukocytes belonging to the adaptive immune response (*3-5*). The adaptive immune response has two major players, B lymphocytes (B cells) and T lymphocytes (T cells). Unlike the innate immunity, the induction of adaptive immune responses relies on distinct receptors highly specific for antigens. This specificity comes from the rearrangement of the variable (V), diversity (D), and joining (J) gene segments of the B cell receptor (BCR) or T cell receptor (TCR) during development, giving rise to clonally varient lymphocytes. Another major difference between the adaptive and innate immunity is that lymphocytes have the ability to acquire long-lasting memory, so that their

response and effector functions are immediate and more robust with a repeated encounter of the same antigen(*6, 7*).

Adaptive immunity is divided into two branches, humoral immunity that is antibody-mediated by B cells, and cellular immunity that is mediated by T cells. BCRs recognize antigens in their native conformational form and can bind antigens in any chemical and physical form. B cells produce antibodies; this neutralizes pathogens or toxins and opsonizes them for elimination via phagocytic cells by binding to them with high specificity (*6, 8*). T cells do not recognize antigens in their native form as B cells do; they only recognize antigens (peptides and polysaccharides) that have been processed and presented on the surfaces of cells. Cytotoxic T cells (CD8+ T cells) recognize antigens bound to major histocompatibility complex class I molecules (MHCI) on the surfaces of all nucleated cells and destroy any cells presenting foreign antigens. Helper T cells (CD4+ T cells) recognize antigens loaded on major histocompatibility complex class II molecules (MHCII) and release cytokines for stimulation of various leukocytes. MHCII is only expressed by professional antigen-presenting cells (APCs), like macrophages, dendritic cells, and B cells. Antigen-presenting cells internalize antigen bound to their receptors, degrade and load them onto MHCII for exocytosis to cell surfaces for interaction with helper T cells (*6, 9, 10*).

1.2 Development and maturation of B cells

B cells develop from hematopoietic precursors in the bone marrow. Here they first start out as progenitor B cells (Pro-B cells), expressing surface pro-BCRs, consisting of calnexin and the signaling transduction heterodimer, Igα and Igβ. Pro-B cells

progress into Pre-B cells after Recombination-activating gene (Rag)-mediated variable (V), diversity (D), and joining (J) gene rearrangement of the heavy μ chain. The heavy chains of IgM are expressed as membrane bound forms (mIgM) in association with surrogate light chains (λ5 and VpreB) and the Igα/Igβ heterodimer to generate the Pre-BCR. Igα/Igβ is the signaling transduction unit of the Pre-BCR and mature BCR by conveying signals from the BCR to cytoplasmic signaling molecules. Signaling though the Pre-BCR is important for transition into immature B cells, that are denoted by expression of mature BCRs, which have replaced the surrogate light chains of pre-BCR for successfully VJ rearranged light chains (κ and λ) (*7, 11-13*). In the bone marrow, immature B cells go through checkpoints to eliminate self-reactive B cells. B cells expressing BCR with high affinity binding to self-antigens are deleted by signaling-induced apoptosis, whereas low affinity binding results in Ig gene editing (further rearrangement of Ig gene) or anergy (unresponsive to antigen) (*14, 15*).

After successful production of non-self reacting BCRs, the immature B cells leave the bone marrow and enter the secondary lymphoid organs, where they become transitional B cells of type 1 (T1) expressing high lvels of IgM and CD93. T1 cells migrate to B cell follicles to develop into transitional B cells of type 2 (T2) and begin to express IgD, Fc receptors for IgE (CD23), and complement receptor (CD21). These T2 cells then become mature B cells, which lose CD93 expression and decrease IgM expression. Mature B cells circulate through the spleen or lymph nodes to seek out pathogens (*11, 16-18*) **(Fig.1.2)**.

Naïve (have not encountered antigen) mature B cells are subdivided into B1 and B2 categories. B1 cells include B1a and B1b cells that are located within the pleural and peritoneal cavities. B1 cells are responsible for generating innate-like antibody responses. Their activation relies on innate signals like TLRs and is independent of T helper cells. B1 B cells mount IgM and IgA antibody responses against non-protein antigens. Such antibody responses are generated without any prior antigen challenge, thereby categorized as natural antibodies (*19-21*). B2 cells have several subsets including marginal zone (MZ), follicular (FO), and germinal center (GC) B cells. MZ B cells share many properties with B1 cells. They express various TLRs and rapidly produce IgM antibodies to TI antigens. MZ B cells reside within the marginal zone of the secondary lymphoid tissues, like the spleen, where they are given access to blood circulating through the lymphoid organs and hence sample for blood-borne pathogens (*21, 22*). Recent studies show that MZ B cells as well as MZ macrophages are capable of transporting antigens into B cell follicules where MZ B cells can present antigen to FO B cells directly or indirectly via follicular dendritic cells (*23*).

B cell activation requires two signals. Antigen binding induces signaling as the first signal for B cell activation. Subsequently, B cells internalize and process antigen as MHC II complexes for the recognition of T helper cells. Interactions of T cells with peptide-loaded MHC II complexes induce T cell activation. Activated T cells provide the second signal for B cell activation, including CD40 ligand to bind to CD40 on the B cell surface and cytokines. After receiving both signals from BCR signaling and T helper cells, B cells undergo rapid proliferation, which leads to

4

Plasma cell

IgD⁺
IgM^low
CD93⁻
CD23⁺
CD21⁺

Mature B cell

Memory B cell

IgM^high
CD93⁺
CD23⁺
CD21⁺

T2 B cell

IgM^high
CD93⁺

T1 B cell

Mature BCR

Immature B cell

Pre-BCR

Surrogate light chains

Pre-B cell

Pro-BCR

Igα Igβ

Calnexin

Pro-B cell

5
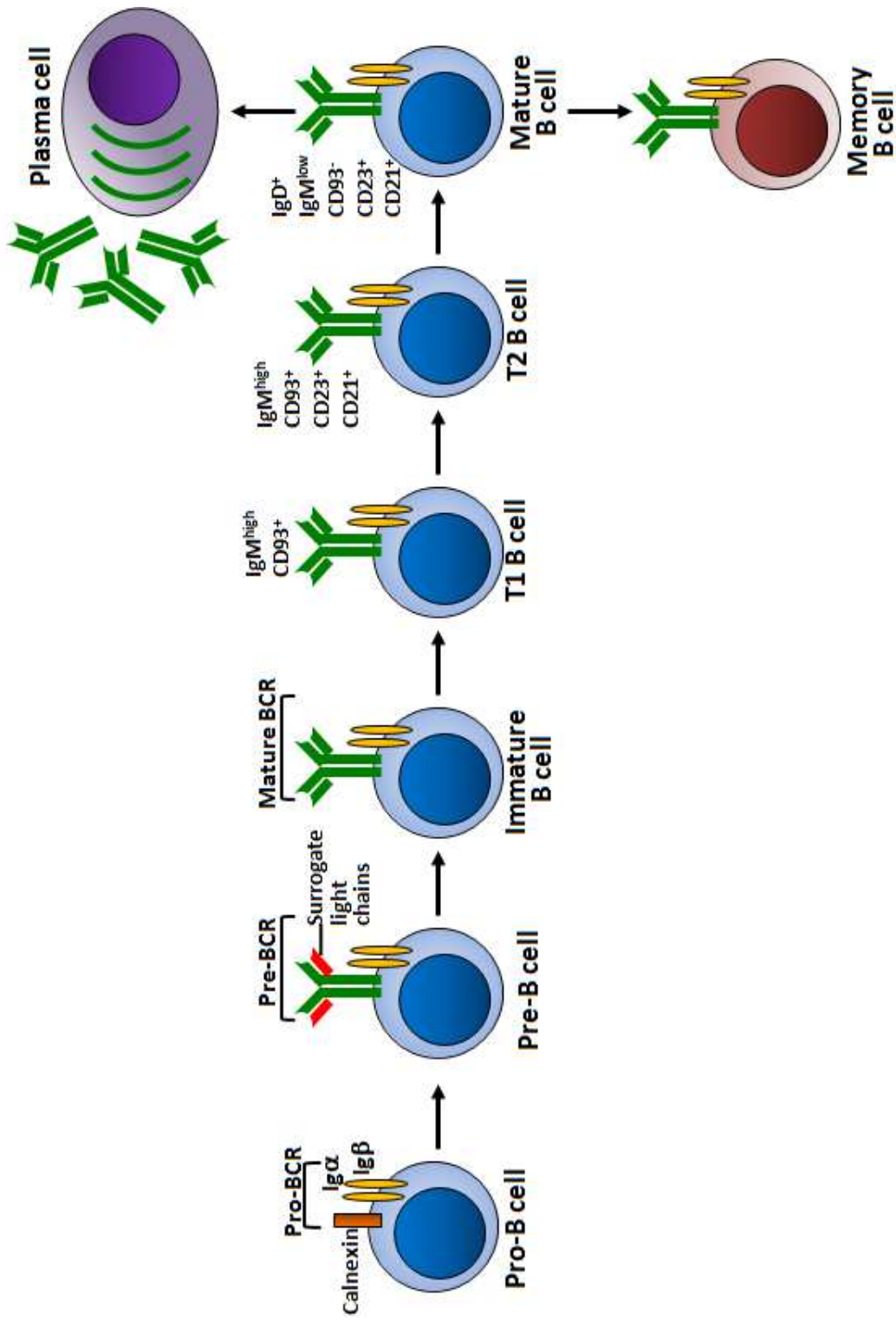
Fig. 1.2: B cell development and maturation. B cell development begins in the bone marrow from hematopoietic precursors. The progenitor B cell (Pro-B cell) produces the Pro-BCR, consisting of calnexin and the signaling transduction heterodimer, Iga and Igb. Expression of the Pre-BCR consisting of rearranged IgM heavy chains and surrogate light chains (VpreB and Vλ5) leads to the development of Pre-B cells. Signaling through the Pre-BCR induces development into the immature B cell, which expresses rearranged IgM heavy chain and light chains (κ and λ) as membrane IgM-based BCR. Immature B cells migrate from the bone marrow to the secondary lymphoid organs where they differentiate into transitional B cells of type 1 (T1) and express IgM and CD93. In the B cell follicles, T1 B cells develop into transitional B cells of type 2 (T2) that gain the expression of CD23 and CD21. T2 B cells become mature B cells that lose expression of CD93 and decrease expression of IgM, while increasing expression of IgD. In the secondary lymphoid organs, mature B cells may encounter their cognate antigen, which activates signaling, and antigen processing and presentation for the recognition of helper T cells. B cell signaling and T cell help enable B cells to differentiation into antibody secreting plasma cells or memory B cells

the differentiation of B cells into short-lived plasma cells and the development of germinal center precursors (*24, 25*). The germinal centers are largely divided into a dark zone and a light zone. The dark zone is made up of rapidly proliferating B cells, while the light zone contains T cells and follicular dendritic cells. In the germinal center, B cells migrate from the dark zone to the light zone to interact with T cells and antigen presented by follicular dendritic cells, which enables isotype switching and affinity maturation of B cells. The variable gene region of Ig genes undergoes somatic hypermutation. Only the B cells expressing BCRs with enhanced affinity to antigen gain survival and differentiation signals from BCR signaling and T helper cells via antigen processing and presentation. These signals enable B cells to differentiate into either long-lived plasma cells or memory B cells (*24, 26, 27*). Long-lived plasma cells migrate to the bone marrow, which provides specialized niches for their survival. In the bone marrow, long-lived plasma cells maintain the level of antibodies, offering extended protection to the host (*28, 29*). Memory B cells are capable of self-renewal and circulate though lymphoid organs, where they remain as resting cells until stimulated by antigen. Upon activation, they undergo rapid clonal expansion and give rise to plasma cells that secrete high affinity antibody to quickly combat the pathogen, which is characteristic of secondary immune responses provided by the adaptive immunity (*30, 31*).

1.3 B cell-mediated antibody responses

Immunoglobulins (Ig) or antibodies are glycoproteins that are essentially the secreted form of the BCR, but lack the hydrophobic membrane-anchoring sequence and

covalently associated Igα/β. They consist of paired heavy and light chains. The structure analysis show that antibody appears as a Y-shape, where the arms of the Y, or F(ab')$_2$ fragment, contains the variable regions that binds to antigen, and the stem of the Y, or F$_c$ fragment, interacts with effector molecules, such as complement, or Fc receptors on cells, like macrophages, to induce phagocytosis of the antibody bound antigen **(Fig. 1.3)**. There are five Ig isotypes, which vary in their F$_c$ fragments and functions: IgM, IgD, IgG, IgA, and IgE. IgM and IgG circulate in the blood and play a major role in opsonization and complement activation, IgA is important for neutralization of pathogens on mucosal surfaces, and IgE is involved in allergic reactions by activating mast cells (*32*).

There are two ways that B cells may become stimulated and produce antibodies: T cell dependent (TD) or T cell independent (TI) activation. For TD activation, a B cell must internalize, process, and present antigen peptides or polysaccharides bound to MHCII to helper T cells. Via antigen presentation, both T and B cells become stimulated, and activated T cells release cytokines that induce B-cell proliferation, antibody production, and memory B cell development. With T cell help through CD40 and release of cytokines, B cells undergo affinity maturation in the germinal center where the variable region of Ig genes undergo hypermutation isotype switching, affinity maturation, and differentiation into antibody producing plasma cells (PC) or memory B cells. Affinity maturation is necessary for developing
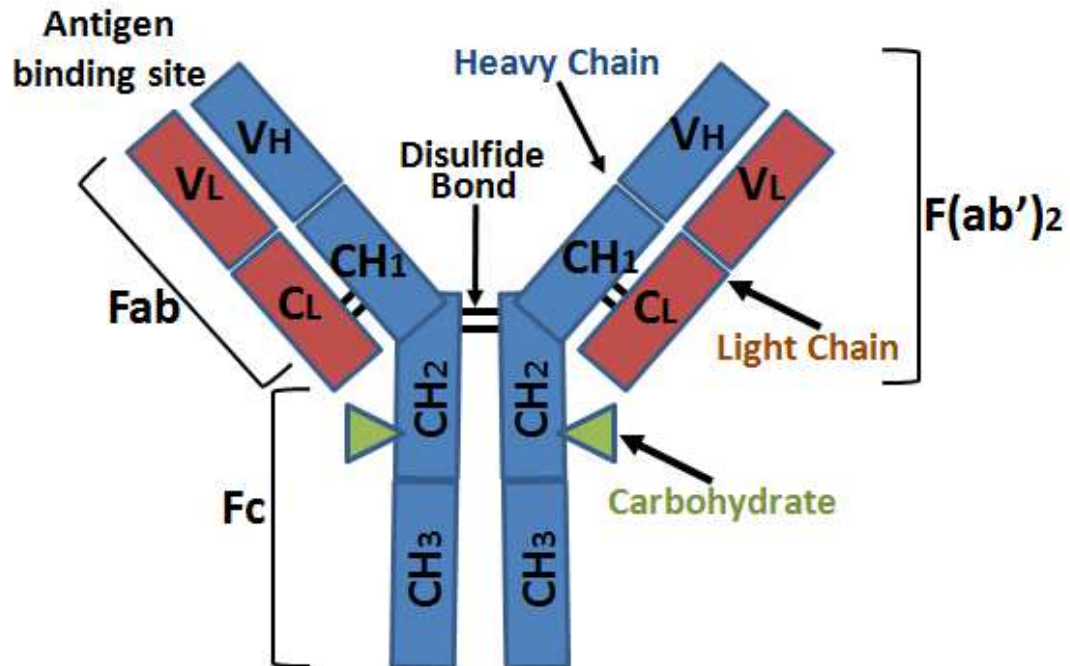
Fig. 1.3: Basic structure of the antibody. Antibodies are the secreted form of the B cell receptor (BCR). They consist of two identical heavy chains held together by disulfide bonds and two identical light chains held to each of the heavy chains through disulfide bonds. The N-terminus of the heavy and light chains contains the variable regions (VL and VH) that form two antigen binding sites. The Fc region of antibodies is glycosylated and consist of a number of constant regions formed by a pair of the heavy and light chains (CH_1) or a pair of the heavy on the C-terminus side (CH_2 and CH_3). The Fab fragment is monovalent and consists of one light chain and its corresponding heavy chain section (CH_1 and VH). The F(ab')$_2$ fragment is divalent and consists of both Fab fragments linked by a disulfide bond.

B cells with enhanced binding affinity to antigen, while isotype switching is important for antibody effector functions. Naïve B cells only express IgM and IgD immunoglobulin on their surfaces. In response to antigenic stimulation and T cell help, the gene encoding the constant regions of IgM and IgD heavy chain are switched to IgG, IgA, or IgE, depending on the type of cytokine directing the B cell. Interleukin 4 (IL-4) induces IgG1 and IgE switching, while interferon-γ (INF-γ) decreases IgG1 and increases IgG2 production. IgA generation is enhanced by transforming growth factor β (TGF-β), IL-2, and IL-5 (*10, 33-35*).

TI activation differs from TD in that it does not require T cell help to produce antibodies; however, TI response is predominately IgM production, lacking affinity maturation and long lasting memory (*36, 37*). TI antigens are generally polysaccharides and are divided into two types, TI type 1 (TI-1) and TI type 2 (TI-2) antigens. TI-1 antigens, such as lipopolysaccharides (LPS), induce polyclonal B cell proliferation. TI-2 antigens, like capsular polysaccharides (PS) from bacterial pathogens, including *Neisseria meningitidis, Haemophilus influenza or Streptococcus pneumonia*, contain multiple repeating antigenic structures that extensively cross-link BCRs and strongly activate receptors (*36-38*). It has been suggested that TI-2 stimulation leads to B cell differentiation into long-lived plasma cells (PC) that secrete IgM or memory PCs. Differentiation of B cells into these memory PCs requires a second signal, such as stimulation through TLRs and cytokines (*21, 38*). B cells express TLRs, including TLR1–TLR2, TLR4, TLR6, TLR7 and TLR9; and it is known that stimulation through TLRs can lead to B cell proliferation and antibody production. TLR expression differs among the various subsets of B cells, with B-1

10

and marginal zone (MZ) B cells having elevated responses to TLR stimulation compared to follicular (FO) B cells, which depend less on TLR activation and mostly on T helper stimulation. B-1 and MZ B cells are a part of the innate immunity, as they can rapidly produce antibody to TI antigen. Although the antibodies they produce are typically low affinity IgM, the antibodies are nonetheless important in combating bacterial pathogens, such as *Streptococcus pneumonia* (*21, 39*).

1.4 B cell receptors and signaling

Activation of the B cell begins with recognition of antigen by B cell receptors (BCRs). BCRs then self-aggregate for initiating signaling. The BCR comprises of a membrane immunoglobulin (mIg) that is non-covalently associated with a heterodimer of Igα (CD79a) and Igβ (CD79b). Igα and Igβ are held together by a disulfide bond. The mIg binds antigen and Igα/Igβ are transmembrane proteins responsible for signal transduction. Both Igα and Igβ contain immunoreceptor tyrosine-based activation motifs (ITAMs) in their cytoplasmic tails **(Fig. 1.4)**. When BCRs are cross-linked by antigen, they become associated with lipid rafts (cholesterol and sphingolipid enriched membrane microdomains) and come into contact with lipid raft-resident protein tyrosine kinases (PTKs), particularly Src-family kinases, including Lyn and Fyn, which phosphorylate the ITAMs in Igα/Igβ (*40-44*). ITAMs with both tyrosines phosphorylated create binding sites for the SH2 domain-
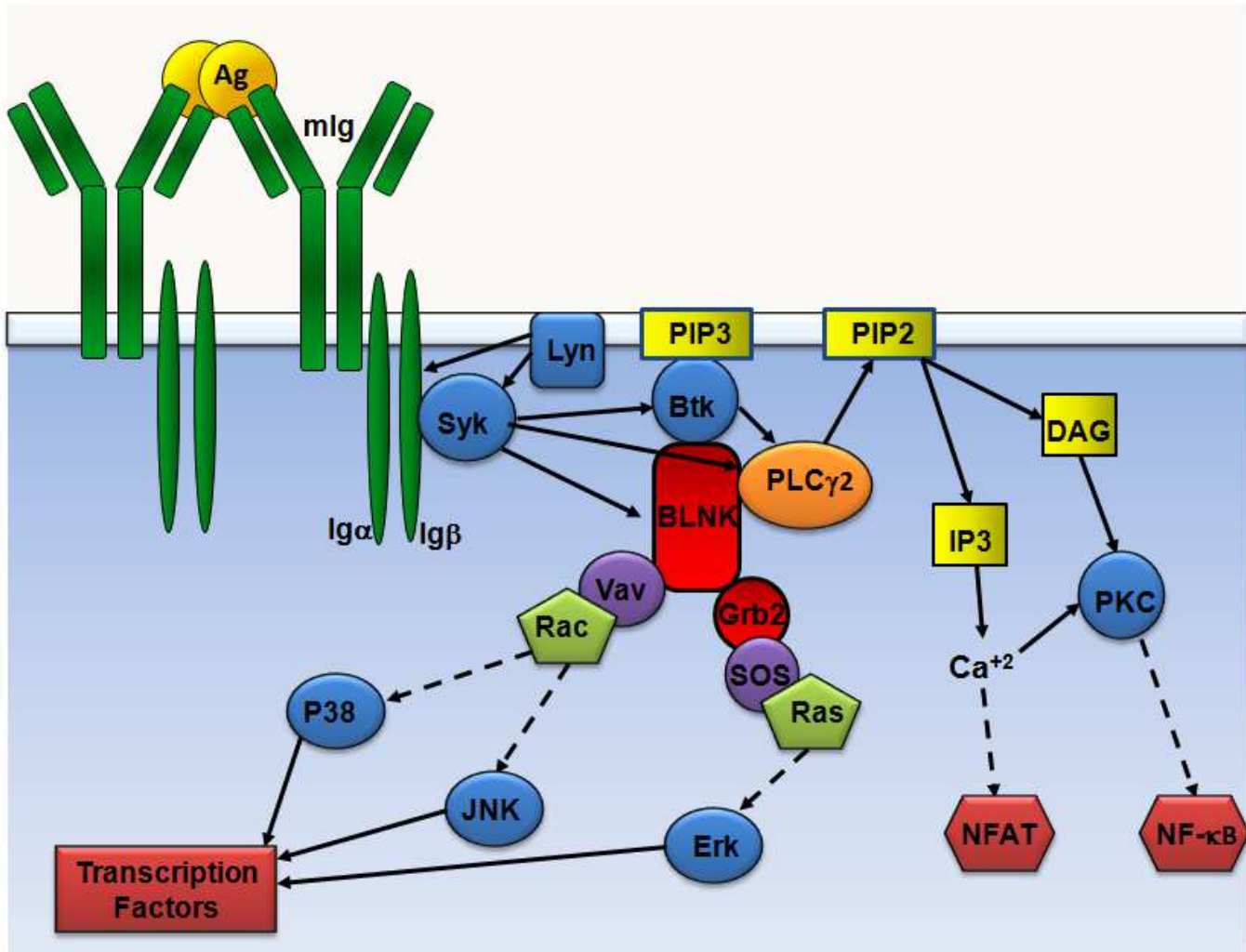
Fig. 1.4: BCR signaling pathways. BCRs aggregated by binding to their cognate antigen initiate signal transduction through the phosphorylation of the immunoreceptor tyrosine-based activation motifs (ITAM) in the cytoplasmic tails of Igα and Igβ. This creates docking sites for spleen tyrosine kinase (Syk), which is then activated by Lyn. Syk activates Bruton's tyrosine kinase (Btk) that associates with B cell linker protein (BLNK), an adaptor molecule that interacts with Vav, Grb2, and phospholipase-Cγ2 (PLCγ2). Vav activates Rac, leading to signaling through the Rac-MAPK pathway and phosphorylation of p38 and JNK. Grb2, an adaptor protein, binds SOS that associates with Ras to initiate the Ras-MAPK family pathway that leads to activation of Erk. PLCγ2 cleaves phosphatidylinositol-4,5-bisphosphate (PIP_2) into diacylglycerol (DAG) and inositol triphosphate (IP_3). IP_3 induces calcium release from the ER and eventual activation of the transcription factor, NFAT, and DAG and calcium activate protein kinase C (PKC), leading to activation of the transcription factor, NF-kB. The activated transcription factors from the signaling pathways promote expression of molecules involved in B cell development, survival, proliferation, and activation.

containing tyrosine kinase, spleen tyrosine kinase (Syk). Syk is vital in BCR-mediated signaling and activates many downstream signaling molecules in signalosomes at the plasma membrane. Syk phosphorylates Bruton's tyrosine kinase (Btk), which is recruited to the cell surface by binding to phosphatidylinositol-3,4,5-triphosphate (PIP_3) via its pleckstrin homology (PH) domain and B cell linker protein (BLNK). BLNK is a key adaptor molecule, serving as a scalfold for the signalosome. Phosphorylated by Syk, BLNK recruits many signaling molecules to signalosomes, such as phospholipase-Cγ2 (PLCγ2), Vav, a guanine nucleotide exchange factor of Rho-family GTPases, and Grb2, an adaptor protein. Grb2 binds SOS, which activates Ras to initiate the Ras-MAPK family pathway. PLCγ2, activated by Syk and Btk, cleave phosphatidylinositol-4,5-bisphosphate (PIP_2) into diacylglycerol (DAG) and inositol triphosphate (IP_3). IP_3 induces calcium release from the ER, and DAG and calcium activate protein kinase Cβ (PKCβ). Calcium flux leads to the activation of the transcription factor, NFAT, and PKCβ is involved in activating the transcription factor, NF-κB (*42, 45-47*). The transcription factors activated through the BCR-mediated signaling pathways promote expression of molecules required for B cell development, survival, proliferation, and activation (*48*).

BCR signaling events are positively or negatively controlled depending on the surface molecules recruited and activated within the vicinity of BCRs. CD19 is a stimulatory co-receptor complexed with the complement receptor CD21 and the tetraspanin protein CD81. CD19 is recruited to BCRs in response to antigenic stimulation and complement opsonized antigen. The CD19-CD21-CD81 complex lowers the threshold of B cell activation in response to complement coated pathogens

and also prolongs BCR-mediated signaling (*45, 49*). Complement coated pathogens cross-link the BCR with the complement receptor, CD21, bringing the CD19-CD21-CD81 complex in close proximity of the BCR, allowing CD19 to be phosphorylated and recruit phosphatidylinositol 3-kinase (PI3K) and Btk. CD19 recruitment of PI3K enhances calcium signaling by supplying the docking sites of Btk, PIP_3 (*45, 46*). CD19 is important in B cell activation and mediating B cell effector functions, as mice that lack CD19 have significant reductions in B cell proliferation after mitogen stimulation, germinal center reactions, and serum antibody levels (*50, 51*). FcγRIIB is an inhibitory co-receptor of the BCR. The FcγRIIB is cross-linked with the BCR when B cells encounter antigen-antibody immune complexes, which leads to phosphorylation of the immunoreceptor tyrosine-based inhibition motif (ITIM) its cytoplasmic tail by Lyn. The phosphorylated ITIM of the cytoplasmic tail recruits the SH2-domain containing inositol 5'-phosphatase 1 (SHIP1). SHIP1 dephosphorylates 5' phosphate groups of PIP_3, thus suppressing calcium signaling by preventing recruitment of Btk and PLCγ to the plasma membrane. FcγRIIB also recruits docking protein 1 (DOK-1) that down regulates Ras activation through recruitment of Ras GTPase-activating protein (GAP) (*43, 52, 53*). It has also been shown that FcγRIIB inhibits early B cell activation by preventing BCR clustering and thus reducing BCR-mediated signaling (*54*). The negative control on BCR signaling by FcγRIIB is essential for normal B cell activation and function, preventing unregulated, over-activation that can have detrimental outcomes. Functionally impaired FcγRIIB and its downstream SHIP-1 are associated with the development of autoimmune diseases, such as systemic lupus erythematosus (*55*).

1.5 BCR and actin dynamics in B-cell activation

In vivo, B cells encounter antigen either as soluble or membrane bound. The majority of antigen in B cell follicules is presented as the membrane bound form by antigen presenting cells (APCs), such as macrophages, follicular dendritic cells, dendritic cells, and marginal zone B cells, which bind oposonized antigens via complement and Fc receptors (*23, 56*). BCR and actin dynamics have been examined extensively using total internal reflection fluorescence microscopy (TIRFM). TIRFM allows for the B cell membrane to be imaged with high resolution at the interface of its attachment site to antigen presenting membranes, enabling detailed examination of BCR clustering, actin dynamics, and synapse formation.

BCR recognition of membrane bound antigen induces BCR clustering and B cell spreading over the target membrane. This increases the B cell contact area with the target membrane and accumulates more antigens for BCR activation. During spreading, the number of BCR clusters increase at the leading edges of the spreading B cell membrane. These BCR clusters signal and begin merging at the center of the B cell contact area. After reaching its maximal spreading, the B cell then contracts, reducing its contact area with the target membrane. BCR clusters reduce in signaling and coalesce to the center of the B cell contact area to form the central BCR cluster (immunological synapse) (*57-59*) **(Fig. 1.5)**.

B cell spreading, BCR clustering, and immunological synapse formation require actin. This has been demonstrated using actin polymerization inhibitors or stabilizers, which obliterate all of these events and ultimately suppresses BCR

signaling and B cell activation (*60-64*). Upon BCR engagement, there is a transient depolymerization of cortical actin, allowing for free later diffusion of surface BCRs (*60, 65, 66*). The BCRs cluster and begin signaling, leading to actin polymerization and co-localization with BCR clusters (*61, 67*). As BCR clustering and signaling continues, the B cell spreads over the target membrane and actin is seen to be distributed along the leading edges of the spreading B cell membrane. When maximal spreading is reached and the B cell membrane contracts, actin is seen as a ring around BCRs, contracting BCR clusters to form the immunological synapse **(Fig. 1.5)** (*61, 64*).

The initiation of BCR clustering induced by membrane bound antigen is suggested to be due to a conformational change in the Cμ4 domain of the mIgM ectodomain. This conformational change exposes an interface that mediates BCR-BCR interaction and induces BCR acquisition of lipid rafts (*68, 69*). This enables BCRs to interact with lipid raft associated Lyn and commence signaling (*44*). Early BCR signaling induces a transient depolymerization of the cortical actin cytoskeleton, which enhances BCR clustering and signaling activity.

The cortical actin cytoskeleton is attached to the plasma membrane through ezrin, a member of the Ezrin-Radixin-Moesin (ERM) family of proteins, which are actin binding proteins and attach F-actin to the plasma membrane by interacting with integral proteins. The cortical actin and ezrin networks have been shown to create diffusion boundaries on the plasma membrane, restricting the lateral movement of BCR clustering and lipid rafts in resting B cells. Upon interacting with membrane

Side View

Bottom View

A — Actin disassembly

spreading   signaling

B — Actin reassembly

spreading   signaling

Start of synapse

C

Decrease in signaling   Contraction and Synapse formation

D

A — Actin disassembly — Signaling initiation

BCR
Activated BCR
ERM
F-actin
Actin poly-merization sites

B — Actin reassembly — IRM — TIRFM

BCR/Actin polymerization sites

C — Cell spreading — Signaling amplification

BCR/F-actin

D — Cell Contraction — Signaling down regulation

BCR/F-actin

18

Fig. 1.5: BCR and actin dynamics in B cell activation.

(A) Upon BCR engagement to membrane bound antigen, the cortical actin depolymerizes to allow clustering of BCRs, which initiates signaling and (B) reassembly of actin to mediate spreading over the membrane to capture more antigen, increase BCR clusters, and amplify BCR signaling. (C) Reaching maximal spreading, BCR clusters begin to decrease in signaling and actin initiates movement of the BCR clusters towards the center of the cell contact area to form the synapse. (D) After maximal spreading, the cell membrane contracts in an actin dependent manner, decreasing the cell contact area and pulling remaining BCR clusters into the synapse.

Interference reflection microscopy (IRM) shows sites of close contact between a cell and substratum.

Total internal reflection fluorescence microscopy (TIRFM) is used to visualize fluorophores present in the near-membrane region of live or fixed cells.

Images from Liu et al. Plos Biology. 2013. e1001704. and Song et al. Immunological Reviews. 256:177-189.

bound antigen, surface BCRs increase lateral diffusion on the membrane surface. The disassembly of the cortical actin is induced by ezrin dephosphorylation, which causes the disassociation of ezrin from F-actin, consequently detaching the actin network from the plasma membrane. In addition, actin undergoes cofilin-dependent depolymerization (*60, 65, 66, 70*). Actin depolymerization also enables BCR clusters to interact with CD19 in lipid rafts (*66*). This interaction enhances BCR clustering, actin rearrangement, BCR signaling, and also B cell spreading on the antigen presenting membrane, which increases the number of BCRs engaging antigen and hence increases the BCR signaling amplification. The ability of the B cell to spread over target membranes and collect more antigen for increasing BCR activation is why membrane bound antigens have more potency than soluble antigen.

BCR clusters that associate with CD19 in lipid rafts recruit signaling molecules, including Syk, Btk, BLNK, Vav, and PLCγ2. The recruitment and function of these signaling molecules have been demonstrated to be necessary in forming signaling BCR clusters (microsignalosomes) that are involved in continuing B cell spreading. Syk, Btk, Vav, and PLCγ2 have been shown to be required for B cell spreading, as signaling induces and enhances actin rearrangement (*58, 63, 71*). Btk activation leads to the activation of Wiskott–Aldrich symptom protein (WASP), an actin nucleation promoting factor (*72, 73*). Btk activates WASP via inducing the phosphorylation of Vav, a guanine-nucleotide exchange factor (GEF) for the Rho GTPases, Rac and Cdc42, and increasing the production of PI-4,5-P$_2$ (*74*). As the B cell membrane continues spreading over the antigen presenting membrane, new BCR clusters form along the expanding edges of the cell. BCR clusters at the outer edges

of the B cell contact zone show the strongest signaling, visualized by phosphotyrosine staining. Signaling BCR clusters on the outer edge are then pulled toward the center of the cell, where BCR clusters coalesce into the central BCR cluster and reduce signaling activity. When the B cell has reached its maximal spreading on the antigen presenting membrane, the B cell contracts its membrane in an actin-dependent manner. This decreases the B cell contact area with the target membrane and the remaining BCR clusters on the outer edges are pulled toward the center of the cell contact area, where F-actin forms a ring like structure surrounding the synapse (*58, 59, 61, 63, 64*).

The growth of the BCR/antigen clusters and formation of the immunological synapse is actin-dependent. Treatment of B cells with Latrunculin A immediately after the B cell has spread over antigen presenting membrane, inhibits antigen accumulation, BCR cluster signaling and movement into the synapse (*60-62*). The inhibitory molecule, SH2-domain containing inositol 5' phosphatase 1 (SHIP1) has been shown to inhibit actin polymerization through suppression of Btk-dependent activation of WASP. Reducing the activation of WASP is necessary for B cell contraction, merging BCR clusters together into the synapse, and signaling attenuation (*73*). Previous work from my lab has demonstrated that Neuronal Wiskott–Aldrich syndrome protein (N-WASP) is required for B cell contraction and BCR signaling attenuation. Furthermore, N-WASP activation inhibits WASP activation (*75*). BCR central cluster formation and stability also require Rap GTPases and Rac, which both are known to be involved in actin cytoskeleton rearrangement (*76, 77*).

1.6 BCR-mediated antigen internalization and processing for presentation

B cells uptake, process and present antigen to acquire T cell help, which provides an essential signaling B cell activation and differentiation into memory B cells. While B cells can non-specifically internalize antigen via pinocytosis, BCRs render B cells the ability to capture specific antigen with high efficiency (*78, 79*). B cells are known to be able to internalize soluble antigens, membrane bound antigen, and immobilized antigens on non-internalizable surfaces. The efficiency of antigen internalization depends on BCR affinity for the antigen and the concentration or density of BCR binding epitope, as higher affinity and density induces greater levels of antigen internalization and therefore better presentation to T cells (*64, 79-81*). Soluble antigens are readily internalized with BCRs. A recent study has shown that B cells can extract antigen immobilized to a surface, and this process involves lysosomal secretion of hydrolases, which remove the antigen from non-internalizable surfaces (*82, 83*). It has also been shown that B cells can internalize antigen form immunological synapses formed with antigen presenting cells, where BCRs internalize antigen along with the target cell's membrane (*81, 84*). Previous studies using *in vitro* approaches indicate that internalization of antigen by BCRs is clathrin and dynamin-dependent.

The binding of antigen to BCRs at the surface induces the recruitment and accumulation of clathrin, leading to their confinement into clathrin coated pits and internalization into the B cell (*85, 86*). The internalization of antigen/BCR complexes

22

is controlled by the cytoplasmic domains of Igα and Igβ, both of which contain internalization motifs in their cytoplasmic domains (*87, 88*). Internalization signal domains are tyrosine-based motifs that are predicted to bind to endocytic adaptor proteins, specifically adaptor protein-2 (AP-2) (*88-90*). Upon binding to cytoplasmic signal domains of receptors, AP2 recruits clathrin to the plasma membrane. Along with curvature inducing proteins and other endocytic proteins, the clathrin-coated plasma membrane bends inward. The invagination of the plasma membrane forms a clathrin-coated pit at the membrane surface. Vesicle scission from the plasma membrane is then mediated through the GTPase, dynamin (*91*). For the internalization of membrane-associated antigen, non-muscle myosin II is required (*84*). Dynamin polymerizes at the neck of the invaginated vesicle and actomyosin provides the tension needed to pull the vesicle from the plasma membrane into the cytoplasm (*92*). Dynamin has been shown to be recruited to the B cell surface via Linker of activated B cells (LAB) and Actin-binding protein 1 (Abp1). B cells with dynamin mutants and Abp1 gene knockout have impaired BCR internalization (*91, 93*). There is a clathrin-independent and actin dependent mechanism reported for BCR internalization in B cells with clathrin heavy chain knockdown. This suggests that clathrin is not the only pathway for BCRs to internalize antigen (*86*).

The clathrin-dependent internalization of antigen/BCR complexes requires lipid rafts, BCR signaling, and actin rearrangement. Pharmacological reagents that disrupt lipid rafts by binding or extracting cholesterol from the plasma membrane

inhibit antigen/BCR internalization (*85, 86, 94*). This is likely because lipid rafts are required for forming BCR-signaling micodomains and it is within these microdomains that signaling and endocytic molecules are recruited and activated, including Vav, Bam32, clathrin, and dynamin (*85, 91, 93, 95*). Many of the signaling molecules known for internalization are involved in actin rearrangement, including Vav, Rac, Btk, Bam32, and Abp1. Actin rearrangement is necessary for antigen/BCR endocytosis, as disruption of actin dynamics by treatment with cytochalasin or latrunculin inhibits antigen/BCR internalization (*86, 96*). B cells deficient in Vav, a GTPase for Rac, or RNA interference of Vav inhibits Rac activation, which significantly reduces antigen/BCR internalization after BCR stimulation (*91, 97*). The recruitment and activation of Vav for internalization depends on the raft associated transmembrane protein, Linker of activated B cells (LAB), and Bruton's tyrosine kinase (Btk) (*91, 97, 98*). Through Vav, Btk activates WASP, consequently inducing actin remodeling (*72*). Two other signaling molecules involved in actin-mediated antigen/BCR internalization include Abp1 and B lymphocyte adaptor molecule of 32 kilodaltons (Bam32). Abp1is phosphorylated and recruited to the cell surface upon BCR engagement to antigen. Abp1 can interact with both F-actin and dynamin, potentially recruiting F-actin to dynamin-restricted clathrin-coated pits (*93*). Bam32 regulates BCR internalization by inducing actin polymerization. It is phosphorylated by the Src tyrosine kinases upon BCR ligation and co-localizes with BCRs, lipid rafts, clathrin, and actin (*95*).

After vesicle scission and entry into the cell, the antigen/BCR complexes are trafficked through endosomal compartments, first entry into early endosomes, then

24

into multivesicular-late endosomes enriched in newly synthesized MHCII (*99-101*) **(Fig. 1.6)**. The fast trafficking of antigen/BCR through endosomal compartments relies on BCR signaling, and cytoskeleton dynamics. Activation of Btk and recruitment of BLNK is necessary for trafficking and fusion of antigen/BCR containing vesicles with MHCII enriched late endosomes(*72, 99*). Both Igα and Igβ are also required for targeting antigen/BCR complexes to MHCII-rich compartments (*87, 88, 102-104*). Trafficking between the endosomal compartments requires actin reorganization, which is mediated through Syk upon BCR stimulation. Prevention of Syk activation has been shown to inhibit the actin rearrangement required for movement and fusion of antigen/BCR containing vesicles with MHCII-rich endosomes (*96, 105*). Along with actin, the actin-associated motor protein, myosin II, is necessary for converging antigen/BCR vesicles with MHCII-rich compartments. Myosin II has been shown to become activated during BCR engagement and thus similar to actin, relies on BCR-mediated signaling for trafficking antigen/BCR vesicles to MHCII enriched compartments (*106*). After reaching MHCII enriched late endosomes, antigen is fragmented by proteases and loaded onto MHCII molecules. Peptide-loaded MHC II complexes are then exported to the B cell surface for T cell recognition (*100*).

Antigen

MHCII

Clathrin

Lipid raft

Actin

BCR

1.

2.

3.

Golgi Apparatus

Invariant Chain

4.

5.

Cathepsin S

MHCII enriched compartment

6.

7.
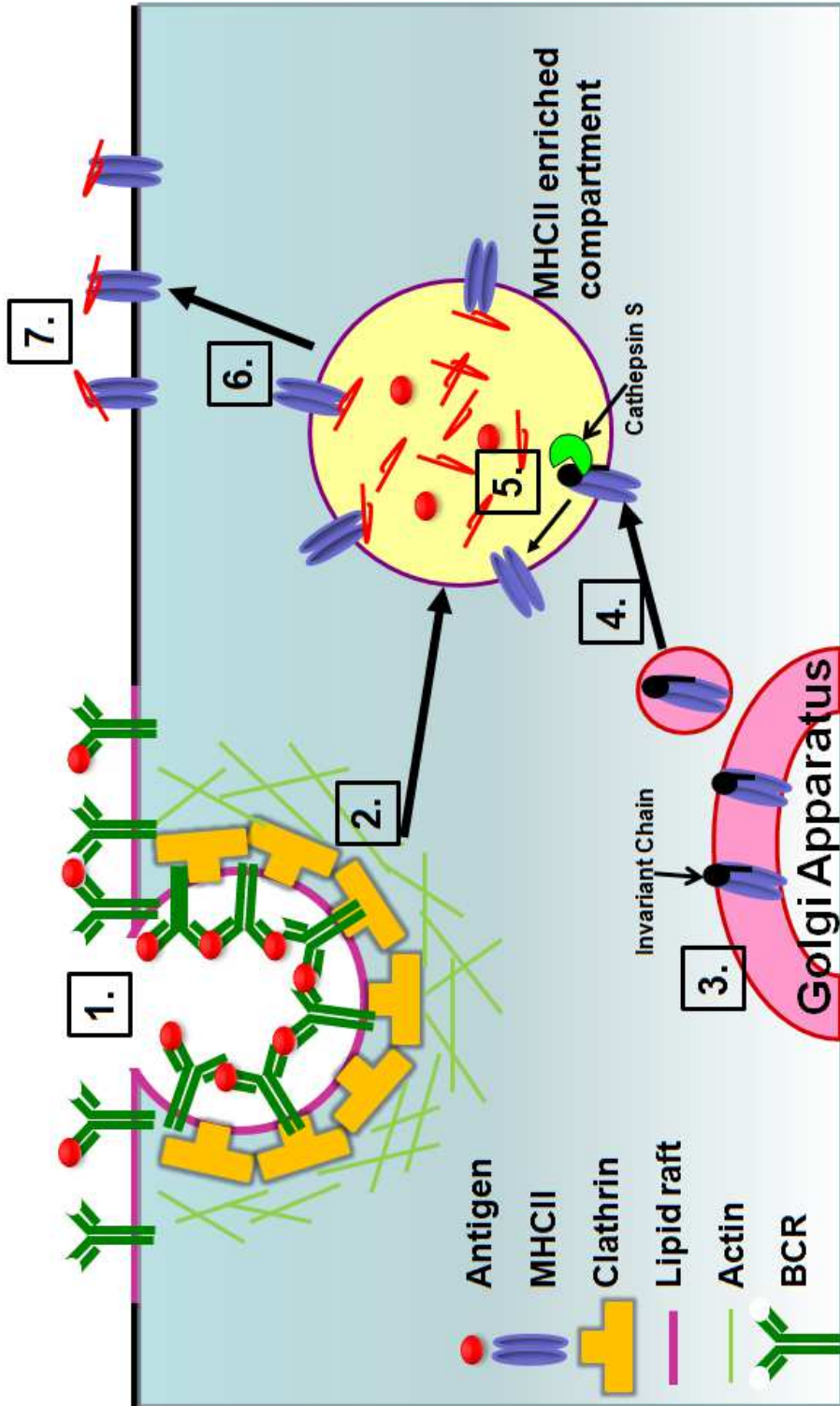
Fig. 1.6: Antigen internalization, processing, and presentation. (1) BCR engagement induces signaling in lipid rafts that leads to activation of molecules involved in actin reorganization. (2)Rearrangement of actin mediates internalization of the antigen/BCR complexes into clathrin coated vesicles that traffic and fuse with endosomes. (3) MHCII molecules are processed, sorted, and transported through the ER and Golgi and then (4) released in vesicles that move along microtubules to fuse with late endosomes. (5) Fusion of antigen/BCR containing endosomes with MHCII enriched late endosomes allows for degradation of the antigen by proteolytic enzymes and loading onto MHCII molecules. Before loading of antigen, MHCII molecules have their invariant chains catalytically removed by cathepsin S. (6) The antigen loaded MHCII molecules are then transported to the B cell surface via microtubules, (7) where they may then present the antigen and interact with T cells.

1.7 Relationship between properties of antigen and the B cell response

The properties of antigen determine the ability of antigen to stimulate B cells, thereby becoming a target of exploration for vaccine design. Increasing antigen avidity is a potential way to enhance its immunogenicity. Avidity measures the overall binding strength between an antigen and its cognate BCR, which depends on both the affinity and valency of the antigen (*58*). Affinity is the binding strength of an antibody to its cognate epitope, while valency is the number of identical epitopes on an antigen. Multivalent antigens containing multiple identical epitopes can cross-link multiple BCRs, which potentially overcomes low affinity interactions of BCRs with antigen (*48*). Avidity is key in determining how B cells respond to antigen, as high avidity induces greater activation of B cells, endocytosis of antigen, and thus enhanced presentation to T cells, which will in turn generate more help from T cells for antibody production and development into memory B cells (*64, 79-81*).

Antigens with higher affinity induce superior BCR signaling, B cell proliferation, antigen internalization and presentation to T cells, and antibody production compared to those with lower affinities. Studies using a model antigen, hen egg lysozyme (HEL), have demonstrated that the soluble wild type form of HEL induces higher levels of protein tyrosine phosphorylation, antigen internalization and presentation to T cells in MD4 transgenic mouse B cells that express HEL specific BCRs, compared to mutated and lower affinity HEL at the same concentration (*25, 80*). With membrane bound HEL, it was discovered that wild type HEL produces greater B cell spreading, antigen accumulation, and intracellular calcium responses compared to the same concentration of lower affinity mutated HEL (*64*). Similarly,

using different antigens in both soluble and membrane bound forms provoke enhanced B cell activation when having higher affinities to the BCRs. Soluble M13 phage peptide with high affinity for 3-83 mouse BCRs induce greater calcium mobilization, tyrosine phosphorylation, cell proliferation, and antibody production compared to M13 phage peptides with lower affinities (*107*). Constructed BCRs with varying affinities for 4-hyroxy-3-iodo-5-nitrophenyl (NIP), showed that B1-8 B cells with high affinity BCRs had a faster calcium response and more quickly clustered BCRs that grew more rapidly than low affinity BCRs at the same concentration of NIP on artificial membranes (*62*).

Corresponding to the effects of higher affinity, higher valency antigens also increase the activation of B cells and induce greater responses of proliferation, antibody production, antigen presentation and stimulation of T cells. BCR oligomerization by antigen cross-linking is required for activating BCR signaling, as F(ab')$_2$ but not Fab fragment of anti-Ig activates B cells (*108, 109*). Due to this, techniques have been designed to increase the valency of antigens to enhance the avidity of antigens and efficiencies of antigen to induce BCRs to cluster together and to elicit B cell responses. The methods that have been employed to increase antigen valency include aggregation, cross-linking, attachment to immobilized substrates, and conjugation to a carrier molecule. Increasing valency is a much more practical way to enhance the avidity of antigens than increasing affinity.

Aggregates of immunogens from pathogens and toxins have been and still are being a common practice for vaccines. Extensive studies have shown that the high

valency created from aggregation elicits enhanced antibody responses. Several methods are described for aggregation of antigens. One way is to heat the antigen until it denatures and clumps together. This strategy is an older method used with many pathogenic proteins, including cholera enterotoxin, which generated a better immunogen that induced high antibody production and increased resistance to lethal challenge in immunized mice (*110*). A much more common method used today is to produce protein immunogens with repetitive antigenic peptides using bioengineering methods. This type of technique is widely used for vaccine development and has been applied for designing vaccines against viruses such as dengue, hepatitis, and HIV (*111-113*), and bacterial toxins like botulinum neurotoxin and tetanus neurotoxin (*114*); all of which showed to elicit sufficient antibody responses that afforded protection against subsequent challenge in animal models.

Chemical cross-linkers have been used to couple multiple antigens together. Multivalent antigens produced through cross-linking show to induce greater BCR signaling, antigen internalization and presentation compared to monovalent antigen *in vitro*. Glutaraldehyde was used to cross-link HEL to produce dimeric, trimeric, and tertrameric HEL. These multivalent HELs were shown to elicit increased phosphotyrosine levels, larger and sustained calcium responses, and greater presentation and ability to activate T cells compared to monomeric HEL (*115*). Streptavidin has been used to cross-link biotinylated antigens, which caused the BCR cap to persist longer at the cell surface and increased and prolonged tyrosine phosphorylation of B cells (*116*).

Another way to increase antigen valency is to link the antigens to immobilized substrates, such as beads or to carrier molecules, including polysaccharides, synthetic polymers, and peptides. Covalent attachment of antigens, such as trinitrophenyl, or anti-Ig antibody to polyacrylamide or agarose beads increases their ability to stimulate B cells and induce proliferation (*108, 117, 118*). Similarly, conjugating anti-Ig antibodies to carrier molecules, such as polysaccharides, ficoll, or dextran, increases B cell proliferation, cell viability, antibody production, and expression of MHC II. Even low affinity anti-Ig antibodies were able to increase B cell activation conjugated to a carrier molecule (*109, 119, 120*). Other carrier molecules, like synthetic polymers or constructed peptides to which dinitrophenyl (DNP) or NIP were covalently linked to have shown to enhance BCR signaling, calcium flux, and antibody production, while their monovalent forms failed to elicit any B cell response at all (*121, 122*).

Besides affinity and valency, the concentration of an antigen is also a factor in determining B cell responses, where increasing the concentration of an antigen increases its ability to activate B cells. Anti-Ig and its dextran conjugate can induce B cell proliferation only at higher concentrations (*109*). Similarly, increasing the density of the model antigen, HEL, on the surface of sheep red blood cells increases antibody production in MD4 mice. Higher densities of HEL attached to artificial membranes induces increased MD4 B cell spreading, HEL accumulation, HEL internalization, and presentation (*25, 64*). Even mutated HELs that bind to the BCR on MD4 B cells in relatively low affinities can activate B cells when attached on membrane at high density (*64*). The enhanced B cell activation response to higher concentrations of

antigen likely results from increased avidity of antigen due to valency increases (*68, 115*).

The effects of the properties of membrane bound antigen on B cell activation has not been as extensively studied as soluble. The majority of antigen presented to B cells *in vivo* are membrane bound (*23*), hence it is important to study the role of properties of membrane bound antigen on B cell activation. Little is known about the effects of valency of membrane bound antigen on B cell activation. Additionally, actin plays a crucial role in B cell activation, it is particularly important for B cell spreading on target membranes, which corresponds to antigen accumulation and BCR signaling (*64*). However, the role of antigen properties of membrane bound antigen on actin dynamics is unknown.

1.8 Membrane damage and repair mechanisms

1.8.1 Cell membrane damage

Most types of cells are under threat of being damaged. For example, epithelial and muscle cells are continuously being exposed to strong mechanical forces. Muscle cells have their cell membranes torn during contraction and epithelial cells endure injuries such as scratches and punctures. These wounds of the plasma membrane are observed in epidermal cells, cardiac muscle, and skeletal muscle through the use of small tracer molecules, such as dextran or peroxidase, that enter the cell through the damaged site (*123*). Another form of mechanical stress on the plasma membrane of cells is the tension and pulling at cell-cell contacts, such as during cellular migration and formation of immunological synapses. It has been shown *in vitro* that moving

chick heart fibroblasts always leave cellular pieces of themselves behind at the detachment site of the cell's trailing edges (*124*). Antigen presenting cells (APCs) may have their membranes damaged at immunological synapses, where B cells and T cells extract antigens with the associated membrane of the APC. It has been demonstrated that during internalization of membrane bound antigen, B cells also internalize some of the target cell's surface membrane (*84*). T cells also acquire membrane and the cell surface molecules from APCs (*125*).

Bacterial toxins, viruses, venom, and even immunological factors, such as perforin and complement, can damage cell membranes by forming pores and causing leakiness in the cells. There are approximately thirty bacterial species that produce pore forming toxins, including hemolysin produced by *E.coli*, pneumolysin produced by *Streptococcus pneumoniae*, streptolysin O (SLO) produced by *Streptococcus pyogenes*, and protective antigen (PA) by *Bacillus anthracis*. Many of the pore-forming toxins are cholesterol dependent cytolysins, including the well studied SLO, which binds cholesterol and oligomerize to form pores in the plasma membrane. The diameter of SLO formed pores is about 30 nm in diameter (*126, 127*). Pore-forming toxins are imperative for microbial pathogenicity. Mutant bacterial strains that do not produce hemolysin or pneumolysin have reduced virulence. This is likely because the pores are required for microbial virulence factors to enter the host cells. For example, PA forms pores for toxin to enter the host cell (*128, 129*). The virulence of group A streptococcus (GAS) is enhanced by SLO, which aids in GAS escape from endosomal/lysosomal pathways following invasion of host cells (*130*). Viruses and venom are also known to damage plasma membranes. Hemolytic viruses, including

hemolytic paramyxoviruses (measles and mumps), respiratory syncytial virus, and parainfluenza viruses, induce permeability changes to the plasma membrane of host cells during entry into the cell, by fusion of an inherently leaky viral envelope with the host's plasma membrane (*131*). Bee venom, melittin, is also known to damage the plasma membrane of host cells and cause leakiness in cells (*131*).

Immunological factors, such as complement and perforin, form pores within membranes to damage and/or lyse target cells. Although these factors are usually directed towards killing pathogens, defects may arise, leading to damages to bystander cells. Complement factors can directly bind to bacterial surfaces or antibody-oposonized pathogen, consequently assembling pores (membrane attack complex created by C5b-C9) that lyse and kill pathogen. Unregulated complement binding leads to complications in the host itself. For example, age-related macular degeneration is caused by a defect in the complement factor H. The complement factor H functions to prevent complement deposition on host cells. When factor H is defective, C5b-C9 is seen deposited in vessels and membranes of eyes of patients (*132*). Perforin, released by cytotoxic T cells, forms pores in target cells to allow access of granzymes and induction of apoptosis. Using this mechanism, cytolytic T cells kill virus infected cells and tumor cells (*133, 134*). Perforin binds phosphorylcholine moieties and oligomerize to form 16 nm pores within the plasma membrane of target cell's membrane (*135*).

1.8.2 Cell membrane repair

After membrane damage, cells repair quickly to survive, resealing the injured site to prevent lethal toxicity by massive extracellular calcium entry or loss of cytoplasmic constituents. Cells repair their injured membrane within seconds to a minute (*123, 136*). For decades it has been known that extracellular calcium is required for membrane repair (*137-139*). The influx of calcium through the membrane wound triggers accumulation and exocytosis of intracellular vesicles to the site of injury (*139-141*). Using TIRFM, it was found that calcium-triggered exocytosis, primarily induces lysosomal fusion with the plasma membrane (*142*). Other studies support this, as lysosomal luminal domain marker, LAMP1, is seen on the cell surface of injured cells and lysosomal enzymes, β-Hexosaminidase (βHex) and acid sphingomyelinase (ASM), are detected in the extracellular media following damage (*143, 144*). Vesicle transport to the plasma membrane requires microtubules, as antibodies against kinesin inhibit fibroblast repair. In sea urchin eggs, vesicle transport by myosin is required and inhibitors of myosin prevent vesicle transport to the plasma membrane and decreased membrane repair (*140, 145*).

In order for the intracellular vesicles to fuse with the plasma membrane, the cortical actin cytoskeleton requires remodeling. In fact, fibroblasts, neurons, and epithelial cells have enhanced resealing with actin destabilizing treatment, conversely actin stabilizing treatment inhibits repair (*146*). Upon reaching the plasma membrane, intracellular vesicles fuse with the plasma membrane via calcium-dependent vesicle fusion proteins. Synaptotagmins (Syts) are transmembrane proteins with two C2 domains in their cytosolic region that, in response to calcium, bind to phospholipids

and soluble N-ethyl-maleimide-sensitive fusion protein attachment protein receptor (SNARE) complexes. SNARE proteins interact with each other to mediate intracellular membrane fusion events by providing the driving force to fuse lipid bilayers. In normal rat kidney epithelial cells (NRK), Syt VII regulates calcium triggered exocytosis of lysosomes. During calcium influx, Syt VII located on lysosomes interacts with the vesicle SNARE (v-SNARE), Vesicle-associated membrane protein 7 (VAMP-7). VAMP-7 then interacts with the target SNAREs (t-SNAREs), SNAP-23 and syntaxin-4, on the plasma membrane to promote lysosomal fusion with the plasma membrane (*144, 147-150*).

Other proteins are also implicated in fusing vesicles with the plasma membrane for repair. Dysferlin, a member of the ferlin family of proteins, have a similar protein structure to Syts and may play a role in vesicle fusion. Dysferlin is known to localize to wound sites during membrane repair and it has been demonstrated that dysferlin is required for muscle membrane repair, as dysferlin deficient mice do not repair their muscle membranes and show symptoms of muscular dystrophy (*151, 152*). Annexins have also been suggested to be involved in membrane fusion events for membrane repair. Annexins are known to mediate membrane fusion and annexin A1 has been shown to move to injured sites in a calcium dependent manner and bind to the plasma membrane in HeLa cells damaged by scrapping or laser injury. Further studies have demonstrated inhibition of membrane repair with the use of an annexin A1 function-blocking antibody and an annexin A1 mutant protein incapable of binding calcium (*152, 153*).

1.8.3 Membrane repair by exocytosis or endocytosis

Observation of vesicle exocytosis at wounded sites set the basis for the "patch hypothesis", which explains the repair of massive membrane wounds, such as the severing of neurons, whereby entry of calcium causes rapid and enormous vesicle-vesicle fusion events beneath the injury, forming a patch of vesicles that then fuses with the plasma membrane in a calcium dependent manner. In the case of massive wounding, it is believed that not just lysosomes are exocytosed to the plasma membrane, but all the available vesicles in the vicinity are used for the patch, including early and late endosomes (*146*). The patch hypothesis explains repair for very large injuries, however, cells damaged by small wounding, such as by pore forming complexes, repair quite differently.

Cells injured by small wounding exocytose lysosomes and then complete the repair of their membrane by removing the lesions. It has been suggested that pore forming complexes are removed from the plasma membrane by enodocytic and/or exocytic processes (*152*). Exocytosis of membrane lesions involves blebbing and shedding of vesicles containing the lesions, whereas endocytosis of the lesions leads to eventual lysosomal degradation of the pore forming complexes. Blebbing is thought to trap the damaged membrane, where it is then sealed off from the cell body to prevent further influx of calcium, which may lead to cell death (*152, 154*). This has been demonstrated in perforin treated HeLa and U937 (monocyte lymphoma cell line) cells, where small molecular dyes, such as trypan blue, were confined within blebs, indicating that the perforin induced pores were isolated from the rest of the cell by the blebs (*139*). Human embryonic kidney 293 (HEK 293) cells permeabilized with SLO

produce blebs and shed vesicles containing SLO pores. HEK 293 cells treated with SLO, translocates annexin A1 to the injured sites of calcium entry to form plugs at the neck of blebs and induce the shedding of vesicles containing SLO pores (*152, 154, 155*). Along with annexin A1, endosomal sorting complex required for transport (ESCRT) is suggested to be involved in creating blebs and regulating vesicle shedding during various types of wounding, including permeabilization by saponin, digitonin, SLO, and laser wounding. ESCRT is known to play a role in various membrane fission events. In membrane repair, ESCRT-III is recruited to wounded sites and accumulates at blebs and vesicle shedding sites, suggesting that repair depends on ESCRT-mediated shedding of damaged membrane portions (*156*). Although there is evidence of blebbing and vesicle shedding, there is also evidence that blebs are retracted back into the cell rather than being shed. Studies have revealed that plasma membrane blebs induced by SLO may completely retract back into the cell body during repair and even micrometer-sized blebs induced by laser wounding have been seen to retract (*138*).

Similar to shedding of vesicles, endocytosis promotes repair of membranes by removing the lesion from the plasma membrane. The endocytosis of membrane lesions has been intensely studied in epithelial and muscle cells. Using endocytosis markers, such as dextran and BSA, and visualizing the number of vesicles in TEM images, it was discovered that fibroblasts and myotubes treated with SLO or scratching have an increase in endocytosis compared to cells without wounding; and that in the case of SLO wounding, the SLO toxin proteins are internalized into vesicles and eventually degraded in lysosomes (*157-159*). Membrane damage by

complement has also been demonstrated to involve internalization of the injured site, where C5b-9 complexes are seen to be internalized by clathrin-coated pits and transported to multivescular bodies (*160*).

The increase in internalization from membrane wounding is necessary for membrane repair and is mediated by acid sphingomyelinase (ASM), which is released from lysosomes during fusion with the plasma membrane and is detected in the surrounding media of cells treated with SLO **(Fig.1.8)**. Treatment with the ASM inhibitor, desipramine (DPA), or using siRNA to silence ASM inhibits endocytosis and membrane repair in HeLa cells. Also Niemann-Pick type A cells, which are deficient in ASM, are defective in endocytosis and membrane repair, however, are rescued with extracellular addition of recombinant human ASM (*143*). The role of ASM in membrane internalization is likely due to its action on the outer leaflet of the plasma membrane to generate ceramide from sphingomyelin. Ceramide is smaller than other plasma membrane lipids and therefore microdomains of ceramide are pushed inward, forming invaginations; also ceramide is known to interact with lipid rafts, which may induce internalization (*138, 143, 158*). The endocytic molecules required for wound repair-mediated internalization includes cholesterol and caveolae, indicating that the internalization for membrane repair is lipid raft-dependent (*161*). Cholesterol depletion by MβCD treatment or RNAi-mediated silencing of Cav1 expression inhibits endocytosis and wound repair (*157, 158*). In fact, it has been shown in SLO treated epithelial and muscle cells that SLO is internalized into caveolae vesicles and that injury by scratching increases the number of caveolae vesicles at the wound site (*158*).
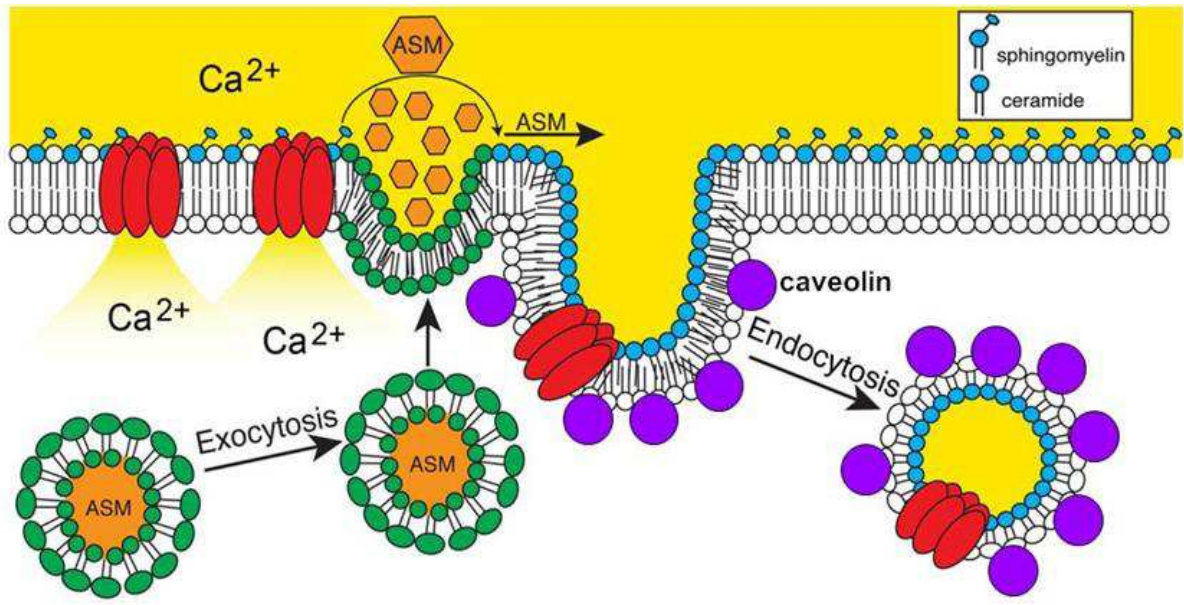
Fig.1.8. Membrane repair of SLO pores via endocytosis. SLO pores (red) allow

entry of calcium into the cell. This induces exocytosis of lysosomes (green) and

fusion of the lysosome with the plasma membrane. Exocytosis of lysosomes releases

acid sphingomyelinase (ASM), which acts on sphingomyelin to generate ceramide.

Ceramide microdomains are invaginated and along with caveolin, mediate

endocytosis of the SLO pores.

Image modified from Tam,C. et al. 2010. JCB. Vol.189. 1027-1038

The last step for endocytosis is scission from the plasma membrane, which typically involves dynamin and actin, however, for epithelial cells damaged with SLO, dynamin and actin are not required for endocytosis and membrane repair. This was demonstrated using a dynamin mutant expressed in NRK cells, which had no effect on internalization and membrane repair when permeabilized by SLO. As for actin, disruption of the cytoskeleton by cytochalasin D actually enhances endocytosis and membrane repair in cells treated with SLO or injured by scratching, indicating that actin polymerization is not needed for endocytosis and repair (*157, 158*). Although damage by SLO is dynamin independent, other studies have revealed that damage by perforin induces a clathrin and dynamin dependent internalization and knockdowns of clathrin heavy chains and dynamin 2 inhibits endocytosis of perforin and prevents membrane repair (*139, 162*).

Overall, for efficient membrane repair, there must be a calcium-triggered exocytosis of intracellular vesicles and removal of the membrane lesion. It has been suggested that the mechanism for membrane lesion removal depends on the type of cell and wounding, where one type of cell may repair differently from another type and this may contrast depending on the size and variety of wounding. Therefore, it may be more efficient for some cells to bud and exocytose membrane lesions, while for other cells, endocytosis works better for membrane repair (*156*). Endocytosis for repair requires caveolin, however, there are cell types that do not express caveolin, such as lymphocytes. If and how lymphocytes repair is unknown; their repairing may reveal alternate mechanisms in membrane repair.

1.9 Role of lipid rafts in B cell activation

Lipid rafts are dynamic structures of the outer leaflet of the plasma membrane and consist of cholesterol and sphingolipids. These structures are less fluid than the surrounding lipids and therefore serve as platforms for organizing and confining protein receptors for creating signaling domains (*161*). BCR signaling and internalization is known to require lipid rafts. Stimulated B cells show co-localization of cholesterol with BCR clusters and evaluation of isolated lipid rafts from activated B cells has shown that BCRs are immediately translocated to lipid rafts upon BCR stimulation, where interaction with lipid raft resident, Lyn, leads to their activation (*163, 164*). Fluorescence resonance energy transfer (FRET) studies have also demonstrated that engaged BCRs move into lipid rafts to associate with Lyn and propagate signaling. Additionally, FRET has shown that BCR association with lipid rafts is prolonged by cross-linking with the co-receptor CD19/CD21; indicating interaction between BCRs with co-receptors stabilizes the signaling domain (*49*). Following BCR entry into lipid rafts and phosphorylation, other signaling molecules are recruited to the rafts and activated, including Syk, Btk, Vav, and PLCγ2 (*165*). This signaling then leads to BCR endocytosis, where it has been demonstrated that lipid rafts are important for retaining the kinases and signaling molecules needed to recruit and activate endocytic molecules (*85, 93, 164*).

The importance of lipid rafts for BCR signaling and internalization is observed with Epstein-Barr virus (EBV) infections. EBV inhibits BCR signaling and internalization by occupying lipid rafts through latent membrane protein 2A

(LMP2A). LMP2A has a binding site for Lyn, which enables it to reside within lipid rafts and exclude BCRs. Latently infected B cells have LMP2A present in their lipid rafts, which prevents BCRs from entering the lipid rafts to signal and internalize, however, this allows for the cell to stay alive so that the virus may persist (*165, 166*).

Lipid rafts may be disrupted by pore forming agents, antibiotics, and cholesterol depleting reagents. All of these reagents typically disrupt lipid rafts by interacting with cholesterol. Toxins like SLO bind cholesterol and create pores in cell membranes; antibiotics such as filipin and nystatin bind to and sequester cholesterol; and methyl-β-cyclodextrin (MβDC) is used to remove cholesterol from membranes (*161*). The role of filipin, nystatin, and MβDC on B cell activation have been examined, however, the role of SLO damage on BCR activation is not known. Disruption of lipid rafts by filipin inhibits calcium flux and activation of the signaling molecule, PLCγ2, however, treatment with MβDC enhances calcium flux from intracellular stores (*167-169*). MβDC and filipin both inhibit BCR movement into lipid rafts, yet these reagents induce tyrosine phosphorylation without BCR stimulation and release Lyn from lipid rafts (*168*). Additionally, nystatin inhibits BCR internalization (*86*). Taken together these studies demonstrate that lipid rafts are vital for regulating proper BCR signaling and internalization. Without lipid rafts to serve as platforms for BCR signaling, there is uncontrolled signaling, possibly because Lyn and other raft resident molecules are no longer retained in lipid rafts, allowing random activation of molecules.

Disruptions of lipid rafts may also occur through plasma membrane damage and wound repair. B cells may have their membranes damaged by bacterial toxins or mechanically injured during cell-cell interactions. It has been shown that activated B cells may transfer portions of their plasma membrane along with BCRs to bystander B cells through close cell-cell contact (*170*). Also B cells serve as APCs and T cells and B cells are able to remove membrane from APCs (*84, 125*). Epithelial and muscle cells repair damaged membranes by lipid raft endocytosis induced by ASM release from exocytosed lysosomes. For B cells, lipid raft internalization would reduce the availability of raft platforms for signaling, which in return could decrease signaling required for BCR internalization. Additionally, ASM release may alter lipid raft composition by decreasing sphingomyelin and increasing ceramide in the plasma membrane, which may also affect BCR signaling.

1.10 Significance and aims

B cells face membrane damage by toxins and mechanical stresses endured during migration and cell-cell contacts with other cells. The first part of this dissertation looks at the membrane repair mechanism of B cells and how this repair mechanism may affect the B cell's response to antigenic stimulation. It is of interest to discover the membrane repair mechanism of B cells. In epithelial and muscle cells, caveolin is necessary for the endocytosis of damaged membrane to promote repair. As B cells do not express caveolae, their mechanism of repair may reveal an alternate route of membrane repair. Further, determining the effects of membrane repair on B cell

activation may reveal how toxins or mechanical stress affect B cell signaling and what this means for the immunological functions of the repaired B cell.

B cells are imperative for efficient immune responses to pathogens. They produce antibodies required for elimination of microbes and toxins. Vaccination relies on the appropriate stimulation to induce antibody production and development of memory B cells. In order to do this, the response of B cells to various forms and properties of antigen must be studied. Antigens in the form of membrane bound are more potent then soluble, however, the role of the properties of membrane bound antigen on B cell activation are not well understood. The second part of this dissertation addresses the effects of antigenic properties on a B cell's response to membrane bound antigen. A novel membrane bound antigen system was employed to accurately determine the role of antigen density and valency on the early events of B cell activation, including actin dynamics, B cell spreading, BCR aggregation, and BCR signaling.

1.10.1. Aim 1. The mechanism of B cell membrane repair and the role of membrane repair on B cell activation

This aim was designed to determine the mechanism of repair of caveolin deficient primary cells and to also examine the effects of membrane repair on B cell activation. To do this, WT Bl6 mouse B cells were damaged with SLO and examined for lysosomal exocytosis and plasma membrane endocytosis; for examining effects on B

cell activation, SLO treated B cells stimulated with antigen were examined for changes in tyrosine phosphorylation (pY), BCR capping, and BCR internalization.

1.10.2 Aim 2. The role of different properties of membrane bound antigen on early B cell activation

This aim was designed to examine how density and valency of membrane bound antigen influences B cell activation. A novel antigen tethered membrane system was developed to present optimally oriented antigen to BCRs. The role of antigen density on actin dynamics, B cell spreading, and BCR aggregation was examined using live imaging of Lifeact primary mouse B cells. For studying effects of valency on B cell activation, B cell spreading, BCR aggregation, and BCR signaling of WT primary B cells were compared between stimulation with either monovalent or bivalent membrane bound antigen.

Chapter 2: Lipid raft-dependent plasma membrane repair interferes with the activation of B-lymphocytes

2.1 Abstract

Cells rapidly repair plasma membrane (PM) damage by a process requiring Ca^{2+}-dependent lysosome exocytosis. Acid sphingomyelinase (ASM) released from lysosomes induces endocytosis of injured membrane through caveolae, membrane invaginations from lipid rafts. How lymphocytes, lacking any known form of caveolin, repair membrane injury is unknown. Here we show that B-lymphocytes repair PM wounds in a Ca^{2+}-dependent manner. Wounding induces surface exposure of the lysosomal protein LIMP2, ASM release, and endocytosis of the lipid-raft marker cholera toxin and dextran. Resealing is reduced by ASM inhibitors and ASM deficiency, and enhanced by extracellular exposure to ASM. B-cell activation via B-cell receptors (BCRs), a process involving lipid rafts, interferes with PM repair. Conversely, wounding inhibits BCR signaling and internalization by disrupting BCR co-clustering with lipid rafts, while inducing endocytosis and formation of tubular-shaped vesicles. Plasma membrane repair and B-cell activation may interfere with one another due to competition for lipid rafts, revealing how frequent membrane injury and repair can impair B-lymphocyte-mediated immune responses.

2.2 Introduction

Plasma membrane wounding can occur during the lifetime of most cells, either by external mechanical forces generated by neighboring or pathogenic cells (*171, 172*), pore-forming proteins secreted by pathogens (*128*), or even internal mechanical forces generated by cell contraction and migration (*124, 173, 174*). Eukaryotic cells can rapidly repair wounds in the plasma membrane, thus avoiding lethal events triggered by massive Ca^{2+} influx and cytosol depletion (*136*). The importance of plasma membrane repair has been demonstrated particularly in muscle fibers, which are frequently injured during contraction. Failure in resealing of the muscle sarcolemma has been identified as a cause of muscular dystrophy (*151*).

Early studies discovered that the rapid membrane repair mechanism is triggered by Ca^{2+} influx through wounds in the plasma membrane (*138, 140*). The Ca^{2+} flux induces lysosome exocytosis, which exposes lumenal lysosomal membrane proteins on the cell surface and releases lysosomal contents (*142-144*). Exposure of the lumenal domain of lysosomal membrane proteins, such as the lysosomal-associated membrane protein 1 (LAMP-1) and the lysosomal synaptotagmin isoform Syt VII are detected a few seconds after wounding, reflecting the Ca^{2+}-dependent fusion of lysosomes with the plasma membrane (*144*). Exocytosed lysosomes were initially suggested to provide the membrane needed for wound sealing, working like a patch to repair open wounds. More recently, it became evident that lysosomal exocytosis is followed by a rapid form of endocytosis that can remove lesions from the plasma membrane (*143, 157, 159*).

Recent studies revealed that plasma membrane wounding by the pore-forming streptolysin-O (SLO) or by mechanical forces triggers endocytosis of caveolae (*158*), plasma membrane invaginations that are preferentially localized in lipid rafts of the plasma membrane (*175*). Evidence supporting this finding includes the co-localization of caveolin and SLO in <80 nm intracellular vesicles, accumulation of budding vesicles with morphological characteristics of caveolae (<80 nm diameter budding vesicles that are flask shaped and lack a dense coat) (*176*) at wound sites in cell lines and primary muscle fibers (*158*), and inhibitory effects of caveolin knockdown on plasma membrane repair (*158, 177*). The involvement of caveolae in the endocytosis-mediated plasma membrane repair process is also consistent with the severe muscle pathology that is observed in mice deficient in caveolin and other caveolae-associated proteins such as cavin (*178, 179*).

Caveolin-mediated endocytosis of injured plasma membrane was shown to be induced by acid sphingomyelinase (ASM) (*143*). Via Ca^{2+}-dependent lysosome exocytosis, ASM is released to the outer leaflet of the plasma membrane, where it generates ceramide from sphingomyelin (*180, 181*). Ceramide was proposed to induce caveolae-mediated endocytosis by facilitating the recruitment of caveolin to lipid rafts and by creating membrane curvature (*138*). The importance of ASM in plasma membrane repair has been demonstrated by the finding that extracellular exposure to ASM restores membrane resealing even in the absence of extracellular Ca^{2+} (*182*). Moreover, inhibition or depletion of ASM reduces wounding-induced endocytosis and plasma membrane resealing (*143*). Thus, increasing evidence supports a closely coordinated process of Ca^{2+}-induced lysosome exocytosis and

49

caveolin-mediated endocytosis as an important mechanism for plasma membrane repair. However, it is not known if this form of plasma membrane repair is universal, or if different cell types that express distinct regulatory proteins have distinct mechanisms to reseal after injury.

Lymphocytes are unique, non-adherent cells that attach to substrates and migrate in response to stimuli (*183, 184*). After maturation in the bone marrow or thymus, lymphocytes circulate through the body in order to survey for the presence of pathogenic substances. In response to pathogenic signals, lymphocytes extravasate, migrating through endothelial cells to reach infected sites. In addition, lymphocytes migrate through dense and well-organized lymphoid tissues, the spleen and lymph nodes, where they recognize antigen presented by antigen-presenting cells and mount responses (*23, 185*). B-cells extract antigen from antigen-presenting cells, internalize and process antigen in late endosomes, and present antigen for T cell recognition (*185, 186*). Through these processes, lymphocytes face ample possibilities of wounding their plasma membrane, such as encountering pore-forming bacterial toxins or complement proteins in infection sites, and particularly, mechanical damage from T cells during antigen presentation, where it has been shown that T cells are able to remove membrane from antigen presenting B cells (*187*) . However, unlike epithelial cells, fibroblasts and myofibers which have been well studied regarding their plasma membrane repair ability, nothing is known about how lymphocytes cope with injury. Different from those well studied cells, lymphocytes do not contain detectable levels of known isoforms of caveolin (*188*), even though B-cells have been reported to express caveolin during differentiation *in vitro* into plasma cells (*189*). Despite the

50

apparent lack of caveolin, the organization of signalosomes and the endocytotic machinery in lymphocytes is known to be highly dependent on lipid rafts (*49, 85, 93, 164, 165*), plasma membrane domains where caveolin normally resides (*175*). B-cell activation is induced by the B-cell antigen receptor (BCR). Upon antigen binding, surface BCRs oligomerize into microclusters in lipid rafts, where the cytoplasmic tails of the receptor are phosphorylated by raft-resident Src kinases in the inner leaflet of the plasma membrane. The phosphorylated cytoplasmic domains of the BCR recruit and activate downstream signaling molecules, propagating signaling cascades (*42, 165*). In addition, lipid rafts are also essential for BCR internalization, by which B-cells capture, uptake, and transport specific antigen for processing and presentation (*86, 94*). We have demonstrated that lipid rafts act to couple BCR signaling and endocytosis by recruiting endocytotic machinery proteins to the vicinity of signalosomes for activation (*72, 85, 93*). The unique properties of lymphocytes, the importance of lipid rafts in their functional properties, and the fact that injury is likely to occur as these cells migrate *in vivo*, raise the question of whether and how lymphocytes repair plasma membrane wounds.

In this study, we show that primary B-lymphocytes can effectively repair membrane wounds in the absence of caveolin. The membrane repair process depends on Ca^{2+} influx, Ca^{2+}-induced lysosome secretion, and lipid raft-mediated endocytosis. Our results suggest that the plasma membrane repair mechanism inhibits the signaling and antigen internalization functions of the BCR by interfering with access of the receptor to lipid rafts.

2.3 Materials and Methods

Mice and B-cell isolation

Splenic B-cells were isolated from wild type (C57BL/6) (Jackson Laboratories) and ASM KO mice (C57BL/6 background, kindly provided by Dr. Edward Schuchman at Mount Sinai School of Medicine and Dr. Silvia Muro at University of Maryland). Mononuclear cells were enriched by Ficoll density-gradient centrifugation (Sigma-Aldrich). T cells were removed by anti-Thy1.2 mAb (BD Biosciences) and guinea pig complement (Rockland Immunochemicals), and monocytes and dendritic cells by panning. All procedures involving mice were approved by the Institutional Animal Care and Usage Committee of the University of Maryland.

Plasma membrane repair assays

Freshly isolated B-cells were incubated with SLO in either Ca^{2+}-containing ($+Ca^{2+}$) or Ca^{2+}-free DMEM ($-Ca^{2+}$) for 5 min at 4°C to allow binding. Cells were then warmed to 37°C for 5 min, immediately transferred to 4ºC and stained with the membrane impermeant dye propidium iodide (PI). Cells were analyzed using a BD FACS Canto II flow cytometer and Flowjo software (Tree Star, Inc.). The percentage of cells repaired in the presence of Ca^{2+} ($+Ca^{2+}$) was determined by [%PI positive ($-Ca^{2+}$) - %PI positive ($+Ca^{2+}$)] x 100/%PI positive ($-Ca^{2+}$). To determine the effect of

sphingomyelinase (SM) on plasma membrane repair, SM from *Bacillus cereus* (Sigma) (50 µM) was included in the medium during the 37°C incubation.

To analyze the effect of BCR cross-linking on the efficacy of plasma membrane repair, surface BCR were labeled with fluorescently conjugated Fab fragments of goat anti-mouse IgM (10 µg/ml, -XL) or F(ab)$_2$ fragment of goat anti-mouse IgM (10 µg/ml, +XL) (Jackson Immunoresearch) at 4°C. After washing off unbound antibodies, the cells were then treated with SLO (200 ng/ml) and analyzed as described above.

Analyses of lysosomal exocytosis

B-cells were incubated with SLO (200 ng/ml) for 5 min at 4°C and then 37°C for 5 min. Cells were transferred to 4°C, stained with rabbit anti-LIMP2 antibody (Sigma) and Cy3-Fab-goat anti-mouse IgM+G for the BCR (Jackson Immunoresearch) at 4°C without permeabilization, and fixed with 4% paraformaldehyde. Cells were then analyzed by flow cytometry (BD FACS Canto II) and confocal fluorescence microscopy (Zeiss LSM 710; Carl Zeiss Microscopy, Thornwood, NY).

Acid sphingomyelinase secretion and inhibition

The secretion of ASM was analyzed by measuring the enzymatic activity of ASM in supernatants. Cells were treated with SLO (200 ng/ml) for 5 min at 4°C, warmed to 37°C for 15 sec, and immediately cooled on ice. The supernatants were collected by centrifugation, and protease inhibitors added. The enzymatic activity of ASM was

determined using an Amplex Red sphingomyelinase assay kit (Molecular Probes), based on manufacturer-provided protocols. Supernatants were also concentrated using centrifugal filtration (Millipore) and analyzed by Western blotting, using rabbit anti-ASM antibody (Abcam). To inhibit ASM, B-cells were pre-incubated with 30 µM of Desipramine (DPA) (Sigma) for 30 min at 37°C. Cells were then treated with SLO as described above.

Dextran endocytosis

B-cells were incubated with SLO (200 ng/ml) for 5 min at 4°C, in the presence of 2.5 mg/ml of 10 kDa lysine fixable Texas Red-dextan (Invitrogen). The cells were warmed to 37°C for 5 min, washed to remove dextran that was not associated with cells, and fixed. The cells were then stained with Alexa Fluor 488 goat anti-mouse IgG (Invitrogen) to mark surface BCRs and imaged by confocal fluorescence microscopy (Zeiss LSM 710; Carl Zeiss Microscopy, Thornwood, NY). For SM treatment, 50 µM of sphingomyelinase (Sigma) was added prior to the 37°C incubation.

BCR capping and activation

B-cells were labeled and/or activated with Cy3-Fab-goat-anti-mouse IgG (Jackson Immunoresearch) or AF546-F(ab)$_2$-goat-anti-mouse IgG (Invitrogen) at 4°C for 30 min, followed by AF488-CTB (Invitrogen) for 10 min. Cells were washed to remove unbound antibody and CTB, and then incubated with SLO (200 ng/ml) for 5 min at 4°C, warmed to 37°C for 5 min, and fixed with 4% paraformaldehyde. Cells were

imaged using a confocal microscope (Zeiss LSM 710; Carl Zeiss Microscopy, Thornwood, NY). For each condition, more than 80 cells were analyzed for each of four independent experiments.

For phosphotyrosine staining, B-cells treated as described above were permeabilized with 0.05% saponin and incubated with anti-phosphotyrosine mAb 4G10 (Millipore), followed by AF488 goat anti-mouse IgG_{2b} secondary antibody (Invitrogen). Cells were analyzed by confocal microscopy (Zeiss LSM 710; Carl Zeiss Microscopy, Thornwood, NY) and flow cytometry (BD FACS Canto II).

Flow cytometry analysis of BCR endocytosis

B-cells were incubated at 4°C with biotinylated F(ab')$_2$ fragments of goat-anti-mouse IgM+IgG (Jackson Immunoresearch) for 30 min. The cells were then incubated with SLO (200 ng/ml) at 4°C for 5 min, warmed to 37°C and fixed at indicated times. The samples were labeled with PE-streptavidin (BD Bioscience) and analyzed using flow cytometry (BD FACS Canto II).

Live cell imaging of BCR/CTB internalization

The surface BCRs were labeled and activated with AF546-F(ab')$_2$-goat anti-mouse IgG and lipid rafts by AF488-CTB (Invitrogen). After 5 min incubation with SLO (200 ng/ml) at 4°C, time lapse images were acquired at 37°C using a Leica SP5 confocal microscope. Kymographs were constructed using Andor IQ to track the internalization of BCR and CTB over time. The co-localization rate of internalized

BCRs with CTB at 10 min was determined using Leica LAS AF Lite imaging software. For each condition, more than eight cells were analyzed for each of three independent experiments.

Immunoelectron microscopy analysis of BCR and CTB distribution

The surface BCRs were labeled with 18 nm gold-conjugated goat anti-mouse IgG+IgM (Jackson Immunoresearch) and lipid rafts by biotinylated CTB (Invitrogen) followed by 10 nm gold-conjugated streptavidin (Sigma) at 4°C. Cells were then incubated with SLO (200 ng/ml) for 5 min at 4°C, warmed to 37°C for 1 and 5 min, and fixed with 2% glutaraldehyde. The cells were post-fixed by 2% osmium tetroxide, embedded in Spurr's replacement embedding medium (Electron Microscopy Sciences), and imaged by transmission EM (Zeiss EM 10CA). For each condition, ≥18 individual cells were analyzed for each of two independent experiments.

Statistical analysis

Statistical analysis was performed by the two-tailed Student's *t* test using Prism software (GraphPad Software, San Diego, CA).

2.4 Results

Primary mouse B-cells repair plasma membrane wounds in a Ca^{2+}-dependent manner

In order to determine whether B-cells are capable of repairing wounds in the plasma membrane, primary B-cells, freshly isolated from mouse spleens, were incubated with increasing concentrations of SLO (0-400 ng/ml) with or without Ca^{2+} in the culture medium. SLO is a bacterial toxin that binds to cholesterol in membranes, oligomerizes and forms pores, thus permeabilizing the plasma membrane. SLO may bind to cholesterol in membranes in the presence or absence of Ca^{2+} (*157*). Cell nuclei were stained with the membrane impermeant dye propidium iodide (PI) 5 min post SLO exposure. B-cells that were injured by SLO and did not repair became PI positive (PI+). The percentage of PI^+ cells was quantified by flow cytometry. In the absence of SLO, a small percentage of cells were PI^+ in the presence or absence of extracellular Ca^{2+} **(Fig. 2.1 A)**, as primary mouse B-cells can undergo spontaneous apoptosis gradually in the absence of stimuli (*190, 191*). In the absence of Ca^{2+}, the percentage of PI^+ B-cells increased with the concentration of SLO, and reached a plateau when the concentration reached 200 ng/ml **(Fig. 2.1, A-B)**. In the presence of Ca^{2+}, the percentages of SLO-treated PI^+ cells were significantly decreased, compared to B-cells treated with SLO in the absence of Ca^{2+}. In the presence of Ca^{2+} the percentage of PI^+ cells was reduced from ~70% to ~30% when the SLO concentration was 200 ng/ml **(Fig. 2.1, A-B)**, indicating that almost half of SLO damaged cells were repaired under these conditions **(Fig. 2.1, B-C).** As expected, even in the presence of
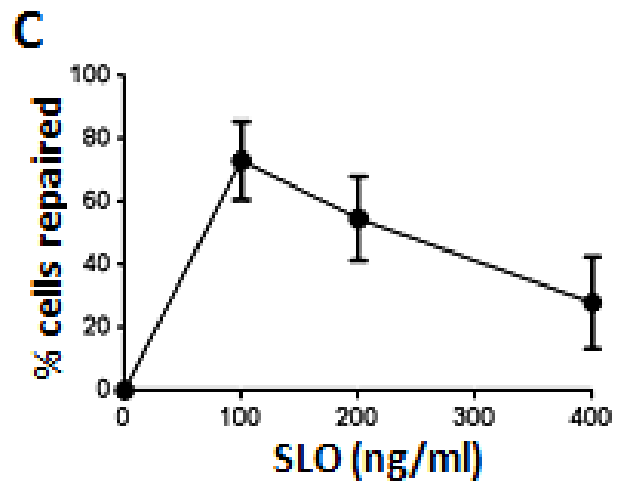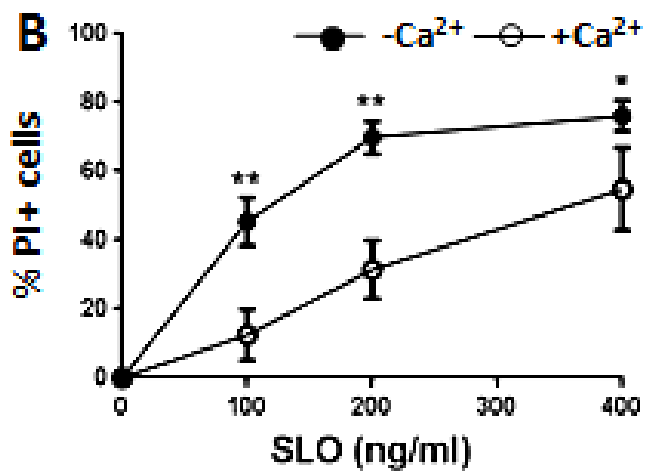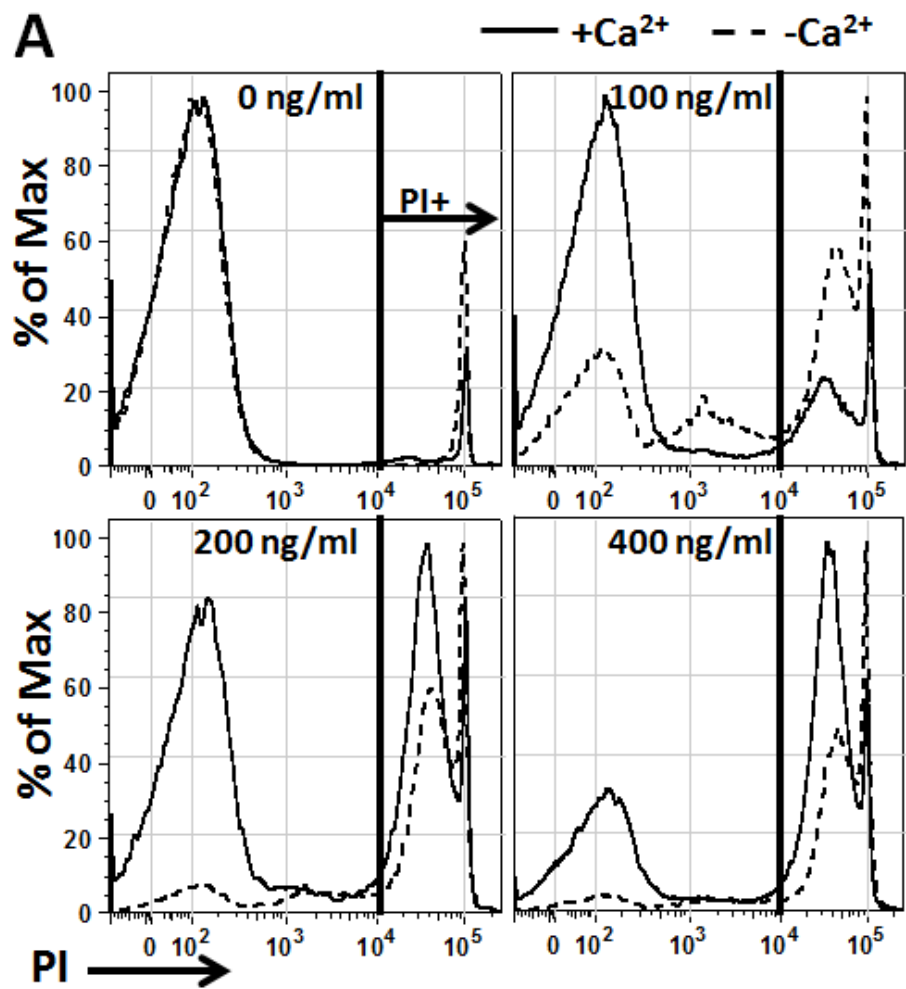
Fig. 2.1. Mouse primary B cells repair SLO-induced membrane damage in a calcium-dependent manner. Primary mouse B cells were incubated with SLO (0 to 400 ng/ml) at 4°C for 5 min and warmed up to 37°C for 5 min in medium with or without calcium. The percentage of PI+ cells were quantified as non-repaired cells using flow cytometry (A) and normalized to untreated cells (B). The percentage of cells repaired was calculated as described in the methods section: [%PI positive ($-Ca^{2+}$) - %PI positive ($+Ca^{2+}$)] x 100/%PI positive ($-Ca^{2+}$) (C). Shown are representative histograms ($-Ca^{2+}$ solid line, $-Ca^{2+}$ dashed line) (A) and the mean ±SD of three independent experiments *$p<0.05$, **$p\leq0.0005$.

Ca^{2+} the percentage of PI^+ cells increased with the concentration of SLO, showing a reduced resealing capacity of B-cells as the SLO concentration rose **(Fig. 2.1, B-C)**. These results indicate that primary mouse B-cells are capable of repairing plasma membrane wounds caused by SLO, and that plasma membrane repair in B-cells is a Ca^{2+}-dependent process.

Wounding-induced lysosomal exocytosis is involved in B-cell plasma membrane repair

Cell wounding induces lysosomal exocytosis, and acid sphingomyelinase (ASM) released from lysosomes is required for plasma membrane repair in epithelial cells, fibroblasts and myofibers (*143, 158*). In contrast to these types of cells, resting primary lymphocytes are significantly smaller and thought to have fewer lysosomes and limited volumes of cytoplasm per cell (*192, 193*). This raises the question of whether wounding the plasma membrane of primary lymphocytes induces lysosome exocytosis, and whether lysosome exocytosis is important for plasma membrane repair in these cells. We analyzed lysosomal exocytosis in SLO-wounded primary B-cells by surface detection of the lysosomal membrane protein LIMP2, and release of the lysosomal enzyme ASM into the medium. Surface LIMP2 was detected using an antibody specific for the lumenal domain of the protein, by both immunofluorescence and flow cytometry without permeabilizing the cells. After 5 min of SLO treatment, LIMP2 was readily detected at the surface of SLO-treated B-cells identified by surface BCR labeling, but not at the surface of untreated B-cells **(Fig. 2.2 A).** Flow cytometry analysis quantitatively confirmed the immunofluorescence microscopy results **(Fig. 2.2 B).** ASM secretion was analyzed by measuring its enzymatic activity
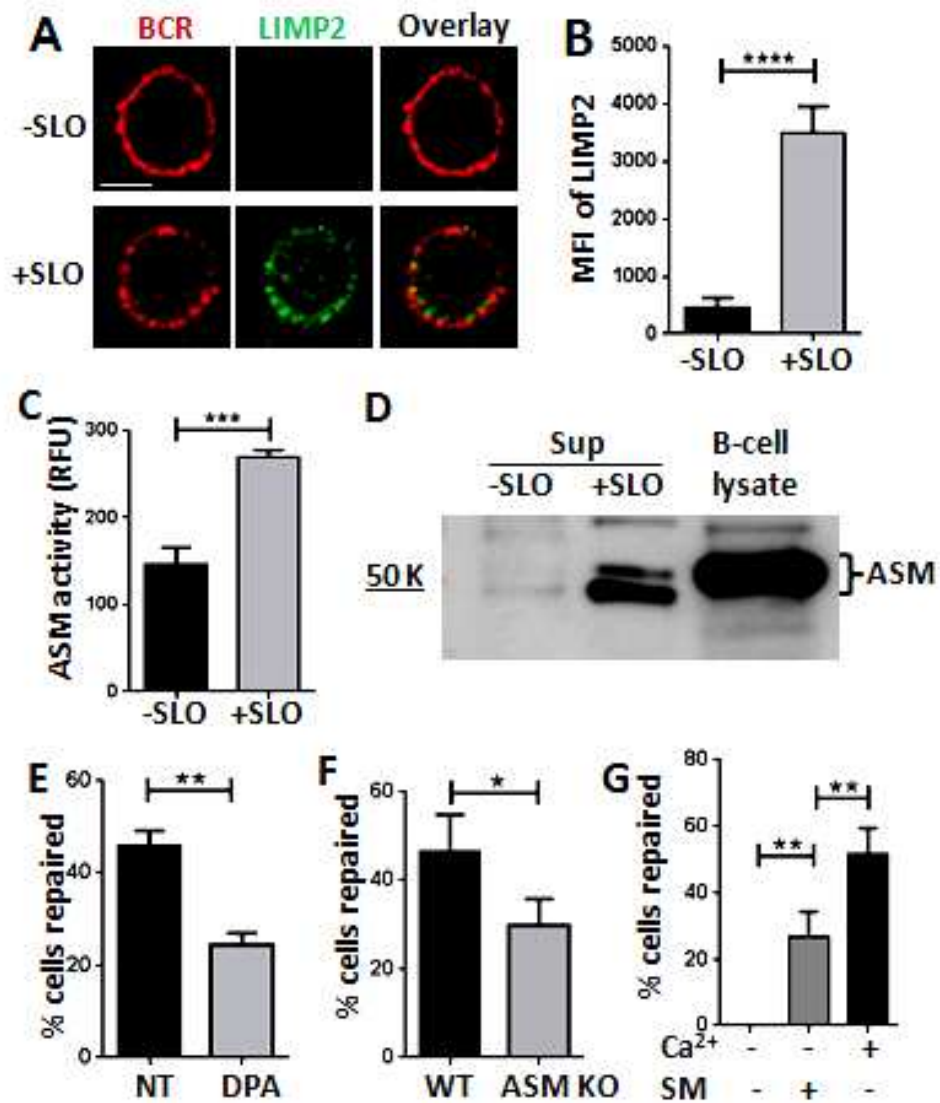
Fig. 2.2. Membrane repair in B cells partially depends on lysosomal secretion and ASM release. (A) Fluorescence confocal images of LIMP2 staining on the membrane surfaces of B cells. Scale bar, 2.5 µm. B cells were exposed to SLO for 5 min at 37˚C and stained for LIMP2 and BCRs at 4˚C without permeabilization. (B) The mean fluorescence intensities of LIMP2 staining on the membrane surfaces of B cells with or without SLO exposure measured by flow cytometry. Shown is the mean (±SD) of three independent experiments. (C) Activity of ASM released from B cells into the medium. B cells were exposed to SLO for 15 sec at 37˚C, protease inhibitors were added and the cells were immediately put on ice. The supernatant was collected and the ASM activity in the supernatants was detected using Amplex Red Sphingomyelinase assay kit, as relative fluorescence units (RFU). Shown is the mean (±SD) of three independent experiments. (D) Release of ASM into the medium was detected using western blotting. (E) Percentage of B cells repaired after exposure to SLO in the presence or absence of the ASM inhibitor, Desipramine (DPA). B cells were pre-incubated with 30 µM of DPA for 30 min at 37°C before 5 min exposure to SLO, followed PI staining and flow cytometry analysis. (F) Comparison of the repair efficiency of B cells from wild type (WT) or ASM KO mice. (G) Comparison of the repair efficiency of B cells in the presence or absence of calcium and sphingomyelinase (SM). B cells were pretreated with SM (50 µM) before SLO exposure, followed by PI staining and flow cytometry. Shown are the means (±SD) of three to five independent experiments. $*p<0.05$, $**p<0.005$, $***p<0.001$, $****p<0.0001$.

and the amount of protein released into the supernatant of the B-cell cultures. The level of ASM activity in the supernatant of B-cells treated with SLO was significantly higher than that of untreated B-cells **(Fig. 2.2 C).** Consistently, there was a much higher level of ASM protein in the supernatant of B-cells injured by SLO than that of untreated B-cells, as shown by western blot **(Fig. 2.2 D).** These results indicate that injury of the B-cell plasma membrane induces lysosome exocytosis.

To determine whether injury-induced release of active ASM is required for B-cells to repair their plasma membrane, we inhibited ASM by a potent inhibitor, desipramine (DPA) (*194*) or used primary B-cells from ASM knockout mice (*195*). DPA treatment reduced the capability of B-cells to repair their plasma membrane by 50%, the same percentage of inhibition previously observed in SLO-wounded NRK cells (*143*). On the other hand, B-cells from ASM knockout mice only showed a ~10% reduction of plasma membrane repair. Since the later results could have been a consequence of compensatory mechanisms developed in ASM knockout mice, we investigated whether addition of purified SM extracellularly, mimicking ASM secretion, was able to restore B-cell plasma membrane repair capability, when the process is blocked by the lack of extracellular Ca^{2+}. Consistent with the results from ASM inhibition, the incubation of SLO-treated B-cells with ASM in the absence of Ca^{2+} significantly increased the percentage of B-cells that fully resealed their plasma membrane **(Fig. 2.2 G).** These data suggest that plasma membrane repair in B-cells requires ASM released by lysosomal secretion.

B-cell injury by SLO induces ASM-dependent fluid phase and lipid raft-mediated endocytosis

Endocytosis of caveolae was shown to be involved in the repair of plasma membrane wounds in fibroblasts and muscle fibers (*158*). To determine whether wounding the plasma membrane of B-cells, which do not express any known forms of the caveolar protein caveolin, also induces endocytosis, we utilized Texas Red-dextran to follow non-specific fluid phase pinocytosis by immunofluorescence microscopy, and cholera toxin subunit B (CTB) for monitoring lipid raft-dependent endocytosis by immunoelectron microscopy. CTB binds glycosphingolipid GM1 which is enriched in lipid rafts, the same membrane domain from where caveolae-mediated endocytosis normally occurs. Dextran endocytosis, detected by the appearance of punctate staining within the cell, was significantly increased after 5 min exposure of B-cells to SLO, when compared to untreated B-cells **(Fig. 2.3, A-B).** These results indicate that plasma membrane wounding triggers rapid endocytosis of dextran by B-cells. To determine whether the dextran endocytosis induced by SLO permeabilization is dependent on ASM released by lysosomal secretion, we examined the effect of extracellular treatment with ASM on dextran endocytosis. We found that ASM treatment alone induced dextran endocytosis to a level similar to SLO treatment **(Fig. 2.3 B)**. These results suggest that the rapid fluid phase endocytic process triggered by wounding in B-cells is ASM-dependent.

We next quantified the endocytosis of CTB, a measure of lipid raft endocytosis, by determining the percentage of surface bound biotin-CTB (marked by gold-labeled streptavidin) entering into individual cells using transmission electron

A

	BCR	Dextran	Overlay
+Ca^{+2} -SLO			
+Ca^{+2} +SLO			
-Ca^{+2} +SLO			

B

% B cells with dextran internalization

SLO	-	+	-
SM	-	-	+

**

C

% CTB internalized/cell

-SLO +SLO   -SLO +SLO
1 min   5 min

**   ****
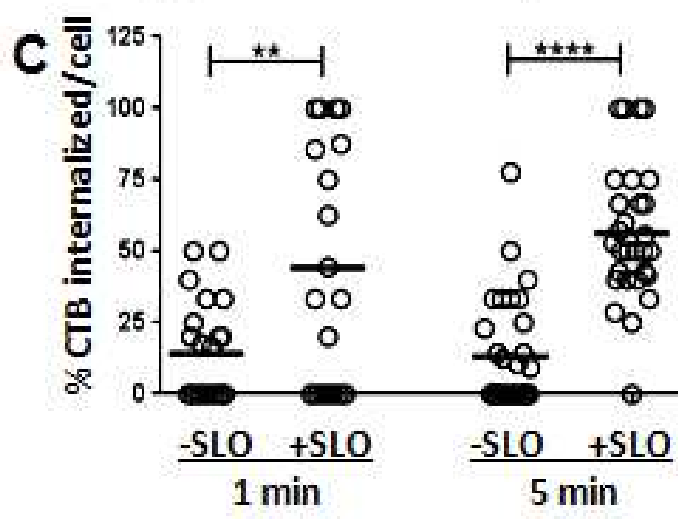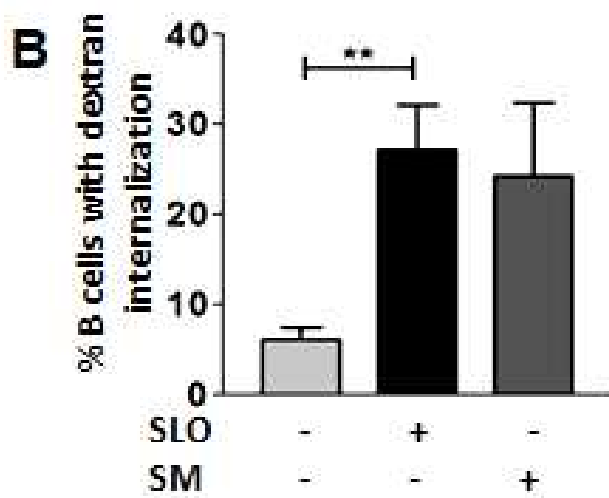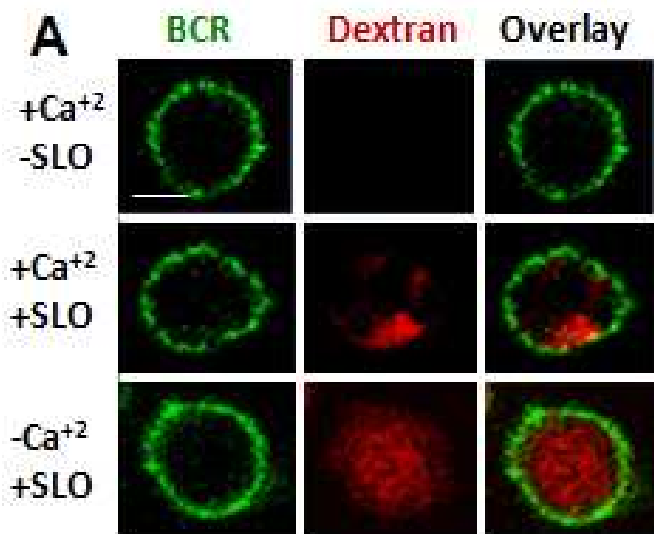
Fig. 2.3. Membrane damage by SLO increases endocytosis. (A) Confocal fluorescence microscopy images of Texas Red-dextran endocytosed at 5 min. B cells were incubated with or without SLO at 4°C for 5 min, and dextran was added right before the 37°C incubation for 5 min. Cells were then washed, fixed, and staining with Alexa Fluor 488 goat anti-mouse IgG to mark the surface BCR. Scale bar, 2.5 μm. (B) Quantification of the percentage of B cells with internalized dextran in the presence or absence of SM by visual inspection of confocal images. Shown is the mean (±SD) of three independent experiments. (C) TEM analysis of the percentage of gold labeled CTB inside B cells. B cells were incubated at 4°C for 15 min with biotin-CTB followed by 30 min with gold-strepavidin (10 nm), and then treated with SLO for 1 and 5 min at 37°C. Shown is the mean (±SD) of more than 16 individual cells per condition from two independent experiments. **p<0.005, ****p<0.0001.

microscopy (TEM). We found that the number of CTB gold particles inside intracellular vesicles was increased after 1 and 5 min of SLO treatment, compared to B-cells that were not treated with SLO **(Fig. 2.3 C).** Using TEM analysis, we did not observe accumulation of a great number of caveolae-like vesicles (<80 nm diameter and flask shaped) within wounded B-cells (data not shown), as previously shown in fibroblasts and muscle cells (*158*), consistent with the absence of caveolae in B-cells. Together, these results indicate that plasma membrane wounding induces caveolae-independent fluid phase and lipid raft-based endocytosis in B-cells, a process regulated by the lysosomal enzyme ASM.

Lipid raft endocytosis is important for B-cell plasma membrane repair

While B-cells do not express classical caveolin, BCR signaling and endocytosis induced by antigenic ligands require the reorganization of lipid rafts and the actin cytoskeleton (*86, 96, 165*). To determine whether lipid raft endocytosis is important for B-cell membrane wound repair, we perturbed lipid rafts by cross-linking (XL) BCRs using antibodies, which activates receptor signaling and endocytosis as well as actin remodeling (*61, 164*). We found that BCR cross-linking significantly reduced the percentage of B-cells that repaired SLO wounds **(Fig. 2.4 A)**, and nearly abolished the SLO-induced rapid endocytosis of CTB **(Fig. 2.4 B).** To determine whether actin dynamics is involved in plasma membrane repair in B-cells, we disrupted or stabilized actin filaments by pretreating B-cells with latrunculin or jasplakinolide. Both treatments significantly reduced the percentage of B-cells that repaired SLO-provoked membrane injury **(Fig. 2.4 C).** These data suggest that
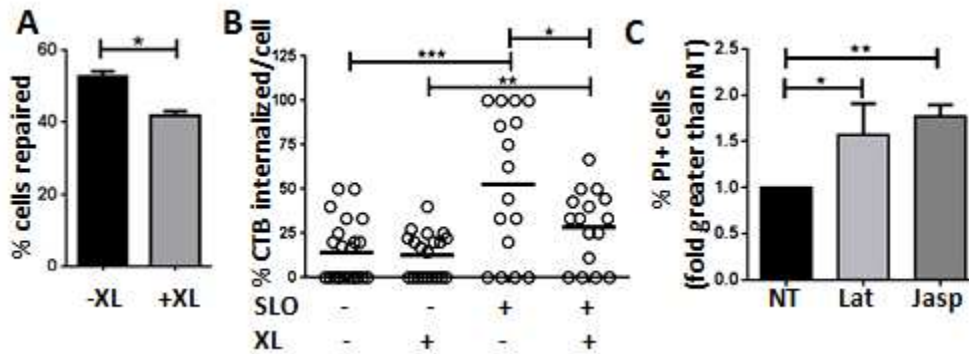
Fig. 2.4. BCR activation and actin disruption interfere with the B cell's repair process of SLO-mediated membrane damage. (A) Percentage of cell repair after 5 min of SLO exposure in the presence or absence of BCR activation by cross-linking antibody. B cells were incubated with either Fab or $F(ab')_2$-anti-mouse IgM for 20 min at 4°C and treated with SLO for 5 min at 37°C, followed by PI staining. Shown is the mean ±SD of three independent experiments. (B) Quantification of the percentage of surface labeled CTB internalized in the presence or absence of SLO and BCR cross-linking antibody. B cells were incubated with or without anti-mouse IgM, biotin-CTB, gold-strep, and SLO at 4°C and warmed to 37°C for 1 min, then processed for TEM. The percentage of gold particles inside individual cells were determined using TEM images. Shown is the mean ±SD of two independent experiments. (C) Disruption of actin during SLO injury decreases membrane repair. B cells were incubated at 37°C with either Latrunculin B (10 μM) or jasplakinolide (2 μM) for 30 min before 5 min exposure to SLO. PI was added and the samples were run on a flow cytometer to identify the percentages of PI+ cells. Shown is the mean ±SD of three independent experiments. *$p<0.05$, **$p<0.01$, ***$p<0.001$.

wounding-induced endocytosis mediates plasma membrane repair in B-cells, and that

BCR activation inhibits repair, possibly by interfering with lipid raft endocytosis and

remodeling actin.

Repair of plasma membrane wounding by SLO inhibits the formation of BCR

signalosomes in lipid rafts

Lipid rafts are critical for B-cell activation by serving as a platform for both BCR

signalosomes and endocytosis (*44, 164*). We investigated whether the plasma

membrane repair process, which also depends on lipid rafts, has any impact on the

BCR signaling and antigen uptake functions. As both these functions are initiated by

BCR clustering in lipid rafts, we analyzed BCR clustering and BCR-lipid raft co-

clustering using immunofluorescence microscopy. Surface BCRs were labeled and

activated with fluorochrome-conjugated F(ab')$_2$ fragment of anti-mouse IgM+G

antibody, and lipid rafts were visualized with fluorescently labeled CTB. To prevent

any possible effect of CTB on BCR clustering, CTB staining was carried out post

BCR activation and at 4°C. Similar to what we previously showed (*116*), BCR cross-

linking induced clustering of surface BCRs to one pole of the cell, forming a

polarized cap **(Fig. 2.5 A).** SLO wounding significantly reduced the percentage of B-

cells with BCR caps, from ~55% to ~35% **(Fig. 2.5 B).** Even though ~35% of SLO-

treated B- cells did display polarized distribution of surface BCRs in response to BCR

cross-linking, the BCR clusters formed were looser and more spread out than those

observed in untreated B-cells **(Fig. 2.5 A).** In the absence of SLO, most of B-cells

with BCR caps (~80%) also showed co-clustering of BCRs with CTB. SLO treatment
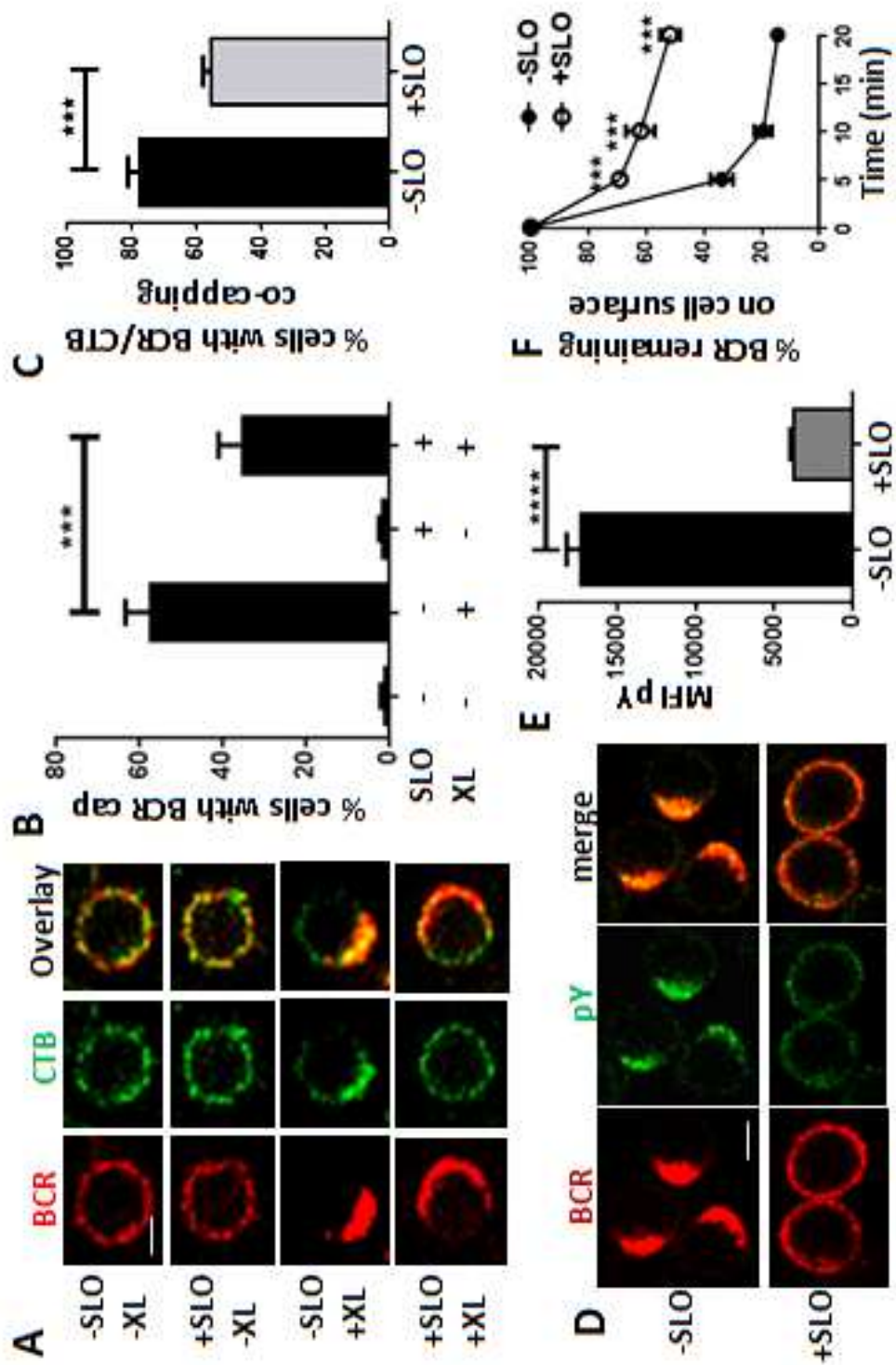
Fig. 2.5. SLO injury reduces BCR activation and internalization. (A-C) Immunofluorescence microscopy analysis of BCR-CTB co-clustering in the presence or absence of SLO. B cells were incubated at 4°C with Alexa Fluor 546 conjugated Fab or F(ab')$_2$ anti-mouse IgM plus Alexa Fluor 488-CTB, and then warmed to 37°C for 5 min with or without SLO, followed by fixation. Shown are representative images (A, scale bar, 2.5 μm) and the average percentages (±SD) of B cells exhibiting polarized BCR clusters among all B cells (B) and BCR-CTB co-clusters among all B cells with polarized BCR clusters (C) by visual inspection of confocal images from four independent experiments (***P=0.0004***P=0.0009). (D and E) Tyrosine phosphorylation (pY) analysis of stimulated B cells treated with or without SLO. B cells were incubated at 4°C with SLO, Alexa Fluor 546 F(ab')$_2$-goat anti-mouse IgM, and warmed to 37°C for 5 min, followed by fixation. Cells were then permeabilized, stained for phosphotyrosine, and analyzed using confocal microscopy (D) and flow cytometry (E). Shown are representative images, Scale bar, 5 μm, (D) and the average (±SD) of the mean fluorescence intensities of phosphotyrosine from three independent experiments (****P<0.0001). (F) Quantification of the effect of SLO treatment on BCR internalization. B cells were incubated at 4°C with biotinylated F(ab')$_2$-anti-mouse IgM, followed by 37°C incubation with or without SLO for indicated times. Cells were then fixed, labeled with PE-strepavidin and analyzed using a flow cytometer to determine the percentage of surface labeled BCRs remaining on the cell surface. Shown is the average percentage (±SD) from three independent experiments ***$p \leq 0.001$, ****$p < 0.0001$.

decreased the percentage to ~55% **(Fig. 2.5 A, C)**. These results indicate that the repair process of plasma membrane wounds inhibits BCR clustering in lipid rafts.

To determine whether the inhibition of BCR-CTB co-clustering affects BCR signaling triggered by receptor cross-linking, we examined tyrosine phosphorylation as a measurement of signaling levels. Immunofluorescence microscopic analysis showed bright staining of anti-phosphotyrosine antibody in BCR caps of untreated B-cells, 5 min post cross-linking. However, most of the SLO-treated cells failed to form BCR caps and exhibited much weaker and uniformly distributed phosphotyrosine staining **(Fig. 2.5 D).** Confirming the results from immunofluorescence, quantitative analysis by flow cytometry showed much lower phosphotyrosine mean fluorescence intensity in SLO-treated B-cells when compared to untreated B-cells **(Fig. 2.5 E).**

We next determined the effect of SLO-induced plasma membrane wounding on BCR endocytosis using flow cytometry. We measured the percentage of reduction in the amount of surface labeled BCR over the incubation time at 37°C to reflect BCR endocytosis. SLO treatment reduced both the kinetics and the overall levels of BCR internalization **(Fig. 2.5 F).** At 20 min, there was still ~50% of surface-labeled BCR remaining at the surface of SLO-treated B-cells, compared to ~10% of surface-labeled BCR at the surface of untreated B-cells **(Fig. 2.5 F).**

Taken together, our data demonstrate that the SLO-wounding and plasma membrane repair process inhibits both the signaling and antigen uptake functions of the BCR.

Repair of plasma membrane wounding leads to segregation of surface BCRs from lipid rafts.

The inhibitory effect of SLO-mediated injury on the co-clustering of surface BCRs with CTB suggests that the plasma membrane repair process prevents surface BCRs from interacting with lipid rafts. To investigate this hypothesis, we analyzed the co-localization between surface-labeled BCRs and CTB using live cell imaging by confocal fluorescence microscopy. B-cells that were not treated with SLO but were activated by cross-linking for 10 min showed internalization of surface labeled BCRs and co-localization of CTB with BCR-containing vesicles **(Fig. 2.6, A, C).** In contrast, there was limited co-localization between internalized BCRs and CTB in B-cells that were injured by SLO **(Fig. 2.6, A, C).** We generated kymographs from time-lapse images to track the co-localization of the BCR with CTB during BCR internalization **(Fig. 2.6 B).** The kymographs showed continuous co-localization between BCRs and CTB during their endocytosis and movement into the cytoplasm of B-cells not injured by SLO. In contrast, in B-cells injured by SLO, internalized BCRs did not co-localize with CTB **(Fig. 2.6 B)**, indicating a segregation of BCRs from lipid rafts during BCR internalization.

We further confirmed this result using immunoelectron microscopy, where surface BCRs were labeled by 18 nm gold particles and CTB by 10 nm gold particles. The co-localization of BCRs with CTB was quantified in individual cells by determining the percentage of CTB gold particles in intracellular vesicles that contained BCR gold particles. Consistent with the results of immunofluorescence
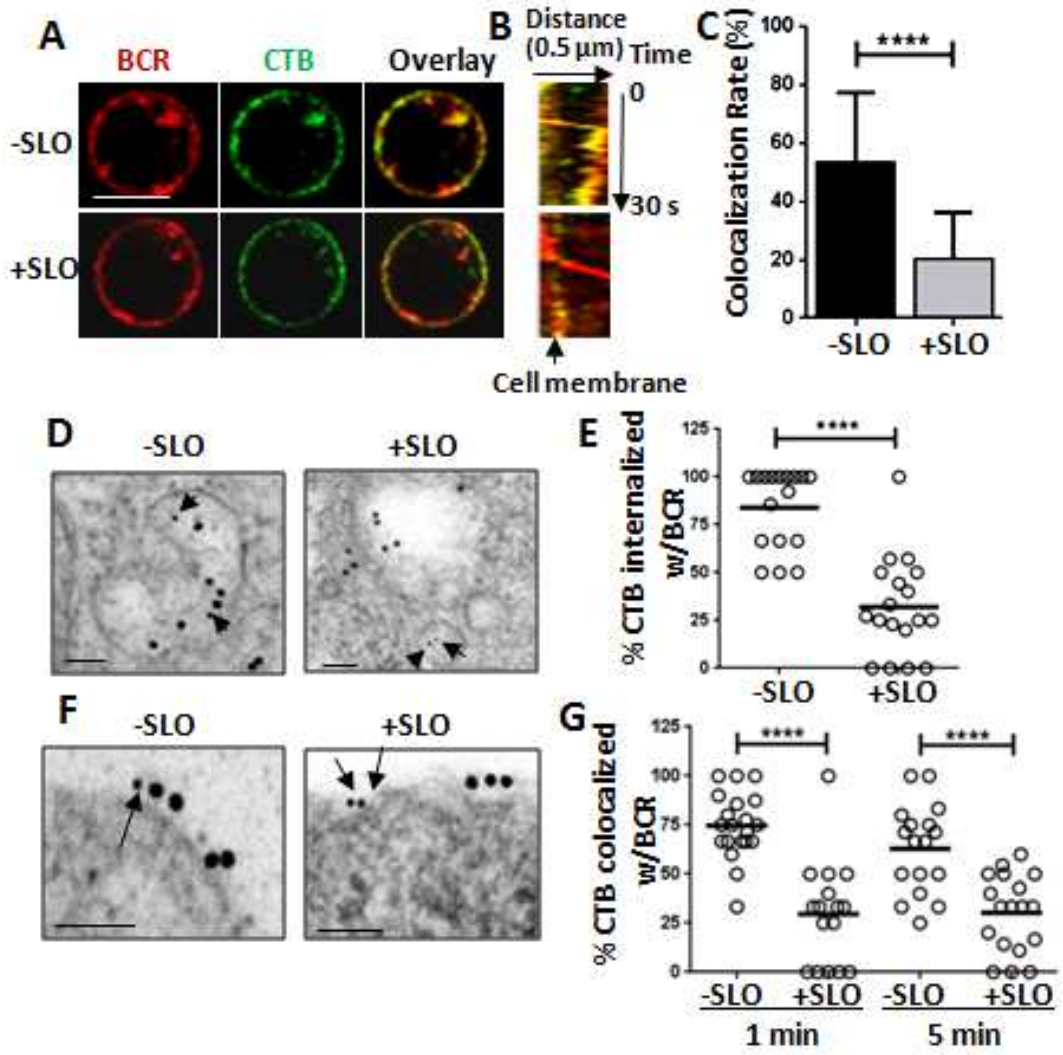
Fig. 2.6. Membrane injury by SLO segregates BCRs from CTB-labeled lipid raft at the cell surface and during BCR internalization. (A-C) Live cell imaging analysis of BCR and CTB internalization. B cells were incubated at 4ºC with Alexa Fluor 546 F(ab')$_2$ goat anti-mouse IgM and Alexa Fluor 488 CTB. Time lapse images were acquired at 37˚C for 10 min in the presence or absence of SLO using a confocal microscope. Shown are representative images at 10 min (A), a kymograph generated from time lapse images (B), the average correlation coefficients (±SD) of BCR and CTB staining at 10 min (C) from three independent experiments. Scale bar, 2.5 µm. (D-G) ImmunoEM analysis of BCRs and CTB in B cells treated with or without SLO. B cells were incubated with gold-anti-mouse IgM (18 nm), biotin-CTB plus gold-strepavidin (10 nm) at 4ºC and then incubated with or without SLO at 37˚C for 1 or 5 min. The percentages of CTB gold particles internalized into vesicles containing BCR gold particles at 5 min (D-E) and in the vicinity (<30 nm) of BCR gold particles at the plasma membrane (F-G) in individual cells were determined. Shown are representative images (scale bar, 100 nm) and the average percentage from ≥16 individual cells and two individual experiments . ****p<0.0001.

microscopy, SLO treatment significantly reduced the percentage of CTB gold particles that co-localized with internalized BCRs at 5 min **(Fig. 2.6, D-E).** In SLO-treated cells, CTB appeared to accumulate in smaller vesicles that did not contain BCR **(Fig. 2.6 D).** To determine whether CTB is segregated from BCRs at the cell surface or during endocytosis, we determined the percentage of CTB gold particles in the close vicinity of BCR gold particles on the plasma membrane using immunoelectron microscopy. Our results showed that SLO treatment significantly reduces the percentage of CTB gold particles localized close to BCR gold particles on the B-cell surface, from ~75% and ~60% to ~25% at 1 and 5 min, respectively **(Fig. 2.6, F-G).** Our data demonstrate a clear segregation between BCRs and lipid rafts at the plasma membrane of B-cells wounded by SLO. Considering that these assays were performed under conditions permissive for resealing (in the presence of Ca^{2+}), we conclude that endocytosis-mediated removal of plasma membrane wounds interferes with the lipid raft-mediated internalization of BCRs.

The segregation of BCRs from CTB during endocytosis suggests that the BCR and CTB are endocytosed into different vesicles. To test this hypothesis, we examined the morphology of vesicles where BCRs and CTB that were just endocytosed (5 min) were located using immunogold staining and TEM. We found that there was a significant increase in the number of tubular-shaped vesicles in SLO wounded B-cells, compared to unwounded B-cells **(Fig. 2.7, A-B).** Based on their morphology, we divided vesicles roughly into four categories: small (<120 nm diameter), medium (120-250 nm), large (>250 nm), and tubular vesicles (200-500 nm) **(Fig. 2.7 A).** We quantified the percentage of BCR- or CTB-containing vesicles

in each category by visual inspection. We found that without SLO-induced wounds, CTB gold particles were primarily concentrated in small vesicles in unstimulated B-cells after a 5 min incubation **(Fig. 2.7 C).** BCR cross-linking did not significantly change the intracellular distribution of endocytosed CTB. In SLO-wounded B-cells, the percentage of CTB-containing small vesicles was significantly reduced, while the percentage of CTB-containing tubular vesicles was significantly increased **(Fig. 2.7 C).** Furthermore, BCR cross-linking reduced the percentage of CTB-containing tubular vesicles and increased CTB-containing small vesicles in SLO-wounded B-cells, compared to unstimulated SLO-wounded B-cells **(Fig. 2.7 C).** This result suggests that the SLO-induced CTB redistribution was partially reversed by BCR cross-linking. Similar to CTB in unwounded B-cells, BCRs were preferentially localized in small vesicles after 5 min incubation in unwounded B-cells **(Fig. 2.7 D).** In contrast to CTB distribution in SLO-wounded B-cells, SLO-triggered wounding and repair did not significantly change the preferential location of endocytosed BCRs in small vesicles **(Fig. 2.7 D).** These data suggest that plasma membrane wounding and repair induce endocytosis of lipid rafts thorough tubular-shaped vesicles, which exclude BCRs.
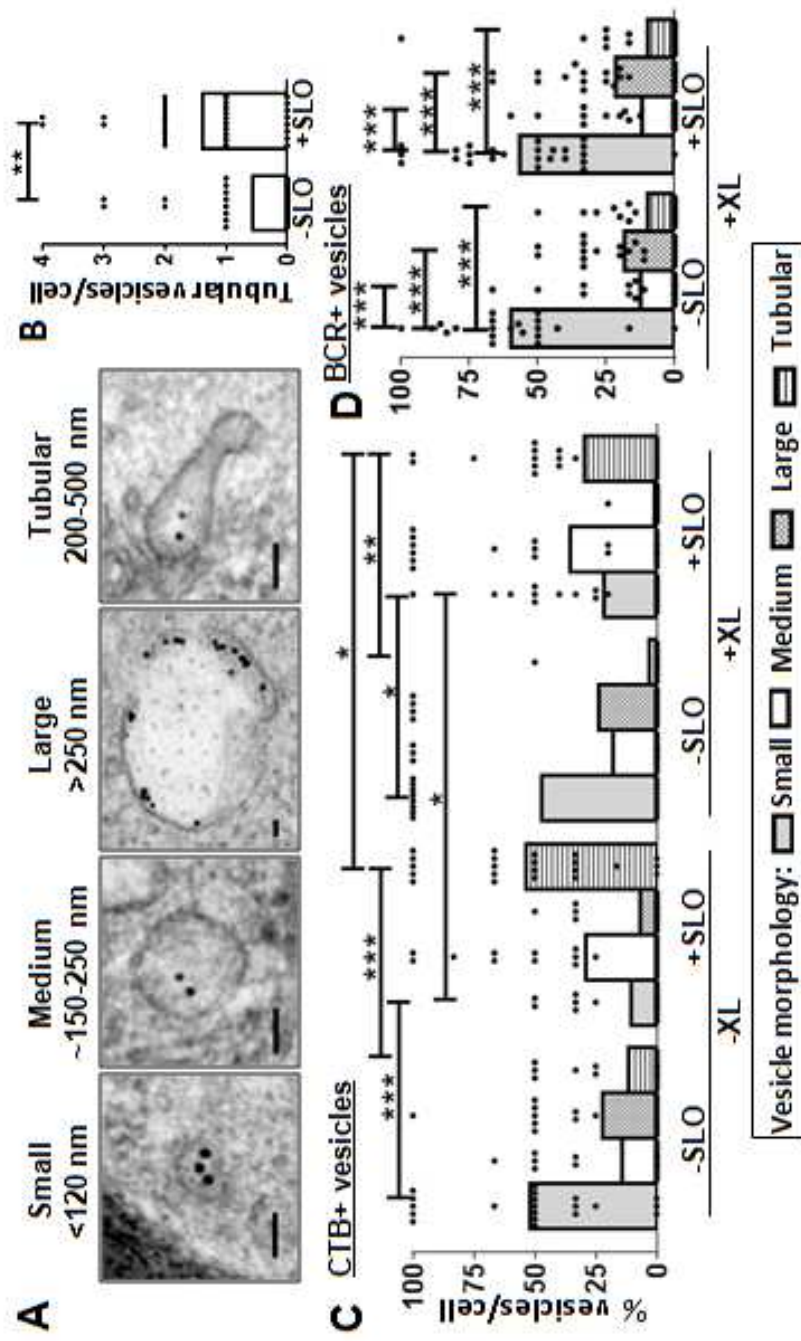
Fig. 2.7. Repair of plasma membrane wounds induces CTB endocytosis into tubular-shaped vesicles. B cells were incubated with gold-anti-mouse IgM (18 nm), biotin-CTB plus gold-streptavidin (10 nm) at 4°C and then incubated with or without SLO at 37°C for 5 min. (A) Representative TEM images of the classifications of vesicle morphologies. Scale bar, 100 nm. (B) The average number of tubular-shaped vesicles per cell countered by visual inspection. (C) The average percentages of individual type of vesicles among all CTB-containing vesicles per cell. (D) The average percentages of individual type of vesicles among all BCR-containing vesicles per cell. The data were generated from ≥18 individual cells from two individual experiments for each condition. *$p<0.05$, **$p<0.01$, ***$p<0.001$.

2.5 Discussion

This study aimed to investigate whether and how lymphocytes repair plasma membrane wounds, and the influence of a putative repair process on B-cell activation. Our results demonstrate that primary mouse B-lymphocytes can rapidly repair plasma membrane wounds caused by the bacterial pore-forming toxin SLO. We found that this B-cell repair process involves lysosomal secretion triggered by Ca^{2+} influx through the wounds, similar to what was previously reported for muscle, fibroblasts and epithelial cells (*143, 158*). Importantly, our results also showed that antigenic activation of B-cells, which activates signaling and internalization of the BCR, interferes with the plasma membrane repair capability of B-cells. Conversely, the plasma membrane repair process suppresses B-cell activation by inhibiting the signal transduction and antigen uptake functions of the BCR. As BCR signaling and internalization require lipid rafts (*164, 165*), the mutual suppression between BCR activation and plasma membrane repair observed in this study uncovers a critical role of lipid rafts in B-cell plasma membrane repair.

This study suggests that B-cells repair repair wounds on their plasma membrane using mechanisms that have several elements in common with those reported for muscle, fibroblasts and epithelial cells: rapid lysosomal exocytosis followed by endocytosis (*157, 158*). Exocytosis of lysosomes in wounded B-cells was determined by surface detection of the lysosomal membrane protein LIMP2, and release of the lysosomal enzyme ASM into the culture medium. Wounding with SLO also triggered endocytosis of the fluid phase tracer dextran, a process that was restored by extracellular addition the lysosomal enzyme ASM when lysosome

80

exocytosis was inhibited. ASM-induced endocytosis was previously shown to be critical for plasma membrane repair by internalizing damaged membrane (*143, 157, 159*). Also similar to other cell types (*143, 157, 159*), inhibition of ASM reduced the ability of B-cells able to repair their plasma membrane. However, B-cells from ASM knockout mice showed only a moderate reduction in their capability of repairing SLO-induced wounds, suggesting that other factors, possibly released by lysosomal exocytosis, are required for efficient B-cell plasma membrane repair. Alternatively, ASM gene deletion in mice may have enhanced the expression of compensatory factors.

Corrotte et al. have recently reported that caveolae-mediated endocytosis mediates the repair of wounds caused by SLO and mechanical forces, in muscle fibers and other cell types such as epithelial cells (*158*). Caveolin is a membrane-associated protein that inserts its lipidated hydrophobic domain into the inner leaflet of lipid raft regions of the plasma membrane, which are dynamic microdomains rich in cholesterol and sphingolipids, such as sphingomyelin and ceramide (*175, 196*). Caveolae are responsible for endocytosis of proteins associated with lipid rafts (*196*). However, lymphocytes do not express detectable amounts of the three known isoforms of caveolin (*176, 197-199*), indicating that endocytosis of plasma membrane wounds in B-cells occurs through a mechanism independent from conventional caveolins. Furthermore, using TEM, we did not observe a significant accumulation of vesicles resembling classical caveolae (~80 nm diameter with flask- or omega-shaped plasma membrane invaginations) (*176*) in B-cells immediately following wounding, as previously described in muscle fibers and other cells (*158*). This observation

further supports a lack of caveolin expression in B-cells, since when wounded these cells do not show the marked accumulation of plasma membrane-proximal caveolae observed in muscle fibers and other cell types (*158*). However, we cannot completely exclude the possibility that an unknown caveolin homologue is expressed in B-cells, a possibility supported by our observation that a caveolin-1 specific antibody recognizes a protein of higher molecular weight than caveolin-1 in B-cell lysates (data not shown).

Our studies strongly suggest that wounding-induced endocytosis in B-cells is lipid raft-dependent, despite the absence of caveolin. This conclusion is supported by our findings that wounding induces the rapid endocytosis of lipid rafts labeled by CTB, and that perturbing lipid rafts by BCR activation inhibits plasma membrane repair. B-cells are known to be capable of endocytosing raft-associated proteins. While BCR endocytosis is primarily mediated by clathrin-dependent vesicles, it requires lipid rafts as well as actin reorganization (*86*). Lipid rafts provide the platform for clathrin to gain phosphorylation and access to endocytosing BCRs, and actin remodeling is required for the fission of clathrin-coated membrane invaginations (*85, 93, 96*). BCRs also have also been reported to be endocytosed via a clathrin-independent but actin- and raft-dependent pathway in cells with a conditional deficiency of the clathrin heavy chain (*86*). Collectively, these data support the notion that B-cells can endocytose wounded plasma membrane via lipid rafts, independent of both clathrin and caveolin.

These observations raise the question of how endocytosis of lipid rafts triggered by plasma membrane wounding is induced without the participation of

clathrin and caveolin. In wounded muscle fibers, epithelial cells and fibroblasts, caveolae-mediated endocytosis of wounded plasma membrane is induced by extracellular ASM, released through lysosomal exocytosis (*143, 158*). ASM converts sphingomyelin into ceramide, creating ceramide-enriched membrane microdomains that can trigger invagination of lipid bilayers (*200, 201*). Here we showed that wound-induced endocytosis in B-cells is also dependent on extracellular ASM, in the absence of caveolin. Furthermore, in wounded B-cells, raft-binding CTB is primarily endocytosed into vesicles with a distinct tubular morphology. While the tubular vesicles still connected to the plasma membrane observed in SLO-wounded B-cells might be considered somewhat similar to caveolae morphologically, their numbers are much lower than what is seen in wounded muscle and other cell types. However, the number of tubular vesicles increases after B-cell wounding and repair, compared to non-wounded B-cells. Together, these results suggest that extracellular ASM delivered by lysosomal exocytosis can induce lipid raft endocytosis independent of caveolin and clathrin - further supporting the notion that an accumulation of ceramide in the plasma membrane due to ASM leads to endocytosis. In the case of B-cells, actin remodeling may further facilitate ceramide-induced endocytosis.

Lipid rafts are critical for both BCR signaling and antigen uptake, two events that are essential for B-cell activation. Binding of antigen to the BCR induces receptor aggregation in lipid rafts, shown here as co-clustering of BCRs with CTB on the cell surface. The clustered BCRs are then phosphorylated by raft-resident Src kinases, initiating signaling cascades required for B-cell activation. As we discussed earlier, lipid rafts are also essential for BCRs to uptake antigen. This scenario raised

83

the question of whether plasma membrane repair, a process shown in other cell types to require lipid raft membrane domains in the form of caveolar endocytosis (*158*), affects BCR activation/signaling/internalization. We found that plasma membrane repair and BCR signaling and internalization suppress one another, most likely by competing for lipid raft domains on the plasma membrane. Plasma membrane repair inhibits BCR signaling and endocytosis via segregation of BCRs from lipid rafts on the cell surface, and during endocytosis. Segregation of BCRs from lipid rafts can reduce BCR phosphorylation by Src kinases required for intiating signaling (*164*), and inhibit clathrin phosphorylation (*85*) or interaction with BCR aggregates. We found that BCRs and raft-bound CTB not only fail to co-localize at the cell surface and during endocytosis, but are also endocytosed in different types of vesicles, small and flask-shaped/tubular respectively, in wounded and resealed B-cells. These findings indicate that plasma membrane repair interferes with the interactions of BCRs with lipid rafts, generating distinct endocytic pathways that compete with each other. It is unclear why the two processes do not share lipid rafts. We can speculate that this competition may be due to different requirements of the two processes for lipid rafts. The formation of BCR signalosomes and endocytosis hot spots may require larger and more stable lipid rafts, when compared to the internalization of wounded plasma membrane. As shown here and previously, the majority of CTB staining on the plasma membrane co-localizes with surface BCRs oo one pole of a stimulated B-cell (*116*). In addition, wounding-induced endocytosis involves a much faster kinetics (seconds) of plasma membrane internalization (*157*) than BCR

84

endocytosis (minutes) (*138*). The mutual suppression further supports the critical role of lipid raft domains in both plasma membrane repair and BCR activation.

We were unable to examine the repair of membrane wounds provoked by mechanical forces in B-cells due to their their high vulnerability to shearing force. While mechanical wounding causes a form of membrane damage that is presumed to be different from SLO, which forms small pores after binding to cholesterol, a previous study showed that the repair of both types of membrane wounds are mediated via ASM-induced endocytosis (*158*). This suggests that in B-cells the repair of SLO pores and mechanical wounds may also involve local generation of ceramide from sphingomyelin and the rapid endocytosis of lipid raft portions of the plasma membrane, a process that is functionally equivalent to the caveolar endocytosis described in muscle fibers and other cell types. This hypothesis remains to be tested.

While B-cell membrane damage has not yet been studied *in vivo*, these cells are frequently in an environment that is likely to cause plasma membrane wounding. In their lifetime, B-cells circulate through narrow blood vessels at high velocity, undergo chemotaxis from blood vessels to infection sites, and migrate through lymphatic organs, an extremely crowded environment. It has been shown that when B-cells present antigen to T cells or other B-cells, fragments of their plasma membrane can be extracted with the antigen by antigen-acquiring cells (*84, 170, 202*). We showed here that B-cells possess a rapid, Ca^{2+}-dependent plasma membrane repair mechanism that protects them from wounding-induced death. Importantly, we also identified an inhibitory effect of the membrane repair process on BCR activation, which may suppress BCR-mediated activation of B-cells that are injured by

presenting antigen and while migrating through narrow spaces. While the physiological significance of this phenomenon remains to be defined, reductions in BCR signaling and antigen uptake may enable them to become better antigen-presenting cells to other B-cells, or facilitate their progress onto the next stage of activation and differentiation in response to T-cell help. Marginal zone B-cells, a subset of mature B-cells, are highly mobile, transporting antigens from the marginal zone to secluded regions of B-cell follicles in the secondary lymph organs (*23*). Our results raise speculation that the inhibitory effects of B-cell plasma membrane damage, possibly provoked by migration and antigen presentation, may sacrifice the activation and antigen-uptake activities of marginal zone B- cells in order to support the activation of other B- cells, by collecting, transporting, and presenting antigen to them. While this hypothesis remains to be tested, our results provide a potential mechanistic explanation for the unique capability of marginal zone B-cells to shuttle antigen.

2.6 Working Model

Figure 2.8 Working Model of lipid raft competition between membrane repair and BCR activation.

Lipid raft distribution during BCR activation-

1. As BCRs bind antigen and aggregate together, they translocate to lipid rafts and begin signaling.
2. BCRs in lipid rafts continue to signal and cluster together to form a central BCR cluster for amplified signaling, including recruitment and activation of molecules for internalization.
3. BCR/antigen complexes are internalized and processed for antigen presentation to T cells.
4. The acquisition of lipid rafts by activated BCRs for signaling and internalization inhibits membrane repair, which uses a lipid raft-dependent internalization mechanism.

Lipid raft distribution during membrane repair:

A. Membrane damage caused by SLO pores allows calcium to enter the cell.
B. The increase of intracellular calcium induces lysosomal exocytosis, allowing the release of acid sphingomyeline (ASM), which induces membrane curvature and internalization.
C. Lipid rafts are internalized for membrane repair, likely by removing the membrane lesion from the cell surface.
D. During BCR activation, the membrane repair pathway may take lipid raft from BCRs
E. As lipid raft is used for membrane repair, BCR clustering and signaling, and antigen internalization is inhibited

Chapter 3: Regulation of the early events of B cell activation by the density and valency of membrane-associated antigen

3.1 Abstract

The immunogenicity of immunogens is the key to the efficacy of vaccines and can be manipulated via the chemical and physical properties of the immunogen. In vivo, the majority of antigens encountered by B cells are presented on membranes. Membrane-associated antigens have been shown to be more efficient than soluble antigens to activate B cells. Antigens initiate B cell activation by binding to B cell receptors (BCRs) that induce signaling cascades. However, how the properties of membrane bound antigens regulate BCR activation is not fully understood. This study investigated the role of density and valency of membrane bound antigen on the early events of BCR activation, including actin-driven BCR clustering and B cell spreading. We have generated a new antigen system that provides optimal orientation on planar lipid bilayers for binding to the BCR and enables alteration of densities and valencies of the antigen. Using interference reflection and total internal reflection fluorescence microscopy, we found that the levels of B cell spreading, BCR self-clustering, and protein tyrosine phosphorylation are increased as the density of antigen increases. However, stimulation of B cells with bivalent versus monovalent antigens on membranes with the same density does not result in any difference in B cell spreading, antigen accumulation, and protein tyrosine phosphorylation. Live cell imaging analysis of B cells from Lifeact transgenic mice showed that higher antigen densities induced greater actin dynamics that correlated with B cell spreading and

BCR clustering. Our results demonstrate that differing from soluble antigen, the density, but not the valency, of membrane bound antigen is critical to BCR activation. Antigen density regulates BCR activation by modulating actin-mediated B cell spreading and antigen accumulation. The method established in this study for creating optimally oriented antigen and the density of membrane bound antigen provide an important tool for studies of B cell activation *in vitro* and optimization of vaccine design.

3.2 Introduction

The humoral immune system consists of B cells that produce antibody and provide humoral immunological memory for protection against invading pathogens. B cells are activated by antigens that bind their specific B cell receptors (BCR). The majority of antigens that B cells encounter *in vivo* are presented on the membranes of other cells, such as marginal zone B cells, macrophages, and follicular dendritic cells (*23*). BCR binding to membrane bound antigen induces BCR clustering and B cell spreading over the target membrane. This increases the contact area between B cells and the target membrane. B cell spreading increases the number of BCRs that bind to antigen and the number of BCR clusters at the leading edges of the spreading B cell membrane. BCR self-clustering is required for initiating signaling. After reaching its maximal spreading, the B cell then contracts, reducing its contact area with the target membrane. B cell contraction drives the coalescence of BCR microclusters into a central cluster (immunological synapse), where signaling is attenuated (*57-59*).

B cell spreading, BCR clustering, and central cluster formation require remodeling of the actin cytoskeleton. Actin inhibitors obliterate all of these events, consequently suppressing BCR signaling and B cell activation (*60-62*). Upon BCR engagement, there is a transient depolymerization of cortical actin, allowing for free later diffusion of surface BCRs and the formation of nano-scale BCR clusters (*60, 65, 66*). BCR clustering activates signaling, leading to actin reassembly at BCR clusters (*61, 67*). As BCR clustering and signaling continues, actin concentrates at the leading edges of the spreading B cell membrane. When maximal spreading is reached, actin forms a ring-like structure around BCR clusters, which is required for cell contraction and central cluster formation (*61, 64*).

Properties of antigens can modulate B cell activation, thereby becoming an important target for vaccine design. Previous studies have demonstrated that the affinity, valency, or concentration of soluble antigen enhance BCR aggregation and signaling (*25, 80, 116*). Similarly, increasing affinity or density of membrane bound antigen induces greater B cell spreading, BCR clustering, and BCR signaling, however, the role of antigen density on actin dynamics is unknown, even though actin dynamics are crucial for inducing B cell spreading and BCR clustering and signaling (*60-62, 64*). The density of membrane bound antigen appears to be able to overcome the lower affinity of the antigens in activation of B cells (*64*). For vaccine design, the density of an antigen is much easier to manipulate than affinity or valency. Although the role of antigen density on BCR activation is becoming clear, how to identify the optimal antigen density and how exactly antigen density regulates BCR activation remains elusive.

In the secondary lymphoid organs, B cells can encounter antigens in both soluble and membrane bound forms. Recent studies have shown that most of antigen have been shuffled by marginal zone macrophages and B cells into B cell follicles and presented by follicular dendritic cells. For soluble antigen, multi-valencies are critical to its immunogenicity as only multi-valent soluble antigen can cross-link BCRs into oligomers, which is required to trigger signaling as well as efficient antigen internalization and presentation to T cells (*23, 110, 115*). For membrane bound antigen, monovalent antigen has been shown to be capable of inducing B cell spreading and BCR clustering and signaling (*68*). However, whether the valency of membrane bound antigen has any effect on BCR activation and how the density of membrane bound antigen regulates BCR activation are not fully understood.

A lack of well-defined antigenic stimulatory systems has hindered our understanding of how antigen density and valency influence BCR activation. Current membrane bound antigen systems use (4-Hydroxy-3-Nitrophenyl)Acetyl (NP)-BSA and biotinylated Fab_2. NP-BSA is made by reaction of the succinic anhydride ester of NP to amines of BSA. The NP-BSA is attached to a histidine tag so that they may bind to nickel labeled lipid bilayers. The exact number of NPs conjugated to a BSA is unknown and thus the valency is unknown, plus the location of the histidine tag is random and there is no way of knowing if all the NPs on the BSA is accessible to BCRs (*68, 203, 204*). Similarly, the biotinylation site of the Fab_2 is unknown and when added to streptavidin coated lipid bilayers, the BCR binding site may not be oriented to bind to the B-cells's BCRs (*63*).

To address these questions, we have designed a novel antigen system, which was designed to generate optimized and homogenous orientation of membrane bound antigen to bind BCRs. This model antigen system allows us to define the density and valency of antigen on membranes, thereby studying their effects on BCR activation. Using this model antigen system combining live-cell imaging with interference reflection (IRM) and total internal reflection fluorescence microscopy (TIRF) of primary B cells from mice expressing LifeAct-GFP transgene, we examined the effects of density and valency of membrane bound antigen on the early events of BCR activation. Our results show that the maximal levels of B-cell spreading, BCR clustering and signaling in the contact zone are antigen-density dependent. Increased B cell spreading is associated with rapid accumulation of F-actin behind spreading membrane, and amplified BCR clustering is linked to faster growth of BCR microclusters. However, the valency of membrane bound antigen had no effect on B-cell spreading, antigen accumulation, and tyrosine phosphorylation. These results show that this model antigen system is useful for studying mechanisms underlying BCR activation and for optimizing immunogen complexes, such as antigen incorporated liposomes, for vaccine development.

3.3 Materials and Methods

Mice and B cell isolation

Splenic B cells were isolated from wild-type (C57BL/6) (Jackson Laboratories), transgenic MD4 mice (Jackson Laboratories), and Lifeact mice of C57BL/6 background (*205, 206*). Mononuclear cells were separated out by Ficoll density-

gradient centrifugation (Sigma-Aldrich). T cells were depleted by anti-Thy1.2 mAb (BD Biosciences) and guinea pig complement (Rockland Immunochemicals), and monocytes were removed by panning for 1 hour. All procedures involving mice were approved by the Institutional Animal Care and Usage Committee of the University of Maryland.

Antibodies and reagents

For intracellular staining, cells were fixed with 4% PFA and permeabilized with 0.05% saponin and incubated for 30 min with anti-phosphotyrosine antibody (clone: 4G10) (Millipore), followed by 30 min with Alexa Fluor 488 goat anti-mouse IgG2b (Invitrogen) for BCR signaling staining.

Biotinylation of antigens

To produce the monobiotinylated goat anti-mouse IgM and IgG Fab' (bFab), a published protocol (*207*) was followed. Briefly, the disulfide bonds of Fab_2' fragments (Jackson Immunoresearch) were reduced by 2-Mercaptoethylamine (Thermo Scientific) and the resulting sulfhydryls were then biotinylated with Maleimide-PEG2-Biotin (Thermo Scientific). EZ Biotin quantitation kit (Pierce Protein) was used for the determination of a 1:1 ratio of biotin to Fab'. The bFab was then labeled with Alexa Fluor 546 (Invitrogen).

Hen egg lysozyme (HEL) (Sigma) was biotinylated with NHS-PEG4-Biotin (Thermo Scientific), which reacts with primary amines and for HEL this would predominantly

biotinylate the N-terminus and thus not likely to block the epitope for BCRs of MD4 mice (*208*). EZ Biotin quantitation kit (Pierce Protein) was used for the determination of a 1:1 ratio of biotin to HEL. The biotinylated HEL (bHEL) was then labeled with Alexa Fluor 546 (Invitrogen).

Preparation of antigen bound artificial membranes

An established protocol described previously was used for making planar lipid bilayers (*44, 209*). Briefly, 1,2-dioleoyl-*sn*-glycero-3-phosphocholine and 1,2-dioleoyl-*sn*-glycero-3-phosphoethanolamine-cap-biotin (Avanti Polar Lipids, Alabaster, AL) at a 100:1 molar ratio in PBS (total concentration of 5 mM) was sonicated to form liposomes, that were then centrifuged and filtered to get rid of any aggregates. Liposomes were added to glass coverslip chambers (Nunc lab-tek) and incubated for 10 min., after which each well was washed with 20 ml PBS. Next 1 µg/ml of streptavidin (Jackson ImmunoResearch Laboratories) was incubated on the planar lipid bilayer coated coverslip for 10 min and washed with PBS. Lastly, the biotinylated antigen was allowed to incubate on the coated coverslip for 10 min and then washed with PBS. For experiments using bFab or bHEL on the lipid bilayer, 1 µg/ml of AF546 bFab or AF546 bHEL was used and non-fluorescent bFab or bHEL was added to make up to the total concentration used.

For experiments testing different concentrations of streptavidin on the lipid bilayer, WT or MD4 B cells were labeled with 5 µg/ml AF546 bFab or 5 µg/ml AF546 bHEL for 30 min at 4°C prior to being added to streptavidin coated lipid bilayers.

Fluorescence imaging

TIRFM and IRM images were taken with a Nikon laser TIRF system on an inverted microscope (Nikon TE2000-PFS), equipped with a 60×, NA 1.49 Apochromat TIRF objective (Nikon Instruments, Melville, NY), a Coolsnap HQ2 charge-coupled device camera (Roper Scientific, Sarasota, FL), and two solid-state lasers of wavelengths 491 and 561 nm. For live cell imaging, time lapse images were taken at the rate of one frame every 2 sec.

Imaging and statistical analysis

Andor iQ software (Andor Technology, Belfast, U.K.) was used to analyze the mean fluorescence intensity line profiles of cells and the fluorescence intensities in the B cell contact area. The B cell contact area was determined from interference reflection microscopy (IRM) images and was analyzed using custom Matlab programs (MathWorks, Natick, MA). BCR cluster tracking was performed using the MATLAB (Mathworks, Natick, MA) image analysis package uTrack version 2.1.3 (http://lccb.hms.harvard.edu/software.html) (*210*). Postprocessing of tracked data was performed with custom programs in MATLAB. At least 30 cells per condition were analyzed for fixed cells and at least 15 cells per condition were analyzed for live imaging.

Prism software (GraphPad Software) was used for all statistical analyses.

3.4 Results

Design of membrane-bound antigen with homogenous and optimized orientation

In order to definably measure the effects of antigen density and valency on B cell activation, we modified a method described by Peluso et al. (*207*) to generate monobiotinylated Fab' fragment (mB-Fab') from F(ab')$_2$ fragment of antibody and tether it onto a streptavidin-coated surface as a microarray to quantify cytokines. We adapted this method to generate mB-Fab' fragment of antibody specific for mouse Ig, a component of the BCR, tethered to planar lipid bilayers. Similar to the published method, we use streptavidin as the linker to hold the mB-Fab' to the lipid bilayer containing biotinylated phospholipid (*63*). To generate the mB–Fab' from F(ab')$_2$-anti-mouse IgG+M, the disulfide bond that links the two Fab' fragments were disrupted using a reducing reagent, 2-mercaptoethylamine. Since all other disulfide bonds remain intact, this reducing reaction generates single sulfhydryl groups at the C-terminal region of each Fab' fragment. The sulfhydryl was then biotinylated with Maleimide-PEG2-Biotin and labeled with Alexa Fluor 546 **(Fig. 3.1 A)**. The binding of the biotin at the C-terminal region to lipid bilayers exposes the antigen binding site at the N-terminus, allowing Fab' to bind to mIg of the BCR. As all Fab' only has single biotin at the same cysteine, all mB-Fab' tethered to lipid bilayers will exhibit same orientation and binding ability to BCRs.

To determine whether mB-Fab'-anti-Ig stimulated BCRs as a bona fide antigen, we used a different stretagy to generate monobiotinylated hen egg lysozyme (mB-HEL) using NHS-PEG4-Biotin. This primary amine-targeted reagent has been shown to biotinylate on the N-terminus of HEL predominantly, which does not block
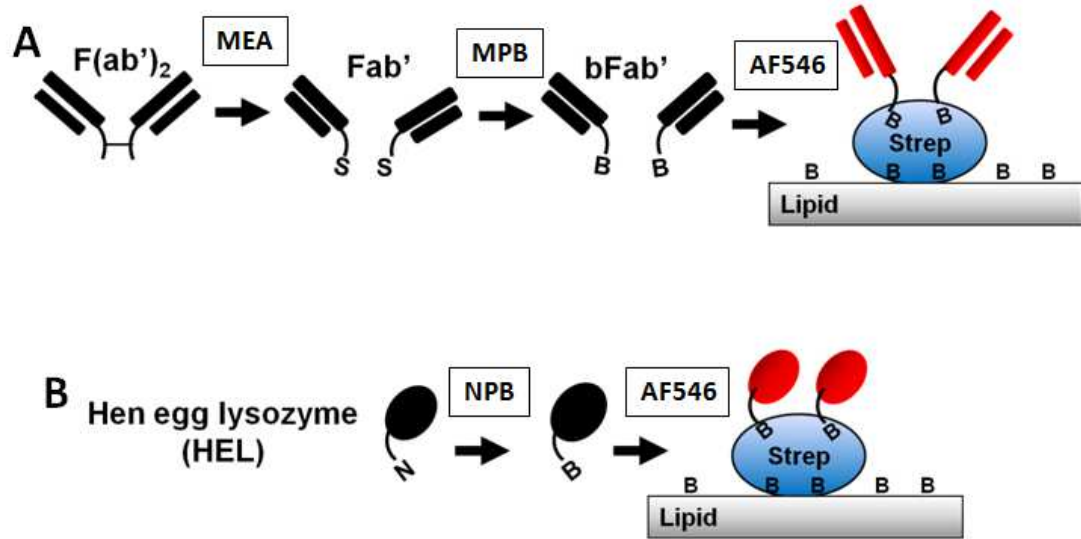
Fig. 3.1: Design of antigen presenting membranes with optimally oriented antigen. (A) To produce monobiotinylated goat anti-mouse IgM and IgG Fab' (bFab), the disulfide bonds of F(ab')$_2$ fragments were reduced by 2-Mercaptoethylamine (MEA) and the resulting sulfhydryls were biotinylated with Maleimide-PEG2-Biotin (MPB). The mB-Fab was then labeled with Alexa Fluor 546 (AF546). Oriented membrane bound antigen was made by coating coverslip chambers with biotinylated lipid, followed by streptavidin, and lastly mB-Fab. (B) Hen egg lysozyme (HEL) was biotinylated with NHS-PEG4-Biotin (NPB), which reacts with primary amines and for HEL this predominantly biotinylates the N-terminus and thus not likely to block the epitope for BCRs of MD4 mice. The biotinylated HEL (mB-HEL) was then labeled with AF 546. The same protocol for making oriented membrane bound mB-Fab was used for mB-HEL.

Image for bFab generation was modified from Peluso et al.Analytical Biochemistry.2003.312.113-124

the binding epitope for BCRs of B cells from MD4 mice (*208*). Similarly, the mB-HEL was then labeled with Alexa Fluor 546 **(Fig. 3.1 B)**.

Monobiotinylation of Fab' and HEL was confirmed by measuring the concentration of both proteins and biotin using Pierce Protein's EZ Biotin quantitation kit, ascertaining a 1:1 ratio of biotin to Fab' or HEL. We also removed $F(ab')_2$ that remained as residues of the reducing reaction using centrifugal filter with a molecular weight cutoff 100 kDa, and the purity was confirmed by Western Blot **(Fig 3.2 A)**. The purity of mB-Fab' was also determined biologically by its incapability of clustering BCRs in the absence of streptavidin. B cells from WT and MD4 mice were first labeled with Alexa Fluor (AF) 546-conjugated mB-Fab' and mB-HEL, respectfully, followed by with or without streptavidin to cross-link bAgs. Only B cells with streptavidin treatment had significant percentages of B cells exhibiting polarized clustering of BCRs to one pole of the cell, called BCR capping. Few B cells showed BCR caps in the absence of streptavidin **(Fig.3.2 B)**. Furthermore, the percentage of B cells showing BCR capping increased as the concentration of streptavidin increased **(Fig 3.2 C)**. These results demonstrate that the generated model Ags are monovalent and monobiotinylated, and after binding to BCRs, their conjugated biotin is readily available for streptavidin to bind.

B cell spreading, BCR clustering and signaling increase as the density of the membrane-bound antigen increases

Using the established model antigen system, we examined the effects of membrane bound antigen density on the early events of BCR activation. We changed antigen

99
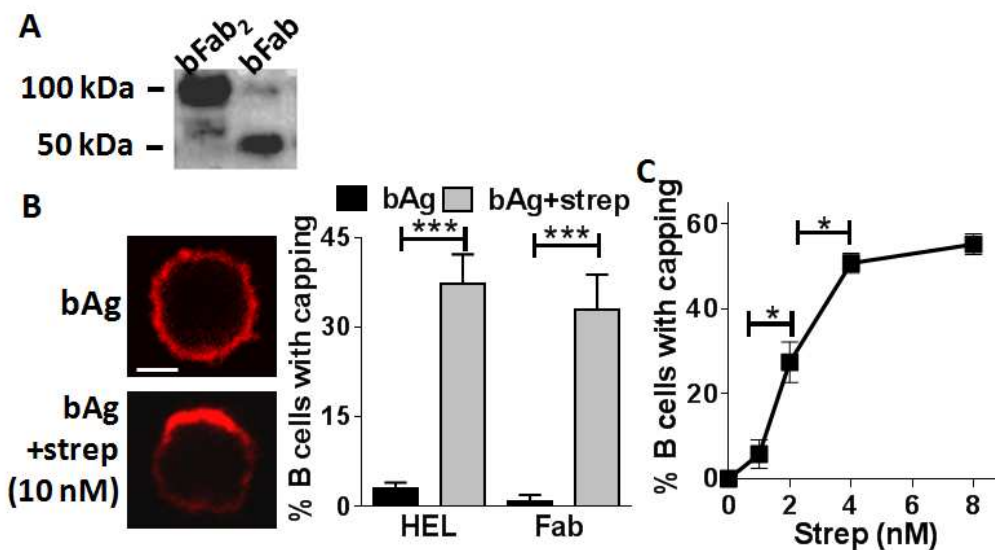
Fig. 3.2: Confirmation of monobiotinylated, monovalent antigen. (A) Western blot for biotin showing that the majority of biotinylated sample is Fab. (B) Testing monobiotinylation and monovalency of antigen by examining the percentage of BCR capping when streptavidin is added to cross-link the mB-Ag (bAg). WT and MD4 B cells were labeled with mB-Fab and mB-HEL respectfully, for 30 min at 4°C. Samples were then incubated with streptavidin for 10 min at 4°C, warmed to 37°C, and fixed at 5 min. Cells were imaged using fluorescence confocal microscopy and the percentage of capped cells were compared between with and without streptavidin. (C) The percentage of capped B cells was determined for increasing the concentration of streptavidin with mB-Fab labeled cells. Scale bar 2.5 μm. Shown is the mean of three independent experiments (± SD), *P≤0.05, ***P≤0.005, Students T Test.

density in two different ways. In the first way, we labeled surface BCRs with AF546-mB-Fab'-anti-Ig or AF546-mB-HEL first and let the B cells to interact with lipid bilayers coated with varying densities of streptavidin (1, 2, 4, 8 nM). This method allowed us to track BCR clustering. Similar to the results with soluble streptavidin, B cells only spread and formed clusters on lipid bilayers teathered with streptavidin. Using the 5-min time point when B cell spreading reached nearly maximal, we found that the B cell contact area and both the mean (MFI) and total fluorescence intensity (TFI) of AF546-Fab'-anti-Ig- or AF546-HEL-labeled BCRs in the contact zone were increased in a proportional fashion as the concentration of streptavidin, indicating streptavidin-dependent enhancement of B cell spreading and BCR clustering at 5 min **(Fig. 3.3 A, B)**. Next, we evaluated the overall signaling level induced by the BCR using phosphotyrosine (pY) staining. The TFI of pY increased dramatically as the density of streptavidin on lipid bilayers, however, the MFI of pY no longer increased when the concentration of streptavidin reached beyond 4 nM, even though the B cell contact area and the MFI of BCRs in the contact zone continuously increased, suggesting when BCR clustering reaches a certain level, it cannot enhance signaling further **(Fig. 3.3 C)**. These results demonstrate that both mB-Fab'-anti-Ig and mB-HEL are effective in stimulating BCRs as membrane bound antigen, and increasing density of streptavidin as cross-linkers proportionally increases B cell spreading, BCR clustering, and enhances BCR signaling.

The second way we changed the antigen density was by varying the amount of mB-Fab'-anti-Ig and mB-HEL to lipid bilayers (20, 60, 120 nM) while keeping the concentration of streptavidin (10 nM) unchanged. Again, we quantified the B cell

A

Fab: B-cell spreading   **BCR clustering**

B

HEL: B-cell spreading   **BCR clustering**

5 min

C

BCR signaling

HEL 5 min
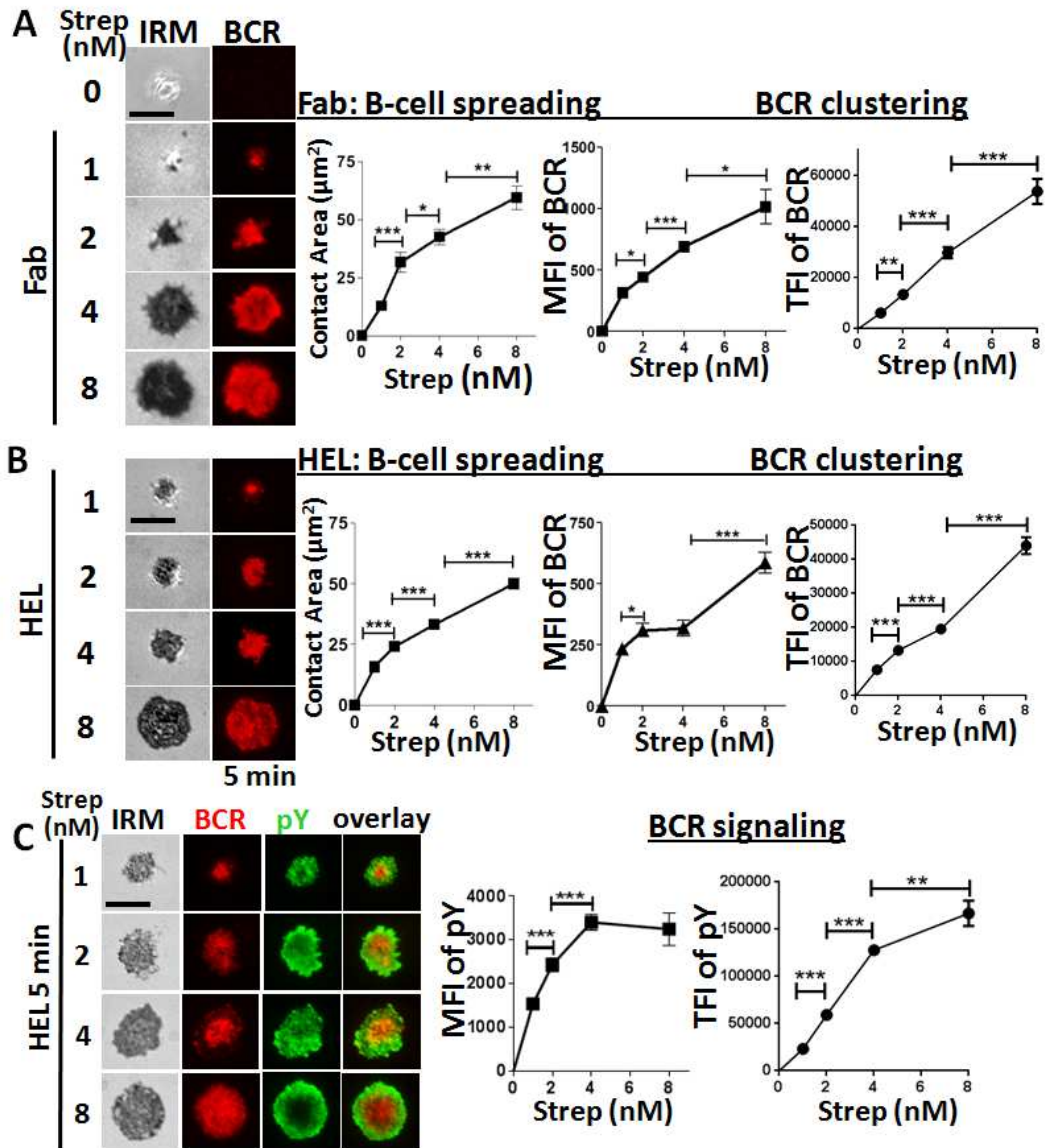
Fig. 3.3: Effects of antigen density on planar lipid bilayers on B cell spreading, BCR clustering, and BCR signaling by changing streptavidin concentration. B cells were labeled with AF546 bFab for 30 min at 4˚C before stimulation for 5 min at 37˚C with varying concentrations of streptavidin on lipid bilayers (A) Representative images using IRM and TIRFM of Alex Fluor 546 mB-Fab labeled B cells at 5 min time points on lipid bilayers containing increasing concentrations of streptavidin; and corresponding quantification of the B cell contact area and BCR mean fluorescence intensities. (B). Same as B, but testing AF546 mB-HEL with MD4 B cells. MD4 B cells were labeled with AF546 mB-HEL for 30 min at 4˚C and stimulated with varying densities of streptavidin tethered to lipid bilayers at 37˚C and fixed at 5 min time points. The samples were then permeabilized and stained for phosphotyrosine. (C) Representative IRM and TIRFM images showing phosphotyrosine distribution of Alexa Fluor 546 mB-HEL labeled cells stimulated with increasing concentrations of membrane bound streptavidin at 5 min time points; and corresponding quantification of the fluorescence intensities of pY in the B cell contact area with increasing concentrations of streptavidin for 5 min time points. Scale bars, 5 μm. Shown is the mean (±SEM), *P≤0.05, **P≤0.005, ***P≤0.0005, Students T Test. The results are representative of three independent experiments.

contact area and the MFI and TFI of antigen in the contact zone 5 min post stimulation. Similar to the B cell response to varying streptavidin densities, both B cell contact area and the MFI and TFI of antigen increased proportionally with increasing densities of antigen. These results together indicate that increasing the density of antigen on membranes enhances B cell activation **(Fig. 3.4)**.

To examine the effect of antigen density on the dynamics of B cell spreading and BCR clustering, time-lapse images were acquired using IRM and TIRF. Higher densities of mB-Fab induced greater levels of B cell spreading and contraction, and BCR fluorescence intensity over time in the contact area **(Fig. 3.5, A,B)**. The increase of BCR intensity in the contact area correlates with the enhanced BCR intensities of individual BCR microclusters tracked over time **(Fig. 3.5 C)**, indicating faster growth of BCR clusters. All together, these results suggest that increasing antigen density enhances B cell spreading and BCR clustering, which correlates to the intensity of individual BCR microclusters that grow and accumulate at the synapse.

Antigen density modulates the level and distribution of the actin cytoskeleton in the B cell contact zone

B cell spreading, BCR clustering and BCR signaling depend on actin dynamics (*67, 70*). The effects of antigen density on these signaling events suggest that antigen density also influences actin remodeling induced by BCR signaling. We examined actin dynamics by live cell images of B cells from mice expressing LifeAct-GFP that binds to F-actin, using IRM and TIRFM. B cells were stimulated with varying densities of AF546-mB- Fab'-anti-Ig on bilayers, and time-lapse images were
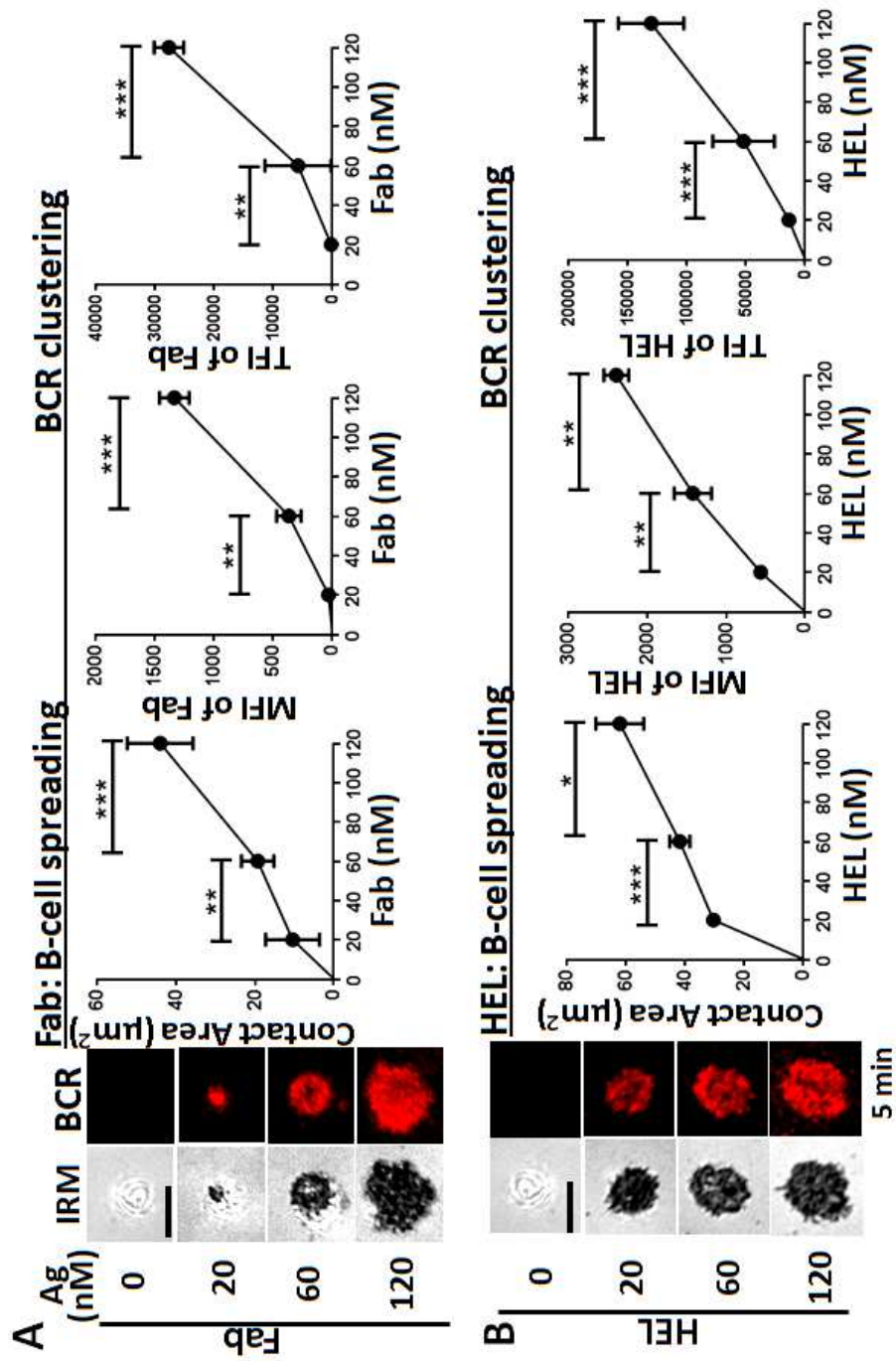
Fig. 3.4: B cell spreading and BCR clustering depends on the density of membrane bound antigen. (A) WT B cells were stimulated with the indicated densities of membrane bound mB-Fab at 37°and fixed at 5 min. Shown are representative IRM and TIRFM images showing the spreading and BCR clustering of B cells stimulated with varying concentrations of mB-Fab tethered to lipid bilayers. Scale bar, 5 μm. Graphs to the right show the quantitative analysis of the contact area and mean and total fluorescence intensities of clustered BCR in the B cell contact area. (B) MD4 B cells were stimulated with indicated concentrations of mB-HEL bound to lipid bilayers at 37° and fixed at 5 min. Shown are representative IRM and TIRFM images showing the spreading and antigen clustering of MD4 B cells stimulated with varying concentrations of mB-HEL tethered to lipid bilayers. Scale bar, 5 μm. Graphs to the right show the quantitative analysis of the contact area and mean and total fluorescence intensities of clustered BCR. Shown is the mean (±SEM). *P≤0.05, **P≤0.005, ***P<0.0001, Students T Test. The results are representative of three independent experiments.
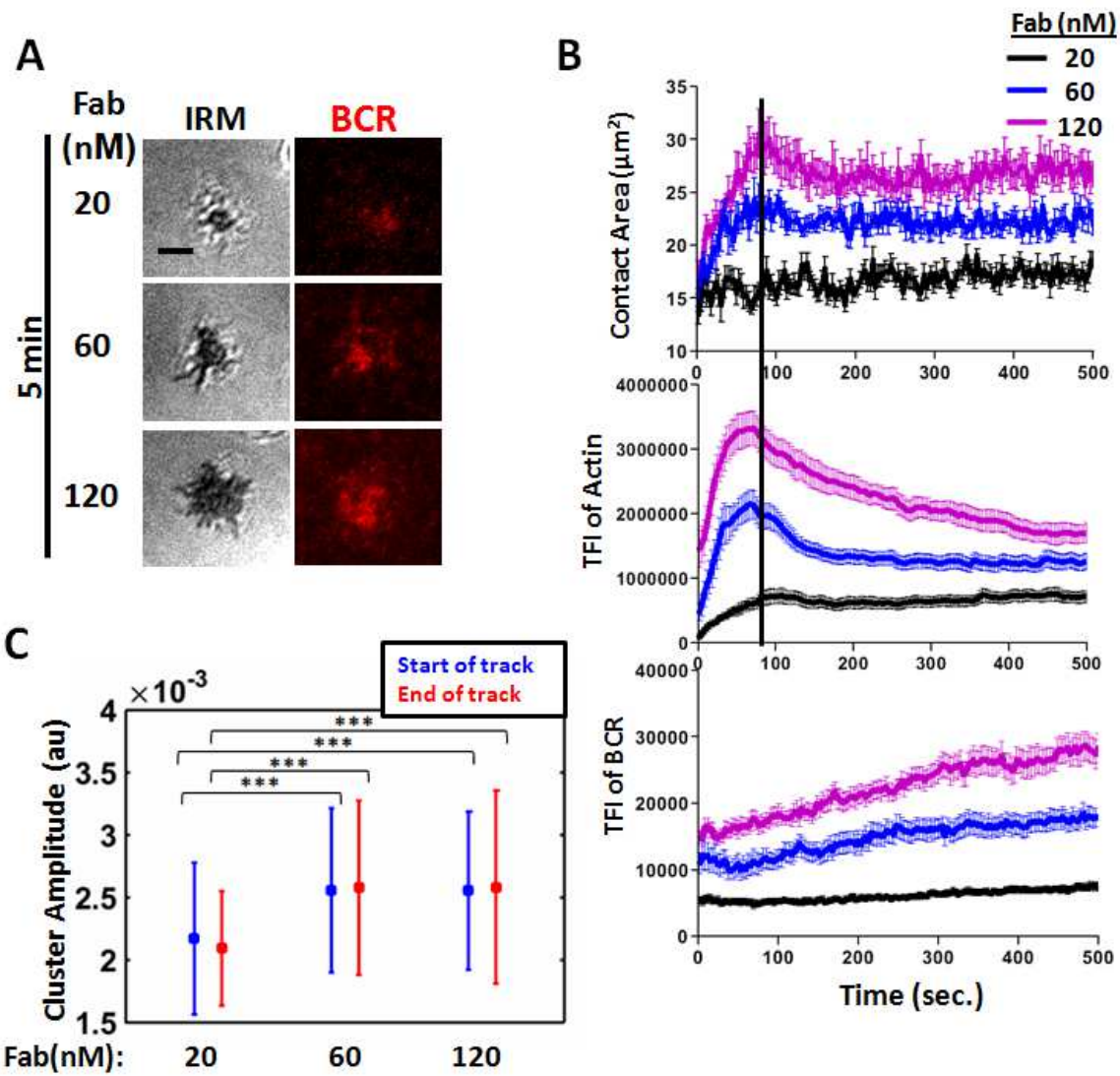
Fig. 3.5: The dynamics of B cell spreading, BCR clustering, and F-actin depends on the density of membrane bound antigen. (A) Representative IRM and TIRFM images of 5 min time points from live images of Lifeact B cells stimulated with increasing concentrations of mB-Fab tethered to lipid bilayers. (B) Analysis of live imaging of the contact area and total (integrated) fluorescence intensities of AF546 mB-Fab and F-actin (Lifeact-GFP) accumulation in the B cell contact area. Verticle line marks the time for the peak of B cell spreading. (C) Fluorescence intensities of individual BCR microclusters induced by the different densities of antigen. Individual BCR microclusters were tracked from their appearance (blue) to their fusion with other BCR microclusters (red). Scale bar, 5 μm. Shown is the mean (±SEM). ***P<0.0001, Students T Test. The results are representative of three independent experiments.

Cluster Amplitude analysis performed by Christy Ketchum

acquired 5 sec after dropping the cells onto lipid bilayers. TIRFM showed that for the lowest density of antigen (20 nM), B cells did not exhibit redistribution of Lifeact-GFP, and the MFI of Lifeact-GFP in the contact zone was much lower than those cells interacting with higher density of antigen **(Fig. 3.5 B; Fig. 3.6 A)**. To examine the spatial relationship of F-actin with spreading membrane, IRM and Lifeact-GFP TIRFM images were overlayed. The results demonstrated that F-actin primarily was accumulated at the periphery of the B cell contact area, forming an actin ring, when the antigen density was 60 nM and higher, but not when the antigen density was reduced to 20 nM **(Fig. 3.6 A, B)**. The greatest F-actin accumulation was seen at sites of actively extending membrane during B cell spreading **(Fig. 3.6 C)**. The intensity of the actin ring decreased during B cell membrane contraction and the highest mB-Fab density induced a greater contraction of the B cells **(Fig. 3.5 B; Fig. 3.6 A).** Measuring the integral of the autocorrelation function of the F-actin fluorescence intensity further demonstrated the lack of extension and retraction of membrane when stimulated with 20 nM, whereas densities of 60 nM and 120 nM induced high actin dynamics at the cell periphery, correlating to movement of the B cell membrane **(Fig. 3.6 D)**. Overall, these results reveal that a higher density of membrane antigen enhances F-actin intensity at the periphery of spreading membranes, which correlates to greater B cell spreading and contraction.

A

Fab (nM)	IRM	Actin	Overlay

1 min (Spreading): 20, 60, 120

5 min (Contraction): 20, 60, 120

B

Fab (nM) — 1 min Spreading | 5 min Contraction

IRM (blue) / Actin (green)

20, 60, 120

MFI — Point along line

C

Spreading Membrane — Actin accumulation

D

20 nM | 60 nM | 120 nM

8 — -2

110
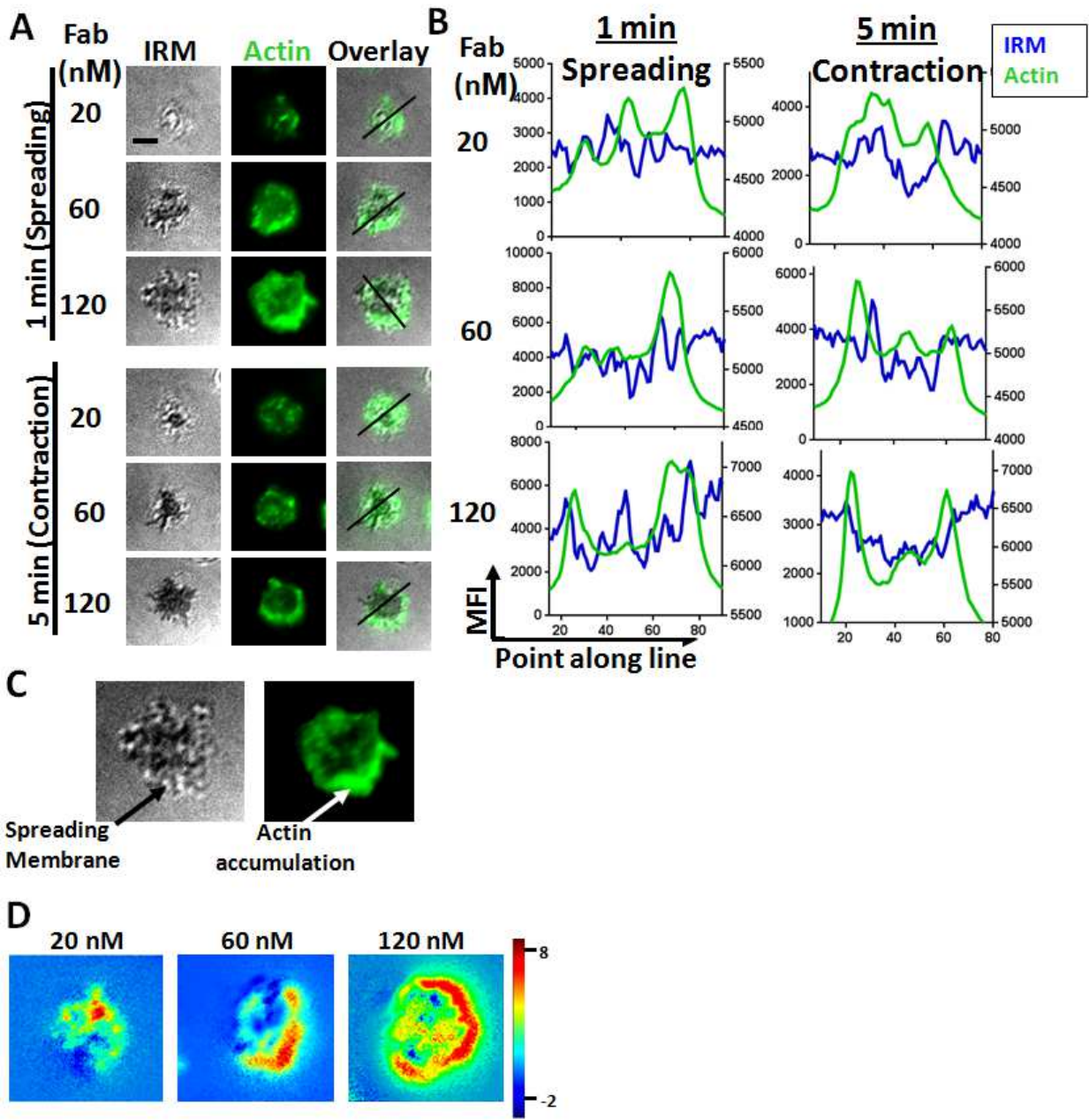
Fig. 3.6: F-actin intensity and distribution depends on the density of membrane bound mB-Fab. (A) Representative IRM and TIRFM images of 1 and 5 min time points from live images of Lifeact B cells stimulated with increasing densities of mB-Fab. 1 min images demonstrate B cell spreading and F-actin accumulation in spreading membranes. 5 min images show B cell membrane contraction and actin ring formation on the border of contact area. (B) Mean fluorescence intensity line profiles of 1 and 5 min times points revealing distribution of F-actin to periphery of contact area. Scale bar,5 μm. The results are representative of three independent experiments. (C) IRM and TIRFM images showing high F-actin intensity accumulated in actively spreading B cell membrane edges. Arrows point to spreading membrane in IRM and dense F-actin intensity in TIRFM image. (D) Integral of the autocorrelation function of the F-actin fluorescence intensity of each image pixel plotted at the original pixel position. High autocorrelations at the cell periphery indicate extensions and retractions of membrane.

Integral of autocorrelation function performed by Christy Ketchum

We have already shown that greater densities of antigen induce enhanced actin dynamics that corresponds to B cell spreading. Actin dynamics are known to mediate BCR clustering and synapse formation. We examined the effects of antigen density on actin and BCR dynamics in the B cell contact area over time. Looking at the fluorescence intensity of BCR clustering over time, it is seen to correlate with actin dynamics. The greater F-actin intensities induced by higher densities of antigen lead to greater BCR clustering, indicating that BCR clustering correlates with actin dynamics **(Fig. 3.5 B)**. Examining the distribution of F-actin and BCR using TIRFM, it was seen that the higher densities induced synapse formation, as seen by the actin ring formation bordering clustered BCRs in the center of the contact area **(Fig. 3.7, A, B)**. The 20 nM density failed to induce BCR clustering and formation of the actin ring typically seen bordering the central BCR cluster **(Fig. 3.7, A, B)**. Taken together, these results indicate that BCR clustering corresponds to actin dynamics, and both depend on antigen density for enhanced intensities in the contact area and distribution to form the synapse.
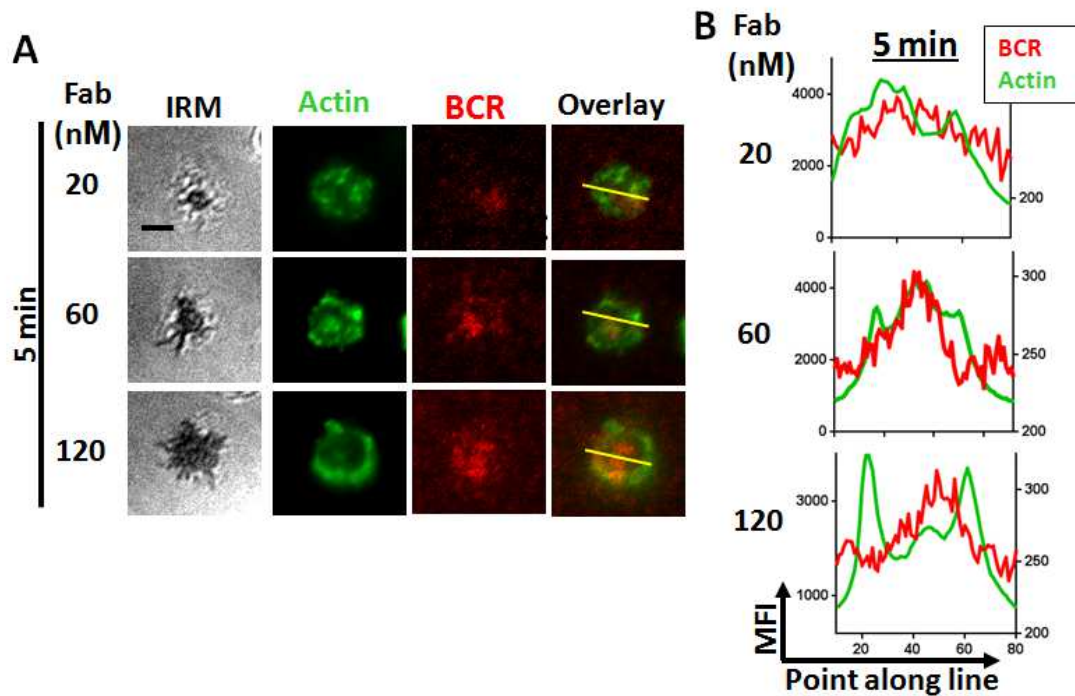
Fig. 3.7: The density of membrane bound antigen effects BCR clustering via actin dynamics (A) Representative IRM and TIRFM images of 5 min time points from live images of Lifeact B cells stimulated with increasing concentrations of mB-Fab tethered to lipid bilayers. Images demonstrate F-actin ring that borders BCRs to form a synapse. (B) Mean fluorescence intensity line profiles of 5 min time point images from (A), revealing F-actin distribution to outside of aggregated BCR. Scale bar, 5 µm. The results are representative of three independent experiments.

The B cell response to membrane bound antigen does not depend on the antigen's valency

To determine the role of antigen valency on B cell activation, we developed a membrane bound antigen system presenting optimally oriented antigen as either monovalent or bivalent **(Fig. 3.8 A)**. Monovalent antigen was made by using a 1:1 ratio of streptavidin to bFab and bivalent used half the streptavidin concentration at a1: 2 ratio. The mean fluorescence intensities were measured to affirm the same densities of antigen for both valency systems **(Fig. 3.8 B)**, thus indicating the valency of each system is correct. WT primary mouse B cells were stimulated with either monovalent or bivalent antigen and B cell spreading, antigen accumulation, and BCR signaling was measured to determine differences in B cell activation. Comparing monovalent to bivalent, there was no significant differences in B cell activation **(Fig. 3.9)**. These results demonstrate that the valency of membrane bound antigen does not affect B cell activation.
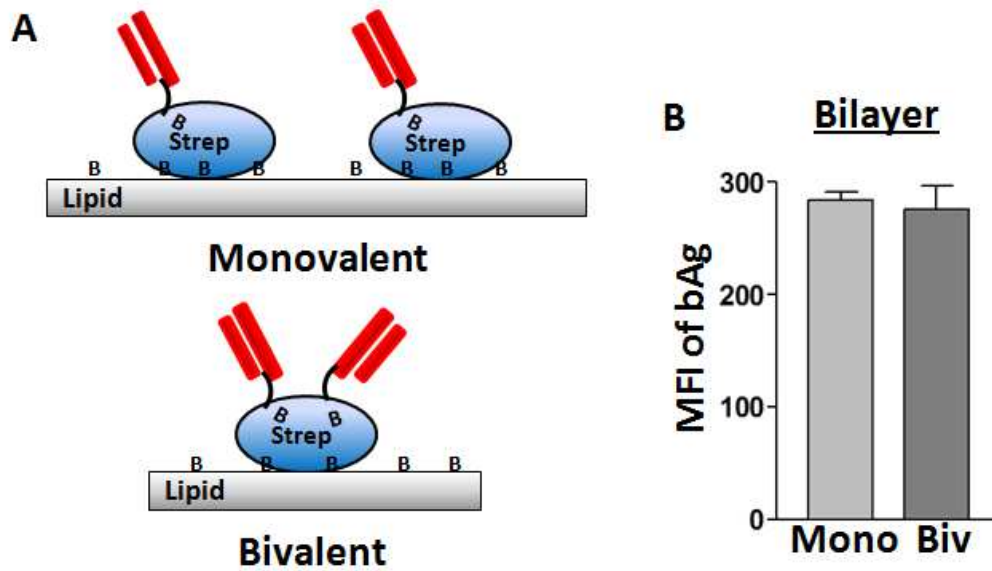
Fig. 3.8: Design of membrane bound valency system. (A) A monovalent membrane bound antigen system was developed using a 1:1 mB-Fab to streptavidin ratio, while for bivalent, a 2:1 mB-Fab to streptavidin ratio was used with half the streptavidin density. (B) Confirmation that the antigen density for both systems was the same, indicating that the valency is increased for the bivalent system. The mean fluorescence intensities of both systems were taken for comparison using TIRFM. Shown is the mean (±SD). The results are representative of three independent experiments.
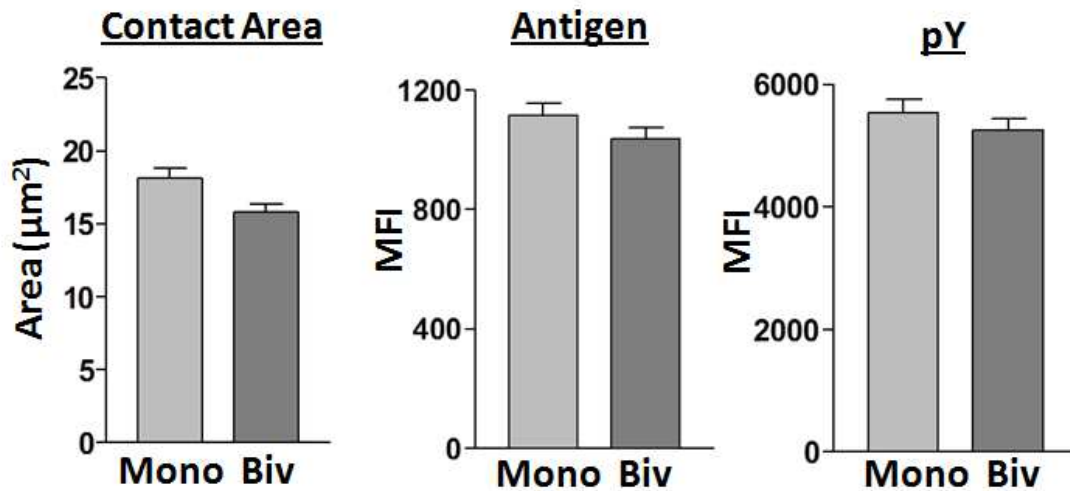
Figure 3.9: The valency of membrane bound antigen has little effect on B cell spreading, antigen clustering, and signaling. WT B cells were stimulated with either monovalent or bivalent mB-Fab on lipid bilayers and fixed at 5 min. The samples were then permeabilized and stained for pY. Quantification of IRM and TIRFM images of the contact area, mean fluorescence intensity of gathered antigen, and mean fluorescence intensity of phosphotyrosine for B cells interacting with either monovalent or bivalent antigen on the lipid bilayer. Shown is the mean (±SD). The results are representative of three independent experiments.

3.5 Discussion

This study addresses the role of antigen properties on B-cell activation. Increasing the affinity, valency, or concentration of soluble antigen enhances B cell activation (*25, 80, 116*). However, the effects of the properties of membrane bound antigen on B-cell activation requires further examination. The majority of antigens *in vivo* are presented to B cells as membrane bound (*23*), suggesting the importance of studying the effects of membrane bound antigen on B-cell activation. Previous studies have shown that increasing the density of membrane bound antigen enhances B cell spreading and antigen accumulation (*64*), yet the effects on actin dynamics have not been determined and the optimal antigen density for BCR activation and exactly how antigen density regulates BCR activation still remains elusive. Plus there are no well-defined antigenic stimulatory systems to use for studying the effects of antigen density and valency on BCR activation. The current membrane bound antigen systems have no way of determining the exact antigen density or valency presented to BCRs.

We developed a novel antigen system to present homogeneous optimally oriented antigen on artificial membranes. Using both Fab' and HEL, we generated antigens that were shown to be monovalent and monobiotinylted, thus obtaining optimal orientation when added to streptavidin coated biotinylated lipid bilayers. This system was demonstrated to be effective for studying the role of density and valency of membrane bound antigen on B-cell activation.

Our system showed that increasing antigen density proportionally increases B cell spreading, BCR clustering, and BCR signaling. Live imaging of LifeAct B cells,

demonstrated that higher antigen densities enhances actin dynamics, which corresponds to greater B cell spreading and BCR clustering. Previous studies from my lab have shown that actin distributes to the edges of the spreading membrane and then forms a ring around the antigen to form the synapse (*61, 73*), this was also seen, and we further demonstrated the role of antigen density on F-actin intensity and distribution. Low antigen density induced decreased actin dynamics, inhibiting B cell spreading and BCR clustering. Since spreading was inhibited, F-actin did not distribute to the edges of spreading membranes and failed to form a synapse. Increasing antigen density enhanced F-actin intensities at the leading edges of the spreading membrane and this in turn related to greater B cell spreading and BCR clustering. These results coincide with previous studies showing increasing densities of membrane antigen enhances B cell spreading and antigen accumulation (*64*), however, our quantification further reveals that the increased B cell activation is proportional to the increase in antigen density. Our work further demonstrates the role of antigen density on actin dynamics and how this relates to B cell activation.

In contrast to antigen density, valency had no effect on B cell spreading, antigen accumulation, or BCR signaling. This data supports the finding that monovalent membrane bound antigen still induces B cell activation due to the induced conformational change in the BCR, which initiates BCR oligomerization (*68*). Thus when presented on membranes, the valency of an antigen has little effect on increasing BCR clustering and initiating signaling and spreading.

Our work suggests that density of membrane bound antigen rather then valency is crucial for activating B cells. Also the orientation of antigen is important,

as presentation of the same epitope at high density induces enhanced B-cell activation on a linear level. The exact density of membrane bound antigen required for efficient B-cell activation has not been determined, but we designed a system where this is possible to do, thus our model will benefit quantitative studies of the molecular mechanisms underlying BCR activation. The results here indicate that manipulations of an antigen's molecular configuration and density can be applied to enhance the immunogenicity of vaccines. Overall, we created an antigen system that will be useful for examining the mechanism of B cell activation *in vivo* and which properties and configurations of antigen would be important for further work in vaccine development.

Chapter 4: Discussion

B cell membrane repair

Mechanism of Repair

We have demonstrated that B cells repair their plasma membranes in a calcium dependent manner. Calcium has been known for decades to be important for membrane repair (*137-139*). The influx of calcium triggers exocytosis of lysosomes in epithelial and muscle cells (*142-144*). This was also seen with B cells after SLO treatment, where there was LIMP2 surface staining and detection of ASM in the surrounding media. Examining whether ASM is required for B cell membrane repair, we discovered using inhibitors and ASM KO mice, that it is important since repair decreased, however, ASM KO mice still repair their cells, thus indicating there may be other lysosomal proteins that may compensate.

After lysosomal exocytosis, it has been suggested that the damaged membrane is removed from the membrane surface by either blebbing and vesicle shedding or endocytosis (*156-159*). We saw no blebbing during live imaging of B cells during SLO treatment or with TEM images; however, there was an increase in internalization of the fluid phase endocytic marker, dextran, after SLO treatment. Also addition of extracellular SM enhanced B cell membrane repair in the absence of calcium after SLO damage, suggesting that inducing internalization alone aids repair. Examining endocytosis of the plasma membrane after injury, it was discovered that

lipid raft internalization was increased using CTB as a lipid raft marker. This increase in lipid raft internalization correlates with previous work demonstrating that cholesterol and caveolin are required for membrane repair of epithelial cells (*157, 158*).

B cells do not express any known form of caveolin (*176, 197-199*), thus it is of interest to examine the types of vesicles the CTB are endocytosed into. Caveolae are responsible for endocytosis of proteins associated with lipid rafts (*196*) and are identified in TEM images as ~80 nm diameter with flask- or omega-shaped plasma membrane invaginations (*176*). Examining our TEM images, no such caveolae invaginations were observed. Although B cells lack caveolin, they still have lipid raft internalization. In fact, BCR internalization requires lipid rafts, actin, and clathrin (*85, 86, 94*). B cells have also been shown to have clathrin-independent internalization, which depends on lipid rafts and actin dynamics (*86*). We have demonstrated that inhibiting actin polymerization reduces B-cell membrane repair, implying that actin remodeling may play a role in one of the steps for membrane repair, which possibly could be internalization. Determining whether actin is required for endocytosis for B cell membrane repair requires further investigation.

Examination of CTB positive vesicles revealed that there was an increase of the lipid raft into tubular-shaped vesicles. Previous identification of these type of structures have been made and are classified as lipid raft-dependent, actin-dependent, and clathrin-independent (*211*). From our TEM images these tubular vesicles do not appear to be clathrin-coated. Tubular vesicles are known to form from the B subunit of Shiga toxin binding to glycosphingolipids (*212*), however, how these vesicles form

and what promotes their formation is unknown (*211, 212*). For B cell membrane repair, these structures may be induced by ASM, which has been demonstrated to induce inward curvature of membranes via production of ceramide from sphingomyelin (*138, 143, 158*). Also, as B cells do not express caveolin, the ASM induced invagination of lipid raft may not be caught and held into small vesicles at the membrane surface, but rather is pushed inward until endocytic molecules are recruited from the cytoplasm. This may be investigated by treatment of B cells with extracellular SM to see if the same tubular structures are formed.

Our results have shown that B cells repair in a similar manner as epithelial and muscle cells, although with several differences that may be due to lack of caveolin, demonstrating a new mechanism for repair. Like epithelial and muscle cells, B cells repair in a calcium dependent exocytosis of lysosomes, which releases ASM to the plasma membrane surface and induces internalization of lipid rafts. Differing from these cells, B cells internalize the lipid rafts into tubular-shaped vesicles; also B cells rely on actin reorganization, but whether it is for internalization requires investigation. Previous work has shown that epithelial cells do not require actin remodeling for membrane repair and that disruption of the actin cytoskeleton actually enhanced endocytosis and repair (*157, 158*). Additionally, epithelial cells do not require dynamin for endocytosis for repair (*139, 162*). Whether the tubular vesicles require dynamin for internalization induced B cell repair is not known, however, other studies have shown that the tubular vesicles may be dynamin dependent or independent (*211*).

We mapped out a repair mechanism for B cells injured with SLO. SLO binds to cholesterol and therefore may alter lipid rafts and modulate membrane repair. Hence, it is important to examine B cell membrane repair of mechanical wounding, such as scratching. Other studies of mechanical wounding have demonstrated that cholesterol and caveolin are required for repair (*157, 158*), indicating that B cells may still repair in a similar mechanism for mechanical wounding.

Effect of membrane repair on B cell activation

We have demonstrated that there may be competition for lipid rafts between repair and BCR activation, as both events interfere with one another. Cross-linking BCRs decreased CTB internalization and repair. BCR activation not only decreased CTB internalization overall, but it also decreased CTB internalization into tubular vesicles. This suggests that BCR activation modulates lipid raft surface distribution, which prevents the availability of rafts for endocytosis and repair.

B cells require lipid rafts for BCR clustering, BCR signaling, and antigen internalization (*85, 93, 164, 165*). Membrane wounding decreased BCR capping and co-capping with lipid rafts. BCR signaling and antigen internalization were also decreased significantly. These results imply that membrane damage by SLO prevents BCRs from entering lipid rafts and thus inhibits overall B cell activation. This is a new finding and demonstrates that membrane injury and repair disrupts lipid rafts that are important for surface receptor signaling. These findings correlate with how the Epstein Barr Virus (EBV) inhibits BCR signaling and internalization by occupying lipid rafts through latent membrane protein 2A

(LMP2A). LMP2A has a binding site for Lyn, which enables it to reside within lipid rafts and exclude BCRs, which prevents BCRs from entering the lipid rafts to signal and internalize antigen (*165, 166*).

Further investigation of the competition for lipid raft, we examined internalization of CTB in relation to BCR. Activation of BCRs induces co-localization of lipid rafts with BCR on the cell surface and internalization together into the same vesicles (*164*). SLO treatment decreased this co-localization and the separation of BCRs from CTB started as early as 1 min on the cell surface. The increase of internalization into separate compartments strongly suggests that there is competition for lipid rafts.

Membrane repair inhibits B cell activation by competing for the same lipid rafts, which decreases the amount of raft available for BCR clustering, BCR signaling, and antigen internalization. The impact this has on later stages of B cell activation and immunological functions requires investigation. There are several possible outcomes for repaired B cells. They could recover completely and regain functions for BCR clustering, signaling, and antigen internalization. Or repaired B cells may lose the ability to become activated and are prevented from presenting antigen to T helper cells, thus blocking development into plasma cells and memory B cells. Another possibility is for the repaired B cell to become inert and function to present antigen to other B cells. We have shown that SLO treatment decreases antigen internalization, which means the antigen will remain on the B cell's surface and is accessible to other B cells. A previous study demonstrated that SLO secreted by

group A streptococcus (GAS) induces keratinocyte lysosomal exocytosis to sites of plasma membrane not localized with the GAS, this then inhibits uptake of the bacteria (*213*). Although this is a strategy used by bacteria to avoid internalization and destruction, in the case of B cells, which are small motile cells, they may migrate to present the bacteria to other B cells.

B cell membrane damage *in vivo*

Although we have not demonstrated that B cells have their membranes damaged *in vivo*, there exists many possibilities for membrane wounding. B cells may have their membranes damaged by bacterial toxins or mechanically injured during migration or by other cell-cell interactions. Lymphocytes extravasate, migrating through endothelial cells to reach infected sites and they also migrate through dense and well-organized lymphoid tissues. Squeezing through these tight spaces is liable to tear membranes. Activated B cells may transfer portions of their plasma membrane along with BCRs to bystander B cells through close cell-cell contact (*170*). Also B cells serve as APCs and T cells and B cells are able to remove membrane from APCs while extracting antigen (*84, 125*). When B cells enter infected sites, they are likely to come in contact with bacteria and bacterial toxins. There are approximately thirty bacterial species that produce pore forming toxins and many of the pore-forming toxins are cholesterol dependent cytolysins (*126, 127*).

We have shown that SLO treatment inhibits B cell activation; this may prevent antibody production and memory B cell development. Thus it is important to

determine how and where B cells are damaged and what implications this may have for immunity and disease.

Properties of antigen and B cell activation

Increasing the valency or concentration of soluble antigen enhances B cell activation (*25, 80, 116*). We sought to determine whether this is the case for membrane-bound antigen, since the majority of antigens *in vivo* are presented to B cells as membrane bound (*23*). Previous studies have shown that increasing the density of membrane bound antigen enhances B cell spreading and antigen accumulation (*64*), however, the current membrane bound antigen systems do not present monovalent antigen that is correctly oriented for directly binding BCRs. We established and characterized a membrane-bound antigen system where all antigenic molecules are optimally orientated for BCR binding. Using both Fab' and HEL, we generated antigens that were shown to be monovalent and monobiotinylted, thus obtaining optimal orientation when added to streptavidin coated biotinylated lipid bilayers.

Using these optimally oriented systems, we determined the role of the density and valancy of membrane-bound antigen on BCR activation. The results show that increases in the density, but not valency of antigen on membranes significantly enhance the magnitudes of the early events of BCR activation. Increasing antigen density proportionally increases B cell spreading, BCR clustering, and BCR signaling. Live imaging of LifeAct B cells, demonstrated that higher antigen densities enhanced actin dynamics, which corresponds to greater B cell spreading and BCR clustering. Previous studies from my lab have shown that actin distributes to the

edges of the spreading membrane and then forms a ring around the antigen to form the synapse (*61, 73*), this was also seen, and we further demonstrated the role of antigen density on actin intensity and distribution. Low antigen density induced decreased actin dynamics, inhibiting B cell spreading and BCR clustering. Increasing antigen density enhanced actin intensities at the edges of the spreading membrane and this in turn related to greater B cell spreading and BCR clustering. These results coincide with previous studies showing increasing densities of membrane antigen enhances B cell spreading and antigen accumulation. Our work further demonstrates that the increase in B cell activation is proportional to the increase in antigen density and this enhanced activation is correlated with greater actin dynamics required for BCR aggregation, B-cell spreading and signaling.

In contrast to antigen density, valency had no effect on B cell spreading, antigen accumulation, or BCR signaling. This data supports the finding that monovalent membrane bound antigen still induces B cell activation due to the induced conformational change in the BCR, which initiates BCR oligomerization (*68*). Thus when presented on membranes, the valency of an antigen has little effect on increasing BCR clustering and initiating signaling and spreading.

Our work suggests that density of membrane bound antigen rather then valency is crucial for activating B cells. Also the orientation of antigen is important, as presentation of the same epitope at high density induces enhanced B-cell activation. The exact density of membrane bound antigen required for efficient B-cell activation has not been determined, but we designed a system where this is possible to do, thus our model will benefit quantitative studies of the molecular mechanisms

underlying BCR activation. The results here indicate that manipulations of an antigen's molecular configuration and density can be applied to enhance the immunogenicity of vaccines.

Bibliography

1. S. Akira, K. Takeda, Toll-like receptor signalling. *Nat Rev Immunol* **4**, 499-511 (2004).

2. K. Newton, V. M. Dixit, Signaling in innate immunity and inflammation. *Cold Spring Harb Perspect Biol* **4**, (2012).

3. R. Medzhitov, Recognition of microorganisms and activation of the immune response. *Nature* **449**, 819-826 (2007).

4. A. Iwasaki, R. Medzhitov, Regulation of adaptive immunity by the innate immune system. *Science* **327**, 291-295 (2010).

5. A. Iwasaki, R. Medzhitov, Toll-like receptor control of the adaptive immune responses. *Nat Immunol* **5**, 987-995 (2004).

6. D. T. Fearon, R. M. Locksley, The instructive role of innate immunity in the acquired immune response. *Science* **272**, 50-53 (1996).

7. D. Jung, C. Giallourakis, R. Mostoslavsky, F. W. Alt, Mechanism and control of V(D)J recombination at the immunoglobulin heavy chain locus. *Annu Rev Immunol* **24**, 541-570 (2006).

8. K. L. Wolniak, R. J. Noelle, T. J. Waldschmidt, Characterization of (4-hydroxy-3-nitrophenyl)acetyl (NP)-specific germinal center B cells and antigen-binding B220- cells after primary NP challenge in mice. *J Immunol* **177**, 2072-2079 (2006).

9. B. A. Cobb, Q. Wang, A. O. Tzianabos, D. L. Kasper, Polysaccharide processing and presentation by the MHCII pathway. *Cell* **117**, 677-687 (2004).

10. F. Y. Avci, X. Li, M. Tsuji, D. L. Kasper, Carbohydrates and T cells: a sweet twosome. *Semin Immunol* **25**, 146-151 (2013).

11. J. C. Cambier, S. B. Gauld, K. T. Merrell, B. J. Vilen, B-cell anergy: from transgenic models to naturally occurring anergic B cells? *Nature Reviews Immunology* **7**, 633-643 (2007).

12. K. Okkenhaug, B. Vanhaesebroeck, PI3K in lymphocyte development, differentiation and activation. *Nat Rev Immunol* **3**, 317-330 (2003).

13. A. G. Rolink *et al.*, B cell development in the mouse from early progenitors to mature B cells. *Immunol Lett* **68**, 89-93 (1999).

14. R. R. Hardy, K. Hayakawa, B cell development pathways. *Annu Rev Immunol* **19**, 595-621 (2001).

15. S. B. Hartley *et al.*, Elimination of self-reactive B lymphocytes proceeds in two stages: arrested development and cell death. *Cell* **72**, 325-335 (1993).

16. R. Carsetti, M. M. Rosado, H. Wardmann, Peripheral development of B cells in mouse and man. *Immunol Rev* **197**, 179-191 (2004).

17. F. Loder *et al.*, B cell development in the spleen takes place in discrete steps and is determined by the quality of B cell receptor-derived signals. *J Exp Med* **190**, 75-89 (1999).

18. D. Allman *et al.*, Resolution of three nonproliferative immature splenic B cell subsets reveals multiple selection points during peripheral B cell maturation. *J Immunol* **167**, 6834-6840 (2001).

19. C. Grönwall, J. Vas, G. J. Silverman, Protective Roles of Natural IgM Antibodies. *Front Immunol* **3**, (2012).

20. P. J. Rauch *et al.*, Innate response activator B cells protect against microbial sepsis. *Science* **335**, 597-601 (2012).

21. T. Defrance, M. Taillardet, L. Genestier, T cell-independent B cell memory. *Curr Opin Immunol* **23**, 330-336 (2011).

22. S. Pillai, A. Cariappa, S. T. Moran, Marginal zone B cells. *Annu Rev Immunol* **23**, 161-196 (2005).

23. F. D. Batista, N. E. Harwood, The who, how and where of antigen presentation to B cells. *Nat Rev Immunol* **9**, 15-27 (2009).

24. U. Klein, R. Dalla-Favera, Germinal centres: role in B-cell physiology and malignancy. *Nature Reviews Immunology* **8**, 22-33 (2008).

25. D. Paus *et al.*, Antigen recognition strength regulates the choice between extrafollicular plasma cell and germinal center B cell differentiation. *J Exp Med* **203**, 1081-1091 (2006).

26. J. Stavnezer, C. E. Schrader, in *J Immunol*. (Inc., 2014), vol. 193, pp. 5370-5378.

27. C. G. Vinuesa, I. Sanz, M. C. Cook, Dysregulation of germinal centres in autoimmune disease. *Nature Reviews Immunology* **9**, 845-857 (2009).

28. A. Radbruch *et al.*, Competence and competition: the challenge of becoming a long-lived plasma cell. *Nature Reviews Immunology* **6**, 741-750 (2006).

29. I. Chernova *et al.*, Lasting antibody responses are mediated by a combination of newly formed and established bone marrow plasma cells drawn from clonally distinct precursors. *J Immunol* **193**, 4971-4979 (2014).

30. D. J. Driver, L. J. McHeyzer-Williams, M. Cool, D. B. Stetson, M. G. McHeyzer-Williams, Development and maintenance of a B220- memory B cell compartment. *J Immunol* **167**, 1393-1405 (2001).

31. L. J. McHeyzer-Williams, M. Cool, M. G. McHeyzer-Williams, Antigen-specific B cell memory: expression and replenishment of a novel b220(-) memory b cell compartment. *J Exp Med* **191**, 1149-1166 (2000).

32. J. Charles A Janeway, P. Travers, M. Walport, M. J. Shlomchik, The structure of a typical antibody molecule. (2001).

33. D. C. Parker, T cell-dependent B cell activation. *Annu Rev Immunol* **11**, 331-360 (1993).

34. L. J. McHeyzer-Williams, L. P. Malherbe, M. G. McHeyzer-Williams, Helper T cell-regulated B cell immunity. *Curr Top Microbiol Immunol* **311**, 59-83 (2006).

35. C. C. Goodnow, C. G. Vinuesa, K. L. Randall, F. Mackay, R. Brink, Control systems and decision making for antibody production. *Nat Immunol* **11**, 681-688 (2010).

36. A. Gonzalez-Fernandez, J. Faro, C. Fernandez, Immune responses to polysaccharides: lessons from humans and mice. *Vaccine* **26**, 292-300 (2008).

37. G. B. Lesinski, M. A. Westerink, Novel vaccine strategies to T-independent antigens. *J Microbiol Methods* **47**, 135-149 (2001).

38. Q. Vos, A. Lees, Z. Q. Wu, C. M. Snapper, J. J. Mond, B-cell activation by T-cell-independent type 2 antigens as an integral part of the humoral immune response to pathogenic microorganisms. *Immunol Rev* **176**, 154-170 (2000).

39. D. J. Rawlings, M. A. Schwartz, S. W. Jackson, A. Meyer-Bahlburg, Integration of B cell responses through Toll-like receptors and antigen receptors. *Nat Rev Immunol* **12**, 282-294 (2012).

40. M. R. Clark *et al.*, The B cell antigen receptor complex: association of Ig-alpha and Ig-beta with distinct cytoplasmic effectors. *Science* **258**, 123-126 (1992).

41. R. Michael, The B-cell antigen receptor complex and co-receptors. *Immunology Today* **16**, 310-313 (1995).

42. J. M. Dal Porto *et al.*, B cell antigen receptor signaling 101. *Mol Immunol* **41**, 599-613 (2004).

43. T. Kurosaki, Regulation of B-cell signal transduction by adaptor proteins. *Nat Rev Immunol* **2**, 354-363 (2002).

44. H. W. Sohn, P. Tolar, S. K. Pierce, Membrane heterogeneities in the formation of B cell receptor-Lyn kinase microclusters and the immune synapse. *J Cell Biol* **182**, 367-379 (2008).

45. A. M. Scharenberg, L. A. Humphries, D. J. Rawlings, Calcium signalling and cell-fate choice in B cells. *Nat Rev Immunol* **7**, 778-789 (2007).

46. M. R. Gold, To make antibodies or not: signaling by the B-cell antigen receptor. *Trends Pharmacol Sci* **23**, 316-324 (2002).

47. T. Kurosaki, Regulation of BCR signaling. *Mol Immunol* **48**, 1287-1291 (2011).

48. A. H. L. A. K. Abbas, *Cellular and Molecular Immunology Updated 5th Edition (Updated Fifth Edition).* (2005).

49. H. W. Sohn, P. Tolar, T. Jin, S. K. Pierce, Fluorescence resonance energy transfer in living cells reveals dynamic membrane changes in the initiation of B cell signaling. *Proc Natl Acad Sci U S A* **103**, 8143-8148 (2006).

50. P. Engel *et al.*, Abnormal B lymphocyte delevopment, activation, and differentiation in mice that lack or overexpress the CD19 signal transduction molecule. *Immunity* **3**, 39-50 (1995).

51. R. C. Rickert, K. Rajewsky, J. Roes, Impairment of T-cell-dependent B-cell responses and B-l cell developmentin CD19-deficient mice. **376**, 352-355 (1995).

52. I. Isnardi *et al.*, Two distinct tyrosine-based motifs enable the inhibitory receptor FcgammaRIIB to cooperatively recruit the inositol phosphatases SHIP1/2 and the adapters Grb2/Grap. *J Biol Chem* **279**, 51931-51938 (2004).

53. H. Phee, W. Rodgers, K. M. Coggeshall, Visualization of negative signaling in B cells by quantitative confocal microscopy. *Mol Cell Biol* **21**, 8615-8625 (2001).

54. W. Liu, H. W. Sohn, P. Tolar, T. Meckel, S. K. Pierce, Antigen-Induced Oligomerization of the B Cell Receptor Is an Early Target of FcγRIIB Inhibition. *J Immunol* **184**, 1977-1989 (2010).

55. R. A. Floto *et al.*, Loss of function of a lupus-associated FcgammaRIIb polymorphism through exclusion from lipid rafts. *Nat Med* **11**, 1056-1058 (2005).

56. Y. R. Carrasco, F. D. Batista, B cells acquire particulate antigen in a macrophage-rich area at the boundary between the follicle and the subcapsular sinus of the lymph node. *Immunity* **27**, 160-171 (2007).

57. D. Depoil *et al.*, Early events of B cell activation by antigen. *Sci Signal* **2**, pt1 (2009).

58. N. E. Harwood, F. D. Batista, New insights into the early molecular events underlying B cell activation. *Immunity* **28**, 609-619 (2008).

59. P. Tolar, H. W. Sohn, S. K. Pierce, Viewing the antigen-induced initiation of B-cell activation in living cells. *Immunol Rev* **221**, 64-76 (2008).

60. B. Treanor, D. Depoil, A. Bruckbauer, F. D. Batista, Dynamic cortical actin remodeling by ERM proteins controls BCR microcluster organization and integrity. *J Exp Med* **208**, 1055-1068 (2011).

61. C. Liu *et al.*, Actin reorganization is required for the formation of polarized B cell receptor signalosomes in response to both soluble and membrane-associated antigens. *J Immunol* **188**, 3237-3246 (2012).

62. W. Liu, T. Meckel, P. Tolar, H. W. Sohn, S. K. Pierce, Antigen affinity discrimination is an intrinsic function of the B cell receptor. *J Exp Med* **207**, 1095-1111 (2010).

63. D. Depoil *et al.*, CD19 is essential for B cell activation by promoting B cell receptor-antigen microcluster formation in response to membrane-bound ligand. *Nat Immunol* **9**, 63-72 (2008).

64. S. J. Fleire *et al.*, B cell ligand discrimination through a spreading and contraction response. *Science* **312**, 738-741 (2006).

65. B. Treanor *et al.*, The membrane skeleton controls diffusion dynamics and signaling through the B cell receptor. *Immunity* **32**, 187-199 (2010).

66. P. K. Mattila *et al.*, The actin and tetraspanin networks organize receptor nanoclusters to regulate B cell receptor-mediated signaling. *Immunity* **38**, 461-474 (2013).

67. F. D. Batista, B. Treanor, N. E. Harwood, Visualizing a role for the actin cytoskeleton in the regulation of B-cell activation. *Immunol Rev* **237**, 191-204 (2010).

68. P. Tolar, J. Hanna, P. D. Krueger, S. K. Pierce, The constant region of the membrane immunoglobulin mediates B cell-receptor clustering and signaling in response to membrane antigens. *Immunity* **30**, 44-55 (2009).

69. P. Tolar, H. W. Sohn, W. Liu, S. K. Pierce, The molecular assembly and organization of signaling active B-cell receptor oligomers. *Immunol Rev* **232**, 34-41 (2009).

70. W. Song *et al.*, Actin-mediated feedback loops in B-cell receptor signaling. *Immunol Rev* **256**, 177-189 (2013).

71. M. Weber *et al.*, Phospholipase C-gamma2 and Vav cooperate within signaling microclusters to propagate B cell spreading in response to membrane-bound antigen. *J Exp Med* **205**, 853-868 (2008).

72.   S. Sharma, G. Orlowski, W. Song, Btk regulates B cell receptor-mediated antigen processing and presentation by controlling actin cytoskeleton dynamics in B cells. *J Immunol* **182**, 329-339 (2009).

73.   C. Liu *et al.*, A balance of Bruton's tyrosine kinase and SHIP activation regulates B cell receptor cluster formation by controlling actin remodeling. *J Immunol* **187**, 230-239 (2011).

74.   N. E. Harwood, F. D. Batista, Early events in B cell activation. *Annu Rev Immunol* **28**, 185-210 (2010).

75.   C. Liu *et al.*, N-wasp is essential for the negative regulation of B cell receptor signaling. *PLoS Biol* **11**, e1001704 (2013).

76.   K. B. Lin *et al.*, The rap GTPases regulate B cell morphology, immune-synapse formation, and signaling by particulate B cell receptor ligands. *Immunity* **28**, 75-87 (2008).

77.   E. Arana *et al.*, Activation of the small GTPase Rac2 via the B cell receptor regulates B cell adhesion and immunological-synapse formation. *Immunity* **28**, 88-99 (2008).

78.   R. W. Chesnut, H. M. Grey, Studies on the capacity of B cells to serve as antigen-presenting cells. *J Immunol* **126**, 1075-1079 (1981).

79.   V. R. Aluvihare, A. A. Khamlichi, G. T. Williams, L. Adorini, M. S. Neuberger, Acceleration of intracellular targeting of antigen by the B-cell antigen receptor: importance depends on the nature of the antigen-antibody interaction. *EMBO J* **16**, 3553-3562 (1997).

80.   .

81.   F. D. Batista, D. Iber, M. S. Neuberger, B cells acquire antigen from target cells after synapse formation. *Nature* **411**, 489-494 (2001).

82.   P. C. Cheng, C. R. Steele, L. Gu, W. Song, S. K. Pierce, MHC class II antigen processing in B cells: accelerated intracellular targeting of antigens. *J Immunol* **162**, 7171-7180 (1999).

83.   M. I. Yuseff *et al.*, Polarized secretion of lysosomes at the B cell synapse couples antigen extraction to processing and presentation. *Immunity* **35**, 361-374 (2011).

84.   E. Natkanski *et al.*, B cells use mechanical energy to discriminate antigen affinities. *Science* **340**, 1587-1590 (2013).

85.   A. Stoddart *et al.*, Lipid rafts unite signaling cascades with clathrin to regulate BCR internalization. *Immunity* **17**, 451-462 (2002).

86.   A. Stoddart, A. P. Jackson, F. M. Brodsky, in *Mol Biol Cell*. (2005), vol. 16, pp. 2339-2348.

87.   C. Bonnerot *et al.*, Role of B cell receptor Ig alpha and Ig beta subunits in MHC class II-restricted antigen presentation. *Immunity* **3**, 335-347 (1995).

88.   C. Jang, S. Machtaler, L. Matsuuchi, The role of Ig-alpha/beta in B cell antigen receptor internalization. *Immunol Lett* **134**, 75-82 (2010).

89.   P. Hou *et al.*, B cell antigen receptor signaling and internalization are mutually exclusive events. *PLoS Biol* **4**, e200 (2006).

90.   K. Busman-Sahay, L. Drake, A. Sitaram, M. Marks, J. R. Drake, Cis and trans regulatory mechanisms control AP2-mediated B cell receptor endocytosis via select tyrosine-based motifs. *PLoS One* **8**, e54938 (2013).

91.   S. Malhotra, S. Kovats, W. Zhang, K. M. Coggeshall, B cell antigen receptor endocytosis and antigen presentation to T cells require Vav and dynamin. *J Biol Chem* **284**, 24088-24097 (2009).

92.   E. a. H. Ungewickell, Lars, Endocytosis: clathrin-mediated membrane budding. **19**, 417–425 (2007).

93.   O. O. Onabajo *et al.*, Actin-Binding Protein 1 Regulates B Cell Receptor-Mediated Antigen Processing and Presentation in Response to B Cell Receptor Activation1. *J Immunol* **180**, 6685-6695 (2008).

94.   M. Blery, L. Tze, L. A. Miosge, J. E. Jun, C. C. Goodnow, Essential role of membrane cholesterol in accelerated BCR internalization and uncoupling from NF-kappa B in B cell clonal anergy. *J Exp Med* **203**, 1773-1783 (2006).

95.   H. Niiro *et al.*, The B lymphocyte adaptor molecule of 32 kilodaltons (Bam32) regulates B cell antigen receptor internalization. *J Immunol* **173**, 5601-5609 (2004).

96.   B. K. Brown, W. Song, The actin cytoskeleton is required for the trafficking of the B cell antigen receptor to the late endosomes. *Traffic* **2**, 414-427 (2001).

97.   S. Malhotra, S. Kovats, W. Zhang, K. M. Coggeshall, Vav and Rac activation in B cell antigen receptor endocytosis involves Vav recruitment to the adapter protein LAB. *J Biol Chem* **284**, 36202-36212 (2009).

98.   C. M. Mutch *et al.*, Activation-induced endocytosis of the raft-associated transmembrane adaptor protein LAB/NTAL in B lymphocytes: evidence for a role in internalization of the B cell receptor. *Int Immunol* **19**, 19-30 (2007).

99.   M. R. Clark, D. Massenburg, K. Siemasko, P. Hou, M. Zhang, B-cell antigen receptor signaling requirements for targeting antigen to the MHC class II presentation pathway. *Curr Opin Immunol* **16**, 382-387 (2004).

100.   F. Vascotto *et al.*, Antigen presentation by B lymphocytes: how receptor signaling directs membrane trafficking. *Curr Opin Immunol* **19**, 93-98 (2007).

101.   W. Song, H. Cho, P. Cheng, S. K. Pierce, Entry of B cell antigen receptor and antigen into class II peptide-loading compartment is independent of receptor cross-linking. *J Immunol* **155**, 4255-4263 (1995).

102.   K. Siemasko *et al.*, Igα and Igβ Are Required for Efficient Trafficking to Late Endosomes and to Enhance Antigen Presentation. (1999).

103.   C. Li, K. Siemasko, M. R. Clark, W. Song, Cooperative interaction of Ig(alpha) and Ig(beta) of the BCR regulates the kinetics and specificity of antigen targeting. *Int Immunol* **14**, 1179-1191 (2002).

104.   M. Zhang *et al.*, Ubiquitinylation of Ig beta dictates the endocytic fate of the B cell antigen receptor. *J Immunol* **179**, 4435-4443 (2007).

105.   D. Le Roux *et al.*, in *Mol Biol Cell*. (2007), vol. 18, pp. 3451-3462.

106.   F. Vascotto *et al.*, The actin-based motor protein myosin II regulates MHC class II trafficking and BCR-driven antigen presentation. *J Cell Biol* **176**, 1007-1019 (2007).

107.   V. Kouskoff *et al.*, Antigens varying in affinity for the B cell receptor induce differential B lymphocyte responses. *J Exp Med* **188**, 1453-1464 (1998).

108.   D. K. Goroff, A. Stall, J. J. Mond, F. D. Finkelman, In vitro and in vivo B lymphocyte-activating properties of monoclonal anti-delta antibodies. I.

Determinants of B lymphocyte-activating properties. *J Immunol* **136**, 2382-2392 (1986).

109.	M. Brunswick *et al.*, Picogram quantities of anti-Ig antibodies coupled to dextran induce B cell proliferation. *J Immunol* **140**, 3364-3372 (1988).

110.	R. A. Finkelstein, K. Fujita, J. J. LoSpalluto, Procholeragenoid: an aggregated intermediate in the formation of choleragenoid. *J Immunol* **107**, 1043-1051 (1971).

111.	E. P. Kelly, J. J. Greene, A. D. King, B. L. Innis, Purified dengue 2 virus envelope glycoprotein aggregates produced by baculovirus are immunogenic in mice. *Vaccine* **18**, 2549-2559 (2000).

112.	S. W. Li *et al.*, A bacterially expressed particulate hepatitis E vaccine: antigenicity, immunogenicity and protectivity on primates. *Vaccine* **23**, 2893-2901 (2005).

113.	C. A. Bricault *et al.*, A Multivalent Clade C HIV-1 Env Trimer Cocktail Elicits a Higher Magnitude of Neutralizing Antibodies than Any Individual Component. *J Virol*, (2014).

114.	Y. Z. Yu *et al.*, Pentavalent replicon vaccines against botulinum neurotoxins and tetanus toxin using DNA-based Semliki Forest virus replicon vectors. *Hum Vaccin Immunother* **10**, 1874-1879 (2014).

115.	Y. M. Kim *et al.*, Monovalent ligation of the B cell receptor induces receptor activation but fails to promote antigen presentation. *Proc Natl Acad Sci U S A* **103**, 3327-3332 (2006).

116.	R. Thyagarajan, N. Arunkumar, W. Song, Polyvalent antigens stabilize B cell antigen receptor surface signaling microdomains. *J Immunol* **170**, 6099-6106 (2003).

117.	J. J. Mond, K. E. Stein, B. Subbarao, W. E. Paul, Analysis of B cell activation requirements with TNP-conjugated polyacrylamide beads. *J Immunol* **123**, 239-245 (1979).

118.	D. C. Parker, J. J. Fothergill, D. C. Wadsworth, B lymphocyte activation by insoluble anti-immunoglobulin: induction of immunoglobulin secretion by a T cell-dependent soluble factor. *J Immunol* **123**, 931-941 (1979).

119.	P. K. Mongini, C. A. Blessinger, P. F. Highet, J. K. Inman, Membrane IgM-mediated signaling of human B cells. Effect of increased ligand binding site valency on the affinity and concentration requirements for inducing diverse stages of activation. *J Immunol* **148**, 3892-3901 (1992).

120.	C. M. Snapper, M. R. Kehry, B. E. Castle, J. J. Mond, Multivalent, but not divalent, antigen receptor cross-linkers synergize with CD40 ligand for induction of Ig synthesis and class switching in normal murine B cells. A redefinition of the TI-2 vs T cell-dependent antigen dichotomy. *J Immunol* **154**, 1177-1187 (1995).

121.	E. B. Puffer, J. K. Pontrello, J. J. Hollenbeck, J. A. Kink, L. L. Kiessling, Activating B cell signaling with defined multivalent ligands. *ACS Chem Biol* **2**, 252-262 (2007).

122.	S. Minguet, E. P. Dopfer, W. W. Schamel, Low-valency, but not monovalent, antigens trigger the B-cell antigen receptor (BCR). *Int Immunol* **22**, 205-212 (2010).

123. P. L. McNeil, R. A. Steinhardt, Loss, restoration, and maintenance of plasma membrane integrity. *J Cell Biol* **137**, 1-4 (1997).
124. W. T. Chen, Mechanism of retraction of the trailing edge during fibroblast movement. *J Cell Biol* **90**, 187-200 (1981).
125. I. Hwang, D. Ki, Receptor-mediated T cell absorption of antigen presenting cell-derived molecules. *Front Biosci* **16**, 411-421.
126. L. Buckingham, J. L. Duncan, Approximate dimensions of membrane lesions produced by streptolysin S and streptolysin O. *Biochim Biophys Acta* **729**, 115-122 (1983).
127. S. Bhakdi, J. Tranum-Jensen, A. Sziegoleit, Mechanism of membrane damage by streptolysin-O. *Infect Immun* **47**, 52-60 (1985).
128. F. C. Los, T. M. Randis, R. V. Aroian, A. J. Ratner, Role of pore-forming toxins in bacterial infectious diseases. *Microbiol Mol Biol Rev* **77**, 173-207 (2013).
129. S. Bhakdi *et al.*, Staphylococcal alpha-toxin, streptolysin-O, and Escherichia coli hemolysin: prototypes of pore-forming bacterial cytolysins. *Arch Microbiol* **165**, 73-79 (1996).
130. J. N. Cole, T. C. Barnett, V. Nizet, M. J. Walker, Molecular insight into invasive group A streptococcal disease. *Nature Reviews Microbiology* **9**, 724-736 (2011).
131. C. L. Bashford *et al.*, Membrane damage by hemolytic viruses, toxins, complement, and other cytotoxic agents. A common mechanism blocked by divalent cations. *J Biol Chem* **261**, 9300-9308 (1986).
132. R. J. Klein *et al.*, Complement factor H polymorphism in age-related macular degeneration. *Science* **308**, 385-389 (2005).
133. C. J. Froelich *et al.*, New Paradigm for Lymphocyte Granule-mediated Cytotoxicity. (1996).
134. L. Shi *et al.*, Granzyme B (GraB) Autonomously Crosses the Cell Membrane and Perforin Initiates Apoptosis and GraB Nuclear Localization. *J Exp Med* **185**, 855-866 (1997).
135. P. Groscurth, L. Filgueira, Killing Mechanisms of Cytotoxic T Lymphocytes. *News Physiol Sci* **13**, 17-21 (1998).
136. M. D. Geeraerts, M. F. Ronveaux-Dupal, J. J. Lemasters, B. Herman, Cytosolic free Ca2+ and proteolysis in lethal oxidative injury in endothelial cells. *Am J Physiol* **261**, C889-896 (1991).
137. P. L. McNeil, T. Kirchhausen, An emergency response team for membrane repair. *Nat Rev Mol Cell Biol* **6**, 499-505 (2005).
138. N. W. Andrews, P. E. Almeida, M. Corrotte, Damage control: cellular mechanisms of plasma membrane repair. *Trends Cell Biol* **24**, 734-742 (2014).
139. D. Keefe *et al.*, Perforin triggers a plasma membrane-repair response that facilitates CTL induction of apoptosis. *Immunity* **23**, 249-262 (2005).
140. R. A. Steinhardt, G. Bi, J. M. Alderton, Cell membrane resealing by a vesicular mechanism similar to neurotransmitter release. *Science* **263**, 390-393 (1994).

141. K. Miyake, P. L. McNeil, Vesicle accumulation and exocytosis at sites of plasma membrane disruption. *J Cell Biol* **131**, 1737-1745 (1995).
142. J. K. Jaiswal, N. W. Andrews, S. M. Simon, Membrane proximal lysosomes are the major vesicles responsible for calcium-dependent exocytosis in nonsecretory cells. *J Cell Biol* **159**, 625-635 (2002).
143. C. Tam *et al.*, Exocytosis of acid sphingomyelinase by wounded cells promotes endocytosis and plasma membrane repair. *J Cell Biol* **189**, 1027-1038 (2010).
144. A. Reddy, E. V. Caler, N. W. Andrews, Plasma Membrane Repair Is Mediated by Ca2+-Regulated Exocytosis of Lysosomes. *Cell* **106**, 157-169 (2001).
145. G. Q. Bi *et al.*, Kinesin- and myosin-driven steps of vesicle recruitment for Ca2+-regulated exocytosis. *J Cell Biol* **138**, 999-1008 (1997).
146. P. L. McNeil, M. Terasaki, Coping with the inevitable: how cells repair a torn surface membrane. *Nat Cell Biol* **3**, E124-129 (2001).
147. I. Martinez *et al.*, in *J Cell Biol*. (2000), vol. 148, pp. 1141-1150.
148. V. Idone, C. Tam, N. W. Andrews, Two-way traffic on the road to plasma membrane repair. *Trends Cell Biol* **18**, 552-559 (2008).
149. S. K. Rao, C. Huynh, V. Proux-Gillardeaux, T. Galli, N. W. Andrews, Identification of SNAREs involved in synaptotagmin VII-regulated lysosomal exocytosis. *J Biol Chem* **279**, 20471-20479 (2004).
150. Y. A. Chen, R. H. Scheller, SNARE-mediated membrane fusion. *Nature Reviews Molecular Cell Biology* **2**, 98-106 (2001).
151. D. Bansal *et al.*, Defective membrane repair in dysferlin-deficient muscular dystrophy. *Nature* **423**, 168-172 (2003).
152. A. Draeger, K. Monastyrskaya, E. B. Babiychuk, Plasma membrane repair and cellular damage control: the annexin survival kit. *Biochem Pharmacol* **81**, 703-712 (2011).
153. A. K. McNeil, U. Rescher, V. Gerke, P. L. McNeil, Requirement for annexin A1 in plasma membrane repair. *J Biol Chem* **281**, 35202-35207 (2006).
154. E. B. Babiychuk, K. Monastyrskaya, S. Potez, A. Draeger, Blebbing confers resistance against cell lysis. *Cell Death Differ* **18**, 80-89 (2011).
155. E. B. Babiychuk, K. Monastyrskaya, S. Potez, A. Draeger, Intracellular Ca(2+) operates a switch between repair and lysis of streptolysin O-perforated cells. *Cell Death Differ* **16**, 1126-1134 (2009).
156. A. J. Jimenez *et al.*, ESCRT machinery is required for plasma membrane repair. *Science* **343**, 1247136 (2014).
157. V. Idone *et al.*, in *J Cell Biol*. (2008), vol. 180, pp. 905-914.
158. M. Corrotte *et al.*, Caveolae internalization repairs wounded cells and muscle fibers. *Elife* **2**, e00926 (2013).
159. M. Corrotte, M. C. Fernandes, C. Tam, N. W. Andrews, Toxin pores endocytosed during plasma membrane repair traffic into the lumen of MVBs for degradation. *Traffic* **13**, 483-494 (2012).
160. C. A. Tegla *et al.*, MEMBRANE ATTACK BY COMPLEMENT: THE ASSEMBLY AND BIOLOGY OF TERMINAL COMPLEMENT COMPLEXES. *Immunol Res* **51**, 45-60 (2011).

161. K. Simons, D. Toomre, Lipid rafts and signal transduction. *Nat Rev Mol Cell Biol* **1**, 31-39 (2000).

162. J. Thiery *et al.*, Perforin activates clathrin- and dynamin-dependent endocytosis, which is required for plasma membrane repair and delivery of granzyme B for granzyme-mediated apoptosis. *Blood* **115**, 1582-1593 (2010).

163. F. G. Karnell, R. J. Brezski, L. B. King, M. A. Silverman, J. G. Monroe, Membrane cholesterol content accounts for developmental differences in surface B cell receptor compartmentalization and signaling. *J Biol Chem* **280**, 25621-25628 (2005).

164. P. C. Cheng, M. L. Dykstra, R. N. Mitchell, S. K. Pierce, A role for lipid rafts in B cell antigen receptor signaling and antigen targeting. *J Exp Med* **190**, 1549-1560 (1999).

165. S. K. Pierce, Lipid rafts and B-cell activation. *Nat Rev Immunol* **2**, 96-105 (2002).

166. M. L. Dykstra, R. Longnecker, S. K. Pierce, Epstein-Barr virus coopts lipid rafts to block the signaling and antigen transport functions of the BCR. *Immunity* **14**, 57-67 (2001).

167. M. J. Aman, K. S. Ravichandran, A requirement for lipid rafts in B cell receptor induced Ca2+ flux. *Current Biology* **10**, 393-396 (2000).

168. M. Awasthi-Kalia, P. P. Schnetkamp, J. P. Deans, Differential effects of filipin and methyl-beta-cyclodextrin on B cell receptor signaling. *Biochem Biophys Res Commun* **287**, 77-82 (2001).

169. R. J. Petrie, P. P. Schnetkamp, K. D. Patel, M. Awasthi-Kalia, J. P. Deans, Transient translocation of the B cell receptor and Src homology 2 domain-containing inositol phosphatase to lipid rafts: evidence toward a role in calcium regulation. *J Immunol* **165**, 1220-1227 (2000).

170. B. J. Quah *et al.*, Bystander B cells rapidly acquire antigen receptors from activated B cells by membrane transfer. *Proc Natl Acad Sci U S A* **105**, 4259-4264 (2008).

171. P. L. McNeil, S. Ito, Molecular traffic through plasma membrane disruptions of cells in vivo. *J Cell Sci* **96 (Pt 3)**, 549-556 (1990).

172. P. L. McNeil, S. Ito, Gastrointestinal cell plasma membrane wounding and resealing in vivo. *Gastroenterology* **96**, 1238-1248 (1989).

173. P. L. McNeil, R. Khakee, Disruptions of muscle fiber plasma membranes. Role in exercise-induced damage. *Am J Pathol* **140**, 1097-1109 (1992).

174. M. S. Clarke, R. W. Caldwell, H. Chiao, K. Miyake, P. L. McNeil, Contraction-induced cell wounding and release of fibroblast growth factor in heart. *Circ Res* **76**, 927-934 (1995).

175. F. Galbiati, B. Razani, M. P. Lisanti, Emerging themes in lipid rafts and caveolae. *Cell* **106**, 403-411 (2001).

176. R. G. Parton, K. Simons, The multiple faces of caveolae. *Nat Rev Mol Cell Biol* **8**, 185-194 (2007).

177. E. Gazzerro, F. Sotgia, C. Bruno, M. P. Lisanti, C. Minetti, in *Eur J Hum Genet*. (England, 2010), vol. 18, pp. 137-145.

178. Y. Hagiwara *et al.*, Caveolin-3 deficiency causes muscle degeneration in mice. *Hum Mol Genet* **9**, 3047-3054 (2000).

179. R. Hnasko, M. P. Lisanti, The biology of caveolae: lessons from caveolin knockout mice and implications for human disease. *Mol Interv* **3**, 445-464 (2003).
180. H. Grassme, V. Jendrossek, J. Bock, A. Riehle, E. Gulbins, Ceramide-rich membrane rafts mediate CD40 clustering. *J Immunol* **168**, 298-307 (2002).
181. M. Xu *et al.*, in *Mol Biol Cell*. (2012), vol. 23, pp. 1546-1557.
182. C. Tam, A. R. Flannery, N. Andrews, Live imaging assay for assessing the roles of Ca2+ and sphingomyelinase in the repair of pore-forming toxin wounds. *J Vis Exp*, e50531 (2013).
183. J. P. Pereira, L. M. Kelly, J. G. Cyster, in *Int Immunol*. (England, 2010), vol. 22, pp. 413-419.
184. M. Brandes, D. F. Legler, B. Spoerri, P. Schaerli, B. Moser, Activation-dependent modulation of B lymphocyte migration to chemokines. *Int Immunol* **12**, 1285-1292 (2000).
185. T. Okada *et al.*, Antigen-Engaged B Cells Undergo Chemotaxis toward the T Zone and Form Motile Conjugates with Helper T Cells. *PLoS Biol* **3**, (2005).
186. M.-I. Yuseff, P. Pierobon, A. Reversat, A.-M. Lennon-Duménil, How B cells capture, process and present antigens: a crucial role for cell polarity. *Nature Reviews Immunology* **13**, 475-486 (2013).
187. A. Aucher, E. Magdeleine, E. Joly, D. Hudrisier, Capture of plasma membrane fragments from target cells by trogocytosis requires signaling in T cells but not in B cells. *Blood* **111**, 5621-5628 (2008).
188. A. M. Fra, E. Williamson, K. Simons, R. G. Parton, Detergent-insoluble glycolipid microdomains in lymphocytes in the absence of caveolae. *J Biol Chem* **269**, 30745-30748 (1994).
189. F. A. Medina, T. M. Williams, F. Sotgia, H. B. Tanowitz, M. P. Lisanti, in *Cell Cycle*. (United States, 2006), vol. 5, pp. 1865-1871.
190. A. L. Wurster, V. L. Rodgers, M. F. White, T. L. Rothstein, M. J. Grusby, in *J Biol Chem*. (United States, 2002), vol. 277, pp. 27169-27175.
191. T. L. Rothstein, Signals and susceptibility to programmed death in b cells. *Curr Opin Immunol* **8**, 362-371 (1996).
192. J. G. Monroe, J. C. Cambier, Sorting of B lymphoblasts based upon cell diameter provides cell populations enriched in different stages of cell cycle. *J Immunol Methods* **63**, 45-56 (1983).
193. B. Hat, B. Kazmierczak, T. Lipniacki, B cell activation triggered by the formation of the small receptor cluster: a computational study. *PLoS Comput Biol* **7**, e1002197 (2011).
194. M. Kolzer, N. Werth, K. Sandhoff, Interactions of acid sphingomyelinase and lipid bilayers in the presence of the tricyclic antidepressant desipramine. *FEBS Lett* **559**, 96-98 (2004).
195. K. Horinouchi *et al.*, Acid sphingomyelinase deficient mice: a model of types A and B Niemann-Pick disease. *Nat Genet* **10**, 288-293 (1995).
196. I. R. Nabi, P. U. Le, Caveolae/raft-dependent endocytosis. *J Cell Biol* **161**, 673-677 (2003).

197. Z. Tang *et al.*, Molecular cloning of caveolin-3, a novel member of the caveolin gene family expressed predominantly in muscle. *J Biol Chem* **271**, 2255-2261 (1996).

198. .

199. A. M. Fra, E. Williamson, K. Simons, R. G. Parton, De novo formation of caveolae in lymphocytes by expression of VIP21-caveolin. *Proc Natl Acad Sci U S A* **92**, 8655-8659 (1995).

200. J. M. Holopainen, M. I. Angelova, P. K. Kinnunen, in *Biophys J*. (United States, 2000), vol. 78, pp. 830-838.

201. K. Trajkovic *et al.*, in *Science*. (United States, 2008), vol. 319, pp. 1244-1247.

202. I. Hwang, D. Ki, Receptor-mediated T cell absorption of antigen presenting cell-derived molecules. *Front Biosci (Landmark Ed)* **16**, 411-421 (2011).

203. P. Tolar, H. W. Sohn, S. K. Pierce, The initiation of antigen-induced B cell antigen receptor signaling viewed in living cells by fluorescence resonance energy transfer. *Nat Immunol* **6**, 1168-1176 (2005).

204. J. M. Dal Porto, A. M. Haberman, M. J. Shlomchik, G. Kelsoe, Antigen drives very low affinity B cells to become plasmacytes and enter germinal centers. *J Immunol* **161**, 5373-5381 (1998).

205. J. Riedl *et al.*, Lifeact: a versatile marker to visualize F-actin. *Nat Methods* **5**, 605-607 (2008).

206. J. Riedl *et al.*, Lifeact mice for studying F-actin dynamics. *Nature Methods* **7**, 168-169 (2010).

207. P. Peluso *et al.*, Optimizing antibody immobilization strategies for the construction of protein microarrays. *Anal Biochem* **312**, 113-124 (2003).

208. K. A. Xavier, R. C. Willson, Association and dissociation kinetics of anti-hen egg lysozyme monoclonal antibodies HyHEL-5 and HyHEL-10. *Biophys J* **74**, 2036-2045 (1998).

209. A. Grakoui *et al.*, The immunological synapse: a molecular machine controlling T cell activation. *Science* **285**, 221-227 (1999).

210. K. Jaqaman *et al.*, Robust single-particle tracking in live-cell time-lapse sequences. *Nature Methods* **5**, 695-702 (2008).

211. M. Kirkham, R. G. Parton, Clathrin-independent endocytosis: new insights into caveolae and non-caveolar lipid raft carriers. *Biochim Biophys Acta* **1745**, 273-286 (2005).

212. C. G. Hansen, B. J. Nichols, Molecular mechanisms of clathrin-independent endocytosis. *J Cell Sci* **122**, 1713-1721 (2009).

213. A. Hakansson, C. C. Bentley, E. A. Shakhnovic, M. R. Wessels, Cytolysin-dependent evasion of lysosomal killing. *Proc Natl Acad Sci U S A* **102**, 5192-5197 (2005).